IN THE UNITED STATES PATENT AND TRADEMARK OFFICE

Application of:	Walke *et al.*		
Serial No.:	09/755,016	Group Art Unit:	1652
Filed:	01/05/2001	Examiner:	C. Fronda

For: Novel Human Proteases and Polynucleotides Encoding the Same

Attorney Docket No.: LEX-0114-USA

APPEAL BRIEF

Mail Stop Appeal Brief - Patents
Commissioner for Patents
P.O. Box 1450

TABLE OF CONTENTS

APPEAL BRIEF

Sir:

Appellants hereby submit an original and two copies of this Appeal Brief to the Board of Patent Appeals and Interferences ("the Board") in response to the Final Office Action mailed on March 6, 2003. The Notice of Appeal was timely submitted on June 6, 2003, and was received in the Patent and Trademark Office ("the Office") on June 9, 2003. This Appeal Brief is timely submitted in light of the concurrently filed Petition for an Extension of Time of one month to and including September 9, 2003, and authorization to deduct the fee as required under 37 C.F.R. § 1.17(a)(1) from Appellants' Representatives' deposit account. The Commissioner is also authorized to charge the fee for filing this Appeal Brief ($160.00), as required under 37 C.F.R. § 1.17(c), to Lexicon Genetics Incorporated Deposit Account No. 50-0892.

Appellants believe no fees in addition to the fee for filing the Appeal Brief and the fee for the extension of time are due in connection with this Appeal Brief. However, should any additional fees under 37 C.F.R. §§ 1.16 to 1.21 be required for any reason related to this communication, the Commissioner is authorized to charge any underpayment or credit any overpayment to Lexicon Genetics Incorporated Deposit Account No. 50-0892.

I. REAL PARTY IN INTEREST

The real party in interest is the Assignee, Lexicon Genetics Incorporated, 8800 Technology Forest Place, The Woodlands, Texas, 77381.

II. RELATED APPEALS AND INTERFERENCES

Appellants know of no related appeals or interferences that will directly affect or be directly affected by or have a bearing on the Board's decision in the pending appeal.

III. STATUS OF THE CLAIMS

The present application was filed on January 5, 2001, claiming the benefit of U.S. Provisional Application Number 60/174,686, which was filed on January 6, 2000, and included original claims 1-4. A Restriction and Election Requirement was set forth during a telephone interview between the Examiner and Appellants' representative Lance K. Ishimoto on October 11, 2001, separating the original claims into three separate and distinct inventions. During this telephone conference, Appellants provisionally elected with traverse the claims of the Group I invention (original claims 1 and 2) for prosecution on the merits.

A First Official Action on the merits ("the First Action") was issued on October 26, 2001, in which claims 1 and 2 were rejected under 35 U.S.C. § 112, first paragraph, as allegedly not described in the specification in such a way as to reasonably convey to one skilled in the relevant art that the inventors, at the time the application was filed, had possession of the claimed invention, claims 1 and 2 were rejected under 35 U.S.C. § 112, first paragraph, as allegedly not enabled, claims 1 and 2 were rejected under 35 U.S.C. § 112, second paragraph, as allegedly indefinite, and claim 1 was rejected under 35 U.S.C. § 102(b) as allegedly anticipated by Tsuruoka *et al.* (GenBank Database Accession Number E13202). In a response to the First Action submitted to the Office on February 7, 2002 ("Response to the First Action"), Appellants cancelled claims 3 and 4 without prejudice and without disclaimer as drawn to non-elected inventions, amended claims 1 and 2 to further improve their clarity, and addressed the rejections of claims 1 and 2.

A Second Official Action ("the Second Action") was issued on September 9, 2002, indicating that the rejection of claims 1 and 2 under 35 U.S.C. § 112, first paragraph, as allegedly not enabled, claim 1 under 35 U.S.C. § 112, second paragraph, as allegedly indefinite, and claim 1 under 35 U.S.C. § 102(b) as allegedly anticipated by Tsuruoka *et al.* (GenBank Database Accession Number E13202) had been overcome by the amendments and remarks submitted in the Response to the First Action, but maintaining the rejection of claims 1 and 2 under 35 U.S.C. § 112, first paragraph, as allegedly not described in the specification in such a way as to reasonably convey to one skilled in the relevant art that the inventors, at the time the application was filed, had possession of the claimed invention, and claim 2 under 35 U.S.C. § 112, second paragraph, as allegedly indefinite, and newly rejecting claims 1 and 2 under

35 U.S.C. § 101 as allegedly lacking a patentable utility, claims 1 and 2 under 35 U.S.C. § 112, first paragraph as allegedly unusable by the skilled artisan due to the alleged lack of patentable utility, and claim 1 under 35 U.S.C. § 102(b) as allegedly anticipated by Strausberg *et al.* (GenBank Database Accession Number AA884376). In a response to the Second Action submitted to the Office on December 4, 2002 ("Response to the Second Action"), Appellants amended claims 1 and 2, added new claims 5-10, and again addressed the rejections of claims 1 and 2.

A Third and Final Official Action ("the Final Action") was issued on March 6, 2003, indicating that the rejection of claim 2 under 35 U.S.C. § 112, first paragraph, as allegedly not described in the specification in such a way as to reasonably convey to one skilled in the relevant art that the inventors, at the time the application was filed, had possession of the claimed invention, claim 2 under 35 U.S.C. § 112, second paragraph, as allegedly indefinite, and claim 1 under 35 U.S.C. § 102(b) as allegedly anticipated by Strausberg *et al.* (GenBank Database Accession Number AA884376) had been overcome by the amendments and remarks submitted in the Response to the Second Action, but maintaining the rejection of claims 1 and 2 (and newly added claims 5-10) under 35 U.S.C. § 101 as allegedly lacking a patentable utility, claims 1 and 2 (and newly added claims 5-10) under 35 U.S.C. § 112, first paragraph as allegedly unusable by the skilled artisan due to the alleged lack of patentable utility, and claim 1 (and newly added claims 7-10) under 35 U.S.C. § 112, first paragraph, as allegedly not described in the specification in such a way as to reasonably convey to one skilled in the relevant art that the inventors, at the time the application was filed, had possession of the claimed invention. In a response to the Final Action submitted to the Office on May 6, 2003 ("Response to the Final Action"), Appellants addressed the rejections of claims 1, 2 and 5-10.

An Advisory Action ("the Advisory Action") was mailed on July 8, 2003, maintaining the rejection of claims 1, 2 and 5-10 under 35 U.S.C. § 101 as allegedly lacking a patentable utility, claims 1, 2 and 5-10 under 35 U.S.C. § 112, first paragraph as allegedly unusable by the skilled artisan due to the alleged lack of patentable utility, and claims 1 and 7-10 under 35 U.S.C. § 112, first paragraph, as allegedly not described in the specification in such a way as to reasonably convey to one skilled in the relevant art that the inventors, at the time the application was filed, had possession of the claimed invention.

Therefore, claims 1, 2 and 5-10 are the subject of this appeal. A copy of the appealed claims are included below in the Appendix (Section IX).

IV. STATUS OF THE AMENDMENTS

As no amendments subsequent to the Final Action have been filed, Appellants believe that no outstanding amendments exist.

V. SUMMARY OF THE INVENTION

The present invention relates to Appellants' discovery and identification of novel human polynucleotide sequences that encode a novel protein that shares structural similarity with mammalian proteases (specification at page 1, lines 9-12), and particularly trypsin-like serine proteases such as enteropeptidase (enterokinase), plasminogen, and acrosin (specification at page 2, lines 2-3 and page 15, lines 30-31).

The presently claimed polynucleotide sequences were compiled from gene trapped cDNAs and clones isolated from a human testis cDNA library (specification at page 3, lines 4-5). Three coding single nucleotide polymorphisms were identified in the claimed sequence - specifically, a C/T polymorphism at nucleotide position 28 of SEQ ID NO:3, a silent polymorphism that results in a leucine at amino acid position 10 of SEQ ID NO:4; a C/T polymorphism at nucleotide position 55 of SEQ ID NO:3, which can result in a tyrosine or histidine at amino acid position 19 of SEQ ID NO:4; and a G/A polymorphism at nucleotide position 379 of SEQ ID NO:3, which can result in an alanine or threonine at amino acid position 127 of SEQ ID NO:4 (specification at page 15, lines 22-29).

The specification details a number of uses for the presently claimed polynucleotide sequences, including in diagnostic assays such as forensic analysis (see, for example, the specification at page 10, lines 13-24), in determining the genomic structure of the protein encoding regions of the corresponding human chromosome (see, for example, the specification at page 10, line 18), and in assessing gene expression patterns, particularly using a high throughput "chip" format (see, for example, the specification at page 5, lines 9-12).

VI. ISSUES ON APPEAL

1. Do claims 1, 2 and 5-10 lack a patentable utility?
2. Are claims 1, 2 and 5-10 unusable by a skilled artisan due to a lack of patentable utility?
3. Do claims 1 and 7-10 lack sufficient written description?

VII. GROUPING OF THE CLAIMS

For the purposes of the outstanding rejections under 35 U.S.C. § 101 and 35 U.S.C. § 112, first paragraph, associated with the utility rejection, the claims will stand or fall together. For the purposes of the outstanding rejection under 35 U.S.C. § 112, first paragraph, associated with written description, claims 1 and 7-10 will stand or fall together.

VIII. ARGUMENT

A. Do Claims 1, 2 and 5-10 Lack a Patentable Utility?

The Final Action first rejects claims 1, 2 and 5-10 under 35 U.S.C. § 101, as allegedly lacking a patentable utility due to not being supported by either a specific and substantial or a well-established utility.

Appellants pointed out both in the Response to the Second Action and the Response to the Final Action that the present nucleic acid sequences have utility in forensic analysis, as described in the specification as originally filed (see, for example, page 10, lines 13-24). As described in the specification at page 15, lines 22-29, the presently claimed sequence defines three coding single nucleotide polymorphisms - specifically, a C/T polymorphism at nucleotide position 28 of SEQ ID NO:3, a silent polymorphism that results in a leucine at amino acid position 10 of SEQ ID NO:4; a C/T polymorphism at nucleotide position 55 of SEQ ID NO:3, which can result in a tyrosine or histidine at amino acid position 19 of SEQ ID NO:4; and a G/A polymorphism at nucleotide position 379 of SEQ ID NO:3, which can result in an alanine or threonine at amino acid position 127 of SEQ ID NO:4. As such polymorphisms are the basis for forensic analysis, which in undoubtedly a "real world" utility, the presently claimed sequence must in itself be useful.

Appellants respectfully point out that the presently described polymorphisms are useful in forensic

analysis exactly as they were described in the specification as originally filed - specifically, to distinguish individual members of the human population from one another based simply on the presence or absence of one or more of the described polymorphisms. The skilled artisan would be able to use the presently described polymorphisms in forensic analysis exactly as they were described in the specification as originally filed, without **any** additional research. It is important to note that simply because the use of these polymorphic markers will necessarily provide additional information on the percentage of particular subpopulations that contain these polymorphic markers does not mean that additional research is needed in order for these markers as they are presently described in the instant specification to be used in forensic science.

This is also not a case of a potential utility. Even in the worst case scenario, the described polymorphisms are each useful to distinguish 50% of the population (in other words, the marker being present in half of the population). Appellants point out that the ability of a polymorphic marker to distinguish at least 50% of the population is an inherent feature of any polymorphic marker, and this feature is well understood by those of skill in the art. Appellants note that as a matter of law, it is well settled that a patent need not disclose what is well known in the art. *In re Wands*, 8 USPQ 2d 1400 (Fed. Cir. 1988). Appellants respectfully point out that all that is required to support Appellants' assertion of utility is for the skilled artisan to believe that the presently described polymorphic markers could be useful in forensic analysis. The fact that forensic biologists use polymorphic markers such as those described by Appellants every day provides more than ample support for the assertion that forensic biologists would also be able to use the specific polymorphic markers described by Appellants in the same fashion. Therefore, the presently claimed sequence clearly has a substantial and well established utility.

The Advisory Action questions this assertion of utility, stating that such uses are "generic utilities that are applicable to any polynucleotide" (Advisory Action at page 2). This argument is flawed in a number of respects. First, Appellants submit that the asserted forensic utility is specific precisely because it cannot be applied to just any polynucleotide. In fact, the basis for forensic analysis is the fact that such polymorphic markers are **not** present in all other nucleic acids, but in fact specific and unique to only a certain subset of the population. Second, until a polymorphic marker is actually described it cannot be used

in forensic analysis. Put another way, simply because there is a likelihood, even a significant likelihood, that a particular nucleic acid sequence will contain a polymorphism and thus be useful in forensic analysis, until such a polymorphism is actually identified and described, such a likelihood is **meaningless**. The Examiner appears to be attempting to use the information presented for the first time by Appellants in the instant specification as hindsight verification that the presently claimed sequence would be expected to have polymorphic markers. Such hindsight analysis based on Appellants discovery is completely improper. Third, the Examiner seems to be confusing the requirements of a **specific** utility with a **unique** utility. The fact that other polymorphic markers have been identified in other genetic loci, or that the use of the presently described polymorphic markers will provide additional information concerning the prevalence of these markers in certain subpopulations, does not mean that use of the polymorphic markers identified by Appellants' in SEQ ID NO:3 in forensic analysis is not a specific utility. As clearly stated by the Federal Circuit in *Carl Zeiss Stiftung v. Renishaw PLC*, 20 USPQ2d 1101 (Fed. Cir. 1991):

> An invention need not be the best or only way to accomplish a certain result, and it need only be useful to some extent and in certain applications: "[T]he fact that an invention has only limited utility and is only operable in certain applications is not grounds for finding a lack of utility." *Envirotech Corp. v. Al George, Inc.*, 221 USPQ 473, 480 (Fed. Cir. 1984)

In other words, just because other (possibly better) polymorphic markers from the human genome have been described, or that additional information about the presently described polymorphic markers can be gained through the use of these markers, does not establish that the presently described polymorphic markers lack a specific utility. If every invention were required to have a unique utility, the Patent and Trademark Office would no longer be issuing patents on batteries, automobile tires, golf balls, golf clubs, and treatments for a variety of human diseases, such as cancer, just to name a few particular examples, because the utility of each of these compositions is applicable to the broad class in which each of these compositions falls: all batteries have the same utility, specifically to provide electrical power; all automobile tires have the same utility, specifically for use on automobiles; all golf balls and golf clubs have the same utility, specifically for use in the game of golf; and all cancer treatments have the same utility, specifically, to treat cancer. However, only the briefest perusal of virtually any issue of the Official Gazette provides numerous examples of patents being granted on each of the above compositions nearly every week.

Furthermore, if a composition needed to be unique to be patented, the entire class and subclass system would be an effort in futility, as the class and subclass system serves solely to group such common inventions, which would not be required if each invention needed to have a unique utility. In view of the above standards and "common sense" analysis, there can be little question that the present sequence clearly meets the requirements of 35 U.S.C. § 101.

Furthermore, as the presently described polymorphisms are a part of the family of polymorphisms that have a well established utility, the Federal Circuit's holding in *In re Brana*, (34 USPQ2d 1436 (Fed. Cir. 1995), "*Brana*") is directly on point. In *Brana*, the Federal Circuit admonished the Patent and Trademark Office for confusing "the requirements under the law for obtaining a patent with the requirements for obtaining government approval to market a particular drug for human consumption". *Brana* at 1442. The Federal Circuit went on to state:

> At issue in this case is an important question of the legal constraints on patent office examination practice and policy. The question is, with regard to pharmaceutical inventions, what must the applicant provide regarding the practical utility or usefulness of the invention for which patent protection is sought. This is not a new issue; it is one which we would have thought had been settled by case law years ago.

Brana at 1439, emphasis added. The choice of the phrase "utility or usefulness" in the foregoing quotation is highly pertinent. The Federal Circuit is evidently using "utility" to refer to rejections under 35 U.S.C. § 101, and is using "usefulness" to refer to rejections under 35 U.S.C. § 112, first paragraph. This is made evident in the continuing text in *Brana*, which explains the correlation between 35 U.S.C. §§ 101 and 112, first paragraph. The Federal Circuit concluded:

> FDA approval, however, is not a prerequisite for finding a compound useful within the meaning of the patent laws. Usefulness in patent law, and in particular in the context of pharmaceutical inventions, necessarily includes the expectation of further research and development. The stage at which an invention in this field becomes useful is well before it is ready to be administered to humans. Were we to require Phase II testing in order to prove utility, the associated costs would prevent many companies from obtaining patent protection on promising new inventions, thereby eliminating an incentive to pursue, through research and development, potential cures in many crucial areas such as the treatment of cancer.

Brana at 1442-1443, citations omitted, emphasis added. As set forth above, the present polymorphisms

are useful in forensic analysis as described in the specification as originally filed, without the need for any further research. As discussed above, even if the use of these polymorphic markers provided additional information on the percentage of particular subpopulations that contain these polymorphic markers, this would not mean that "additional research" is needed in order for these markers as they are presently described in the instant specification to be of use to forensic science. As stated above, using the polymorphic marker as described in the specification as originally field can definitely distinguish members of a population from one another. However, even if, *arguendo*, further research might be required in certain aspects of the present invention, this does not preclude a finding that the invention has utility, as set forth by the Federal Circuit's holding in *Brana*, which clearly states, as highlighted in the quote above, that "pharmaceutical inventions, necessarily includes the expectation of further research and development" (*Brana* at 1442-1443, emphasis added). In assessing the question of whether undue experimentation would be required in order to practice the claimed invention, the key term is "undue", not "experimentation". *In re Angstadt and Griffin*, 190 USPQ 214 (CCPA 1976). The need for some experimentation does not render the claimed invention unpatentable. Indeed, a considerable amount of experimentation may be permissible if such experimentation is routinely practiced in the art. *In re Angstadt and Griffin*, *supra*; *Amgen, Inc. v. Chugai Pharmaceutical Co., Ltd.*, 18 USPQ2d 1016 (Fed. Cir. 1991). Again, as a matter of law, it is well settled that a patent need not disclose what is well known in the art (*In re Wands*, *supra*).

Importantly, it has been clearly established that a statement of utility in a specification must be accepted absent reasons why one skilled in the art would have reason to doubt the objective truth of such statement. *In re Langer*, 503 F.2d 1380, 1391, 183 USPQ 288, 297 (CCPA, 1974; "*Langer*"); *In re Marzocchi*, 439 F.2d 220, 224, 169 USPQ 367, 370 (CCPA, 1971). As set forth in *In re Langer* (183 USPQ 288 (CCPA 1974); "*Langer*"):

> As a matter of Patent Office practice, a specification which contains a disclosure of utility which corresponds in scope to the subject matter sought to be patented must be taken as sufficient to satisfy the utility requirement of § 101 for the entire claimed subject matter unless there is a reason for one skilled in the art to question the objective truth of the statement of utility or its scope.

Langer at 297, emphasis in original. As set forth in the MPEP, "Office personnel must provide evidence

sufficient to show that the statement of asserted utility would be considered 'false' by a person of ordinary skill in the art" (MPEP, Eighth Edition at 2100-40, emphasis added). Thus, absent such evidence from the Examiner concerning the use of the presently described polymorphisms in forensic analysis, the present claims clearly meet the requirements of 35 U.S.C. § 101.

Additionally, Appellants pointed out in the Response to the Second Action that a sequence sharing 100% percent identity at the protein level over an extended region of the claimed sequence is present in the leading scientific repository for biological sequence data (GenBank), and has been annotated by third party scientists at the National Center for Biotechnology Information who are *wholly unaffiliated with Appellants* as a "serine protease" (GenBank accession number XM_171629; alignment and GenBank report shown in **Exhibit A**). Appellants further pointed out in the Response to the Final Action that an additional sequence sharing almost 100% percent identity at the amino acid level over an even greater length of the described sequence is present in the leading scientific repository for biological sequence data (GenBank), and has also been annotated by third party scientists *wholly unaffiliated with Appellants* as a "serine protease" (GenBank accession number XM_208689; alignment and GenBank report shown in **Exhibit B**). The legal test for utility simply involves an assessment of whether those skilled in the art would find any of the utilities described for the invention to be credible or believable. Given these two GenBank annotations, there can be no question that those skilled in the art would clearly believe that Appellants' sequence is a serine protease. Thus, the present sequence clearly meets the requirements of 35 U.S.C. § 101.

In the Final Action the Examiner questioned Appellants' assertion that the presently claimed sequence encodes a human serine protease, citing articles by Attwood and Miller (2001, Comput. Chem. 25:329-339) and Ponting (2001, Breif. Bioinform. 2:19-29) in an attempt to support this position. The PTO has repeatedly attempted to deny the utility of nucleic acid sequences based on a small number of spurious publications that call into doubt the usefulness of bioinformatic predictions, of which these two articles are merely the latest examples. Appellants readily agree that there is not 100% consensus within the scientific community regarding prediction of protein function from homology information, and further agree that prediction of protein function from homology information is not 100% accurate. However,

Appellants respectfully point out that the lack of 100% consensus on prediction of protein function from homology information is **completely irrelevant** to the question of whether the claimed nucleic acid sequence has a substantial and specific utility, and that 100% accuracy of prediction of protein function from homology information is **not the standard** for patentability under 35 U.S.C. § 101. Appellants respectfully point out that, as discussed above, the legal test for utility simply involves an assessment of whether those skilled in the art would find any of the utilities described for the invention to be **believable**. Appellants submit that the overwhelming majority of those of skill in the relevant art would **believe** prediction of protein function from homology information and the usefulness of bioinformatic predictions to be powerful and useful tools, as evidenced by hundreds if not thousands of journal articles (which Appellants will submit to the Office if the Board truly doubts Appellants' assertion that the overwhelming majority of those of skill in the art place a high value on prediction of protein function from homology information and the usefulness of bioinformatic predictions), and would thus **believe** that Appellants sequence is a serine protease. As **believability** is the standard for meeting the utility requirement of 35 U.S.C. § 101, and **not** 100% consensus or 100% accuracy, Appellants submit that the present claims must clearly meet the requirements of 35 U.S.C. § 101.

Thus, while Appellants have provided evidence of record that conclusively establishes that those skilled in the art would believe that the specifically claimed sequence encodes a serine protease, the Examiner has provided no evidence that directly establishes that the specifically claimed sequence does not encode a serine protease. Accordingly, the evidence of record compels a finding that the present invention has a patentable utility. Furthermore, the **PTO itself** does not require 100% identity between proteins to establish functional homology. Example 10 of the Revised Interim Utility Guidelines Training Materials, discussed above, only requires a similarity score greater than 95% to establish functional homology. Thus, scientific publications that generally assert that very small changes between amino acid sequences can lead to changes in function, or publications describing specific examples of proteins, distinct from Appellants sequence, where a minor change in amino acid sequence has lead to a change in function, have been viewed by the PTO itself as irrelevant to the question of utility, and thus do not support the Examiner's allegation that the presently claimed sequence lacks utility. Therefore, the present utility rejection must fail

as a matter of policy, as a matter of science, and as a matter of law.

In the Response to the Second Action and the Response to the Final Action, Appellants detailed an additional example of the utility of the present nucleotide sequences, as described in the specification on page 5, lines 9-12, specifically that the present nucleotide sequences have utility in assessing gene expression patterns using high-throughput DNA chips. Such "DNA chips" clearly have utility, as evidenced by hundreds of issued U.S. Patents, as exemplified by U.S. Patent Nos. 5,445,934 (**Exhibit C**), 5,556,752 (**Exhibit D**), 5,744,305 (**Exhibit E**), 5,837,832 (**Exhibit F**), 6,156,501 (**Exhibit G**) and 6,261,776 (**Exhibit H**). Evidence of the "real world" substantial utility of the present invention is further provided by the fact that there is an entire industry established based on the use of gene sequences or fragments thereof in a gene chip format. Perhaps the most notable gene chip company is Affymetrix. However, there are many companies that have, at one time or another, concentrated on the use of gene sequences or fragments, in gene chip and non-gene chip formats, for example: Gene Logic, ABI-Perkin-Elmer, HySeq and Incyte. In addition, one such company (Rosetta Inpharmatics) was viewed to have such "real world" value that it was acquired by large a pharmaceutical company (Merck) for significant sums of money (net equity value of the transaction was $620 million). The "real world" substantial industrial utility of gene sequences or fragments would, therefore, appear to be widespread and well established. Clearly, there can be no doubt that the skilled artisan would know how to use the presently claimed sequences (see Section VIII(B), below), strongly arguing that the claimed sequences have utility. Given the widespread utility of such "gene chip" methods using *public domain* gene sequence information, there can be little doubt that the use of the presently described *novel* sequences would have great utility in such DNA chip applications. As the present sequences are specific markers of the human genome (see below), and such specific markers are targets for the discovery of drugs that are associated with human disease, those of skill in the art would instantly recognize that the present nucleotide sequences would be ideal, novel candidates for assessing gene expression using such DNA chips. Clearly, compositions that enhance the utility of such DNA chips, such as the presently claimed nucleotide sequences, must in themselves be useful. Thus, the present claims clearly meet the requirements of 35 U.S.C. § 101.

The Final Action did not specifically address this assertion of utility, but merely stated that "further

research" is needed "to identify the biological function and possible diseases associated with the [claimed] nucleic acids", and that this "further research" confirms that the claimed sequences do not have a "real world" utility (the Final Action at page 3). Appellants respectfully point out that, with regard to a "real world" usage, as opposed to the nebulous concept of a "real world" usage expressed by the Examiner in the Second Action and the Final Action, nucleic acid sequences similar to those set forth in SEQ ID NO:3 are used throughout the biotechnology industry every day, for example in such gene chip applications. Appellants are completely at a loss to understand how the Examiner can consider the biotechnology industry, an industrial sector that has a market capitalization of hundreds of billions of dollars, not to be a part of the "real world". This argument is also thwarted by the fact that skilled artisans already have used and continue to use sequences such as Appellants in gene chip applications every day, without any further experimentation. Appellants respectfully point out that this is exactly how most gene chip applications are carried out. Expression profiling does **not** require a knowledge of the function of the particular nucleic acid on the chip - rather the gene chip indicates which DNA fragments are expressed at greater or lesser levels in two or more particular tissue types.

The Advisory Action states once again that such uses are "generic utilities that are applicable to any polynucleotide" (Advisory Action at page 2). Appellants first point out that the present sequence, which has been biologically validated to be expressed, has a much greater utility than sequences that are merely predicted to be expressed based on bioinformatic analysis. Second, not "any nucleotide sequence" can be used to track gene expression, but rather, only those small percentage of nucleotide sequences that are expressed can be used in such a manner. Third, the Examiner again seems to be confusing the requirements of a **specific** utility with a **unique** utility (*Carl Zeiss Stiftung v. Renishaw PLC, supra*). The fact that other expressed sequences can be used to track gene expression, or that additional information concerning the presently claimed sequence might make it even more useful in certain gene chip embodiments, does not mean that the use of Appellants' sequence to track gene expression on a gene chip is not a specific utility. Therefore, this argument also fails to support the alleged lack of utility of the presently claimed compositions.

Clearly, persons of skill in the art, as well as venture capitalists and investors, readily recognize the

utility, both scientific and commercial, of genomic data in general, and specifically human genomic data. Billions of dollars have been invested in the human genome project, resulting in useful genomic data (see, *e.g.*, Venter *et al.*, 2001, Science *291*:1304; **Exhibit I**). The results have been a stunning success as the utility of human genomic data has been widely recognized as a great gift to humanity (see, *e.g.*, Jasny and Kennedy, 2001, Science *291*:1153; **Exhibit J**). Clearly, the usefulness of human genomic data, such as the presently claimed nucleic acid molecules, is substantial and credible (worthy of billions of dollars and the creation of numerous companies focused on such information) and well-established (the utility of human genomic information has been clearly understood for many years).

Although Appellants need only make one credible assertion of utility to meet the requirements of 35 U.S.C. § 101 (*Raytheon v. Roper*, 220 USPQ 592 (Fed. Cir. 1983); *In re Gottlieb*, 140 USPQ 665 (CCPA 1964); *In re Malachowski*, 189 USPQ 432 (CCPA 1976); *Hoffman v. Klaus*, 9 USPQ2d 1657 (Bd. Pat. App. & Inter. 1988)), Appellants noted in the Response to the First Action and the Response to the Final Action, as a further example of the utility of the presently claimed polynucleotide, as described in the specification at least at page 10, line 18, the present nucleotide sequence has a specific utility in "determining the genomic structure" of the protein encoding regions of the corresponding human chromosome. This is evidenced by the fact that SEQ ID NO:3 can be used to map the 5 coding exons on chromosome 12 (present within the chromosome 12 clone described in GenBank Accession Number AC008121; the alignment and the first page from the GenBank report are presented in **Exhibit K**). Appellants respectfully remind the Board that only a minor percentage (2-4%) of the genome actually encodes exons, which in-turn encode amino acid sequences. The presently claimed polynucleotide sequence provides biologically validated empirical data (*e.g.*, showing which sequences are transcribed, spliced, and polyadenylated) that *specifically* define that portion of the corresponding genomic locus that actually encodes exon sequence. Equally significant is that the claimed polynucleotide sequence defines how the encoded exons are actually spliced together to produce an active transcript (*i.e.*, the described sequences are useful for functionally defining exon splice-junctions). Such biologically validated splice junctions are superior to splice junctions that may have been predicted from genomic sequence alone, and, as detailed in the specification, at least at page 10, lines 19-24, that "sequences derived from regions

adjacent to the intron/exon boundaries of the human gene can be used to design primers for use in amplification assays to detect mutations within the exons, introns, splice sites (*e.g.*, splice acceptor and/or donor sites), *etc.*, that can be used in diagnostics and pharmacogenomics". Appellants respectfully submit that the practical scientific value of biologically validated, expressed, spliced, and polyadenylated mRNA sequences is readily apparent to those skilled in the relevant biological and biochemical arts.

Clearly, the present polynucleotide provides exquisite specificity in localizing the specific region of human chromosome 12 that contains the gene encoding the given polynucleotide, a utility not shared by virtually any other nucleic acid sequences. In fact, it is this specificity that makes this particular sequence so useful. Early gene mapping techniques relied on methods such as Giemsa staining to identify regions of chromosomes. However, such techniques produced genetic maps with a resolution of only 5 to 10 megabases, far too low to be of much help in identifying specific genes involved in disease. The skilled artisan readily appreciates the significant benefit afforded by markers that map a specific locus of the human genome, such as the present nucleic acid sequence. For further evidence in support of the Appellants' position, the Board is requested to review, for example, section 3 of Venter *et al.* (*supra*, at pp. 1317-1321, including Fig. 11 at pp.1324-1325; **Exhibit I**), which demonstrates the significance of expressed sequence information in the structural analysis of genomic data. The presently claimed polynucleotide sequence defines a biologically validated sequence that provides a unique and specific resource for mapping the genome essentially as described in the Venter *et al.* article. Thus, the present claims clearly meet the requirements of 35 U.S.C. § 101.

The Advisory Action also dismisses this asserted utility, once again stating that such uses are "generic utilities that are applicable to any polynucleotide" (Advisory Action at page 2). Appellants first point out that only those small percentage of nucleotide sequences that are located in this region of chromosome 12 can be used in such a manner. Second, the Examiner again seems to be confusing the requirements of a **specific** utility with a **unique** utility. The fact that a small number of other nucleotide sequences could be used to map the protein coding regions in this specific region of chromosome 12 does not mean that the use of Appellants' sequence to map the protein coding regions of chromosome 12 is not a specific utility (*Carl Zeiss Stiftung v. Renishaw PLC*, *supra*).

Regarding the utility requirements under 35 U.S.C. § 101, the Federal Circuit has clearly stated "(t)he threshold of utility is not high: An invention is 'useful' under section 101 if it is capable of providing some identifiable benefit." *Juicy Whip Inc. v. Orange Bang Inc.*, 185 F.3d 1364, 51 USPQ2d 1700 (Fed. Cir. 1999) (citing *Brenner v. Manson*, 383 U.S. 519, 534 (1966)). Additionally, the Federal Circuit has stated that "(t)o violate § 101 the claimed device must be totally incapable of achieving a useful result." *Brooktree Corp. v. Advanced Micro Devices, Inc.*, 977 F.2d 1555, 1571, 24 USPQ2d 1401 (Fed. Cir. 1992), emphasis added. *Cross v. Iizuka* (753 F.2d 1040, 224 USPQ 739 (Fed. Cir. 1985); "*Cross*") states "any utility of the claimed compounds is sufficient to satisfy 35 U.S.C. § 101". *Cross* at 748, emphasis added. Indeed, the Federal Circuit recently emphatically confirmed that "anything under the sun that is made by man" is patentable *(State Street Bank & Trust Co. v. Signature Financial Group Inc.*, 149 F.3d 1368, 47 USPQ2d 1596, 1600 (Fed. Cir. 1998), citing the U.S. Supreme Court's decision in *Diamond vs. Chakrabarty*, 447 U.S. 303, 206 USPQ 193 (U.S., 1980)). Thus, based on the relevant case law, the present claims clearly meet the requirements of 35 U.S.C. § 101.

Finally, While Appellants are well aware of the new Utility Guidelines set forth by the USPTO, Appellants respectfully point out that the current rules and regulations regarding the examination of patent applications is and always has been the patent laws as set forth in 35 U.S.C. and the patent rules as set forth in 37 C.F.R., not the Manual of Patent Examination Procedure or particular guidelines for patent examination set forth by the USPTO. Furthermore, it is the job of the judiciary, not the USPTO, to interpret these laws and rules. Appellants are unaware of any significant recent changes in either 35 U.S.C. § 101, or in the interpretation of 35 U.S.C. § 101 by the Supreme Court or the Federal Circuit that is in keeping with the new Utility Guidelines set forth by the USPTO. This is underscored by numerous patents that have been issued over the years that claim nucleic acid fragments that do not comply with the new Utility Guidelines. As examples of such issued U.S. Patents, the Board is invited to review U.S. Patent Nos. 5,817,479 (**Exhibit L**), 5,654,173 (**Exhibit M**), and 5,552,281 (**Exhibit N**; each of which claims short polynucleotides), and recently issued U.S. Patent No. 6,340,583 (**Exhibit O**; which includes no working examples), none of which contain examples of the "real-world" utilities that the Examiner seems to be requiring. As issued U.S. Patents are presumed to meet all of the requirements for patentability,

including 35 U.S.C. §§ 101 and 112, first paragraph (see Section VIII(B), below), Appellants submit that the present polynucleotides must also meet the requirements of 35 U.S.C. § 101. While Appellants understand that each application is examined on its own merits, Appellants are unaware of any changes to 35 U.S.C. § 101, or in the interpretation of 35 U.S.C. § 101 by the Supreme Court or the Federal Circuit, since the issuance of these patents that render the subject matter claimed in these patents, which is similar to the subject matter in question in the present application, as suddenly non-statutory or failing to meet the requirements of 35 U.S.C. § 101. Thus, holding Appellants to a different standard of utility would be arbitrary and capricious, and, like other clear violations of due process, cannot stand.

For each of the foregoing reasons, Appellants submit that the rejection of claims 1, 2 and 5-10 under 35 U.S.C. § 101 must be overruled.

B. Are Claims 1, 2 and 5-10 Unusable Due to a Lack of Patentable Utility?

The Final Action next rejects claims 1, 2 and 5-10 under 35 U.S.C. § 112, first paragraph, since allegedly one skilled in the art would not know how to use the invention, as the invention allegedly is not supported by either a clear asserted utility or a well-established utility.

The arguments detailed above in Section VIII(A) concerning the utility of the presently claimed sequences are incorporated herein by reference. As the Federal Circuit and its predecessor have determined that the utility requirement of Section 101 and the how to use requirement of Section 112, first paragraph, have the same basis, specifically the disclosure of a credible utility (*In re Brana*, *supra*; *In re Jolles*, 628 F.2d 1322, 1326 n.11, 206 USPQ 885, 889 n.11 (CCPA 1980); *In re Fouche*, 439 F.2d 1237, 1243, 169 USPQ 429, 434 (CCPA 1971)), Appellants submit that as claims 1, 2 and 5-10 have been shown to have "a specific, substantial, and credible utility", as detailed in Section VIII(A) above, the present rejection of claims 1, 2 and 5-10 under 35 U.S.C. § 112, first paragraph, cannot stand.

Appellants therefore submit that the rejection of claims 1, 2 and 5-10 under 35 U.S.C. § 112, first paragraph, must be overruled.

C. Do Claims 1 and 7-10 Lack Sufficient Written Description?

The Final Action next rejected claims 1 and 7-10 under 35 U.S.C. § 112, first paragraph, as allegedly containing subject matter that was not described in the specification in such a way as to reasonably convey to one skilled in the relevant art that the inventors, at the time the application was filed, had possession of the claimed invention.

The Examiner states that the present claims lack sufficient written description support because "the claims encompass any polynucleotide of any biological function" (the Advisory Action at page 2). Appellants respectfully point out that there is **no requirement whatsoever** that novel fragments of a novel sequence have the **exact same function** as the full length sequence in order to be patented. If this were to be the case, hundreds, if not thousands, of issued U.S. Patents would be instantly invalidated, as they each claim nucleotide fragments that have not been demonstrated to have the exact same function as the full length nucleotide sequence. Appellants therefore submit that the claimed sequence meets the written description requirement of 35 U.S.C. § 112, first paragraph.

As set forth by Appellants in the Response to the First Action, the Response to the Second Action, and the Response to the Final Action, 35 U.S.C. § 112, first paragraph, requires that the specification contain a written description of the invention. The Federal Circuit in *Vas-Cath Inc. v. Mahurkar* (19 USPQ2d 1111 (Fed. Cir. 1991); "*Vas-Cath*") held that an "applicant must convey with reasonable clarity to those skilled in the art that, as of the filing date sought, he or she was in possession *of the invention*." *Vas-Cath*, at 1117, emphasis in original. However, it is important to note that the above finding uses the terms reasonable clarity to those skilled in the art. Further, the Federal Circuit in *In re Gosteli* (10 USPQ2d 1614 (Fed. Cir. 1989); "*Gosteli*") held:

> Although [the applicant] does not have to describe exactly the subject matter claimed, . . . the description must clearly allow persons of ordinary skill in the art to recognize that [he or she] invented what is claimed.

Gosteli at 1618, emphasis added. Additionally, *Utter v. Hiraga* (6 USPQ2d 1709 (Fed. Cir. 1988); "*Utter*"), held "(a) specification may, within the meaning of 35 U.S.C. § 112 ¶1, contain a written description of a broadly claimed invention without describing all species that claim encompasses" (*Utter*, at 1714). Therefore, all Appellants must do to comply with 35 U.S.C. § 112, first paragraph, is to convey

the invention with reasonable clarity to the skilled artisan.

Further, the Federal Circuit has held that an adequate description of a chemical genus "requires a precise definition, such as by structure, formula, chemical name or physical properties" sufficient to distinguish the genus from other materials. *Fiers v. Revel*, 25 USPQ2d 1601, 1606 (Fed. Cir. 1993; "*Fiers*"). *Fiers* goes on to hold that the "application satisfies the written description requirement since it sets forth the . . . nucleotide sequence" (*Fiers* at 1607). In other words, provision of a structure and formula - the nucleotide sequence - renders the application in compliance with 35 U.S.C. § 112, first paragraph.

More recently, the standard for complying with the written description requirement in claims involving chemical materials has been explicitly set forth by the Federal Circuit:

> In claims involving chemical materials, generic formulae usually indicate with specificity what the generic claims encompass. One skilled in the art can distinguish such a formula from others and can identify many of the species that the claims encompass. Accordingly, such a formula is normally an adequate description of the claimed genus. *Regents of Univ. of California v. Eli Lilly and Co.*, 43 USPQ2d 1398, 1406 (Fed. Cir. 1997).

Thus, a claim describing a genus of nucleic acids by structure, formula, chemical name or physical properties sufficient to allow one of ordinary skill in the art to distinguish the genus from other materials meets the written description requirement of 35 U.S.C. § 112, first paragraph. As further elaborated by the Federal Circuit in *Regents of Univ. of California v. Eli Lilly and Co.*:

> In claims to genetic material ... a generic statement such as 'vertebrate insulin cDNA' or 'mammalian insulin cDNA', without more, is not an adequate written description of the genus because it does not distinguish the claimed genus from others, except by function. It does not specifically define any of the genes that fall within its definition. It does not define any structural features commonly possessed by members of the genus that distinguish them from others. One skilled in the art cannot, as one can do with a fully described genus, visualize or recognize the identity of members of the genus. (Emphasis added)

Thus, as opposed to the situation set forth in *Regents of Univ. of California v. Eli Lilly and Co.* and *Fiers*, the nucleic acid sequences of the present invention are not distinguished on the basis of function, or a method of isolation, but in fact are distinguished by structural features - a chemical formula, *i.e.*, the *sequence itself*

Using the nucleic acid sequences of the present invention (as set forth in the Sequence Listing), the skilled artisan would readily be able to **distinguish** the claimed nucleic acids from other materials on the basis of the specific **structural** description provided. Polynucleotides comprising at least 60 contiguous bases from SEQ ID NO:3 are within the genus of the instant claims, while those that lack this structural feature lie outside the genus. The claimed genus of polynucleotides is clearly defined in structural terms, which is **all that is required** of claims 1 and 7-10 to meet the written description requirement of 35 U.S.C. § 112, first paragraph.

For each of the foregoing reasons, Appellants submit that the rejection of claims 1 and 7-10 under 35 U.S.C. § 112, first paragraph, must be overruled.

IX. APPENDIX

The claims involved in this appeal are as follows:

1. (Twice Amended) An isolated nucleic acid molecule comprising at least 60 contiguous nucleotides from SEQ ID NO:3.

2. (Twice Amended) An isolated nucleic acid molecule comprising a nucleotide sequence that:

(a) encodes the amino acid sequence shown in SEQ ID NO: 4; and

(b) hybridizes to the nucleotide sequence of SEQ ID NO:3 or the complement thereof under highly stringent conditions of 0.5 M $NaHPO_4$, 7% sodium dodecyl sulfate (SDS) and 1 mM EDTA at 65°C and washing in 0.1x SSC/0.1%SDS at 68°C.

5. The isolated nucleic acid molecule of claim 1, wherein said isolated nucleic acid molecule comprises the nucleotide sequence of SEQ ID NO:3.

6. An isolated nucleic acid molecule comprising a nucleotide sequence that encodes the amino acid sequence shown in SEQ ID NO:4.

7. A recombinant expression vector comprising the isolated nucleic acid molecule of claim 1.

8. The recombinant expression vector of claim 7, wherein said isolated nucleic acid molecule comprises a nucleotide sequence that encodes the amino acid sequence shown in SEQ ID NO:4.

9. The recombinant expression vector of claim 8, wherein said isolated nucleic acid molecule comprises the nucleotide sequence of SEQ ID NO:3.

10. A host cell comprising the recombinant expression vector of claim 7.

X. CONCLUSION

Appellants respectfully submit that, in light of the foregoing arguments, the Final Action's conclusion that claims 1, 2 and 5-10 lack a patentable utility and are unusable by the skilled artisan due to a lack of patentable utility, and that claims 1 and 7-10 are not enabled and lack sufficient written description, is unwarranted. It is therefore requested that the Board overturn the Final Action's rejections.

Respectfully submitted,

September 9, 2003
Date

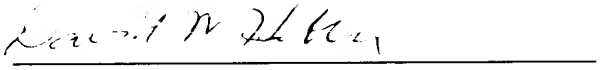

David W. Hibler Reg. No. 41,071
Agent For Appellants

LEXICON GENETICS INCORPORATED
8800 Technology Forest Place
The Woodlands, TX 77381
(281) 863-3399

Customer # 24231

TABLE OF AUTHORITIES

CASES

STATUTES

The Sequence of the Human Genome

J. Craig Venter,[1*] Mark D. Adams,[1] Eugene W. Myers,[1] Peter W. Li,[1] Richard J. Mural,[1] Granger G. Sutton,[1] Hamilton O. Smith,[1] Mark Yandell,[1] Cheryl A. Evans,[1] Robert A. Holt,[1] Jeannine D. Gocayne,[1] Peter Amanatides,[1] Richard M. Ballew,[1] Daniel H. Huson,[1] Jennifer Russo Wortman,[1] Qing Zhang,[1] Chinnappa D. Kodira,[1] Xiangqun H. Zheng,[1] Lin Chen,[1] Marian Skupski,[1] Gangadharan Subramanian,[1] Paul D. Thomas,[1] Jinghui Zhang,[1] George L. Gabor Miklos,[2] Catherine Nelson,[3] Samuel Broder,[1] Andrew G. Clark,[4] Joe Nadeau,[5] Victor A. McKusick,[6] Norton Zinder,[7] Arnold J. Levine,[7] Richard J. Roberts,[8] Mel Simon,[9] Carolyn Slayman,[10] Michael Hunkapiller,[11] Randall Bolanos,[1] Arthur Delcher,[1] Ian Dew,[1] Daniel Fasulo,[1] Michael Flanigan,[1] Liliana Florea,[1] Aaron Halpern,[1] Sridhar Hannenhalli,[1] Saul Kravitz,[1] Samuel Levy,[1] Clark Mobarry,[1] Knut Reinert,[1] Karin Remington,[1] Jane Abu-Threideh,[1] Ellen Beasley,[1] Kendra Biddick,[1] Vivien Bonazzi,[1] Rhonda Brandon,[1] Michele Cargill,[1] Ishwar Chandramouliswaran,[1] Rosane Charlab,[1] Kabir Chaturvedi,[1] Zuoming Deng,[1] Valentina Di Francesco,[1] Patrick Dunn,[1] Karen Eilbeck,[1] Carlos Evangelista,[1] Andrei E. Gabrielian,[1] Weiniu Gan,[1] Wangmao Ge,[1] Fangcheng Gong,[1] Zhiping Gu,[1] Ping Guan,[1] Thomas J. Heiman,[1] Maureen E. Higgins,[1] Rui-Ru Ji,[1] Zhaoxi Ke,[1] Karen A. Ketchum,[1] Zhongwu Lai,[1] Yiding Lei,[1] Zhenya Li,[1] Jiayin Li,[1] Yong Liang,[1] Xiaoying Lin,[1] Fu Lu,[1] Gennady V. Merkulov,[1] Natalia Milshina,[1] Helen M. Moore,[1] Ashwinikumar K Naik,[1] Vaibhav A. Narayan,[1] Beena Neelam,[1] Deborah Nusskern,[1] Douglas B. Rusch,[1] Steven Salzberg,[12] Wei Shao,[1] Bixiong Shue,[1] Jingtao Sun,[1] Zhen Yuan Wang,[1] Aihui Wang,[1] Xin Wang,[1] Jian Wang,[1] Ming-Hui Wei,[1] Ron Wides,[13] Chunlin Xiao,[1] Chunhua Yan,[1] Alison Yao,[1] Jane Ye,[1] Ming Zhan,[1] Weiqing Zhang,[1] Hongyu Zhang,[1] Qi Zhao,[1] Liansheng Zheng,[1] Fei Zhong,[1] Wenyan Zhong,[1] Shiaoping C. Zhu,[1] Shaying Zhao,[12] Dennis Gilbert,[1] Suzanna Baumhueter,[1] Gene Spier,[1] Christine Carter,[1] Anibal Cravchik,[1] Trevor Woodage,[1] Feroze Ali,[1] Huijin An,[1] Aderonke Awe,[1] Danita Baldwin,[1] Holly Baden,[1] Mary Barnstead,[1] Ian Barrow,[1] Karen Beeson,[1] Dana Busam,[1] Amy Carver,[1] Angela Center,[1] Ming Lai Cheng,[1] Liz Curry,[1] Steve Danaher,[1] Lionel Davenport,[1] Raymond Desilets,[1] Susanne Dietz,[1] Kristina Dodson,[1] Lisa Doup,[1] Steven Ferriera,[1] Neha Garg,[1] Andres Gluecksmann,[1] Brit Hart,[1] Jason Haynes,[1] Charles Haynes,[1] Cheryl Heiner,[1] Suzanne Hladun,[1] Damon Hostin,[1] Jarrett Houck,[1] Timothy Howland,[1] Chinyere Ibegwam,[1] Jeffery Johnson,[1] Francis Kalush,[1] Lesley Kline,[1] Shashi Koduru,[1] Amy Love,[1] Felecia Mann,[1] David May,[1] Steven McCawley,[1] Tina McIntosh,[1] Ivy McMullen,[1] Mee Moy,[1] Linda Moy,[1] Brian Murphy,[1] Keith Nelson,[1] Cynthia Pfannkoch,[1] Eric Pratts,[1] Vinita Puri,[1] Hina Qureshi,[1] Matthew Reardon,[1] Robert Rodriguez,[1] Yu-Hui Rogers,[1] Deanna Romblad,[1] Bob Ruhfel,[1] Richard Scott,[1] Cynthia Sitter,[1] Michelle Smallwood,[1] Erin Stewart,[1] Renee Strong,[1] Ellen Suh,[1] Reginald Thomas,[1] Ni Ni Tint,[1] Sukyee Tse,[1] Claire Vech,[1] Gary Wang,[1] Jeremy Wetter,[1] Sherita Williams,[1] Monica Williams,[1] Sandra Windsor,[1] Emily Winn-Deen,[1] Keriellen Wolfe,[1] Jayshree Zaveri,[1] Karena Zaveri,[1] Josep F. Abril,[14] Roderic Guigó,[14] Michael J. Campbell,[1] Kimmen V. Sjolander,[1] Brian Karlak,[1] Anish Kejariwal,[1] Huaiyu Mi,[1] Betty Lazareva,[1] Thomas Hatton,[1] Apurva Narechania,[1] Karen Diemer,[1] Anushya Muruganujan,[1] Nan Guo,[1] Shinji Sato,[1] Vineet Bafna,[1] Sorin Istrail,[1] Ross Lippert,[1] Russell Schwartz,[1] Brian Walenz,[1] Shibu Yooseph,[1] David Allen,[1] Anand Basu,[1] James Baxendale,[1] Louis Blick,[1] Marcelo Caminha,[1] John Carnes-Stine,[1] Parris Caulk,[1] Yen-Hui Chiang,[1] My Coyne,[1] Carl Dahlke,[1] Anne Deslattes Mays,[1] Maria Dombroski,[1] Michael Donnelly,[1] Dale Ely,[1] Shiva Esparham,[1] Carl Fosler,[1] Harold Gire,[1] Stephen Glanowski,[1] Kenneth Glasser,[1] Anna Glodek,[1] Mark Gorokhov,[1] Ken Graham,[1] Barry Gropman,[1] Michael Harris,[1] Jeremy Heil,[1] Scott Henderson,[1] Jeffrey Hoover,[1] Donald Jennings,[1] Catherine Jordan,[1] James Jordan,[1] John Kasha,[1] Leonid Kagan,[1] Cheryl Kraft,[1] Alexander Levitsky,[1] Mark Lewis,[1] Xiangjun Liu,[1] John Lopez,[1] Daniel Ma,[1] William Majoros,[1] [illegible] McDaniel, [illegible]ean Murphy, Matthew Newman, [illegible]ung Nguyen, [illegible]ngo Nguyen, [illegible] Nguyen, [illegible]ue Pan, [illegible]m Peck, Marshall Peterson, William Rowe, Robert Sanders, John Scott, Michael Simpson,[1] Thomas Smith,[1] Arlan Sprague,[1] Timothy Stockwell,[1] Russell Turner,[1] Eli Venter,[1] Mei Wang,[1] Meiyuan Wen,[1] David Wu,[1] Mitchell Wu,[1] Ashley Xia,[1] Ali Zandieh,[1] Xiaohong Zhu[1]

A 2.91-billion base pair (bp) consensus sequence of the euchromatic portion of the human genome was generated by the whole-genome shotgun sequencing method. The 14.8-billion bp DNA sequence was generated over 9 months from 27,271,853 high-quality sequence reads (5.11-fold coverage of the genome) from both ends of plasmid clones made from the DNA of five individuals. Two assembly strategies—a whole-genome assembly and a regional chromosome assembly—were used [illegible] publicly funded genome effort. The public data were shredded into 550-bp segments to create a 2.9-fold coverage of those genome regions that had been sequenced, without including biases inherent in the cloning and assembly procedure used by the publicly funded group. This brought the effective coverage in the assemblies to eightfold, reducing the number and size of gaps in the final assembly over what would be obtained with 5.11-fold coverage. The two assembly strategies yielded very similar results that largely agree with independent mapping data. The assemblies effectively cover the euchromatic regions of the human chromosomes. More than 90% of the genome is in scaffold assemblies of 100,000 bp or more, and 25% of the genome is in scaffolds of 10 million bp or larger. Analysis of the genome sequence revealed 26,588 protein-encoding transcripts for which there was strong corroborating evidence and an additional ~12,000 computationally derived genes with mouse matches or other weak supporting evidence. Although gene-dense clusters are obvious, almost half the genes are dispersed in low G+C sequence separated by large tracts of apparently noncoding sequence. Only 1.1% of the genome is spanned by exons, whereas 24% is in introns, with 75% of the genome being intergenic DNA. Duplications of segmental blocks, ranging in size up to chromosomal lengths, are abundant throughout the genome and reveal a complex evolutionary history. Comparative genomic analysis indicates vertebrate expansions of genes associated with neuronal function, with tissue-specific developmental regulation, and with the hemostasis and immune systems. DNA sequence comparisons between the consensus sequence and publicly funded genome data provided locations of 2.1 million single-nucleotide polymorphisms (SNPs). A random pair of human haploid genomes differed at a rate of 1 bp per 1250 on average, but there was marked heterogeneity in the level of polymorphism across the genome. Less than 1% of all SNPs resulted in variation in proteins, but the task of determining which SNPs have functional consequences remains an open challenge.

Decoding of the DNA that constitutes the human genome has been widely anticipated for the contribution it will make toward understanding human evolution, the causation of disease, and the interplay between the environment and heredity in defining the human condition. A project with the goal of determining the complete nucleotide sequence of the human genome was first formally proposed in 1985 (*1*). In subsequent years, the idea met with mixed reactions in the scientific community (*2*). However, in 1990, the Human Genome Project (HGP) was officially initiated in the United States under the direction of the National Institutes of Health and the U.S. Department of Energy with a 15-year, $3 billion plan for completing the genome sequence. In 1998 we announced our intention to build a unique genome-sequencing facility, to determine the sequence of the human genome over a 3-year period. Here we report the penultimate milestone along the path toward that goal, a nearly complete sequence of the euchromatic portion of the human genome. The sequencing was performed by a whole-genome random shotgun method with subsequent assembly of the sequenced segments.

The modern history of DNA sequencing [illegible] DNA using chain-terminating nucleotide analogs (*3*). In the same year, the first human gene was isolated and sequenced (*4*). In 1986, Hood and co-workers (*5*) described an improvement in the Sanger sequencing method that included attaching fluorescent dyes to the nucleotides, which permitted them to be sequentially read by a computer. The first automated DNA sequencer, developed by Applied Biosystems in California in 1987, was shown to be successful when the sequences of two genes were obtained with this new technology (*6*). From early sequencing of human genomic regions (*7*), it became clear that cDNA sequences (which are reverse-transcribed from RNA) would be essential to annotate and validate gene predictions in the human genome. These studies were the basis in part for the development of the expressed sequence tag (EST) method of gene identification (*8*), which is a random selection, very high throughput sequencing approach to characterize cDNA libraries. The EST method led to the rapid discovery and mapping of human genes (*9*). The increasing numbers of human EST sequences necessitated the development of new computer algorithms to analyze large amounts of sequence data, and in 1993 at The Institute for Genomic Research (TIGR), an algorithm was developed that permitted assembly and analysis of hundreds of thousands of ESTs. This algorithm permitted characterization and annotation of human genes on the basis of 30,000 EST assemblies (*10*).

The complete 49-kbp bacteriophage lambda genome sequence was determined by a shotgun restriction digest method in 1982 (*11*). When considering methods for sequencing the smallpox virus genome in 1991 (*12*), a whole-genome shotgun sequencing method was discussed and subsequently rejected owing to the lack of appropriate software tools for genome assembly. However, in 1994, when a microbial genome-sequencing project was contemplated at TIGR, a whole-genome shotgun sequencing approach was considered possible with the TIGR EST assembly algorithm. In 1995, the 1.8-Mbp *Haemophilus influenzae* genome was completed by a whole-genome shotgun sequencing method (*13*). The experience with several subsequent genome-sequencing efforts established the broad applicability of this approach (*14*, *15*).

A key feature of the sequencing approach used for these megabase-size and larger genomes was the use of paired-end sequences (also called mate pairs), derived from subclone libraries with distinct insert sizes and cloning characteristics. Paired-end sequences are sequences 500 to 600 bp in length from both ends of double-stranded DNA clones of prescribed lengths. The success of using end sequences from long segments (18 to 20 kbp) of DNA cloned into bacteriophage lambda in [illegible] bacterial genomes led to the

[1]Celera Genomics, 45 West Gude Drive, Rockville, MD 20850, USA. [2]GenetixXpress, 78 Pacific Road, Palm Beach, Sydney 2108, Australia. [3]Berkeley *Drosophila* Genome Project, University of California, Berkeley, CA 94720, USA. [4]Department of Biology, Penn State University, 208 Mueller Lab, University Park, PA 16802, USA. [5]Department of Genetics, Case Western Reserve University School of Medicine, BRB-630, 10900 Euclid Avenue, Cleveland, OH 44106, USA. [6]Johns Hopkins University School of Medicine, Johns Hopkins Hospital, 600 North Wolfe Street, Blalock 1007, Baltimore, MD 21287–4922, USA. [7]Rockefeller University, 1230 York Avenue, New York, NY 10021–6399, USA. [8]New England BioLabs, 32 Tozer Road, Beverly, MA 01915, USA. [9]Division of Biology, 147-75, California Institute of Technology, 1200 East California Boulevard, Pasadena, CA 91125, USA. [10]Yale University School of Medicine, 333 Cedar Street, P.O. Box 208000, New Haven, CT 06520–8000, USA. [11]Applied Biosystems, 850 Lincoln Centre Drive, Foster City, CA 94404, USA. [12]The Institute for Genomic Research, 9712 Medical Center Drive, Rockville, MD 20850, USA. [13]Faculty of Life Sciences, Bar-Ilan University, Ramat-Gan, 52900 Israel. [14]Grup de Recerca en Informàtica Mèdica, Institut Municipal d'Investigació Mèdica, Universitat [illegible] 08003 Barcelona, Catalonia, Spain.

neously map and sequence the human genome by means of end sequences from 150-kbp bacterial artificial chromosomes (BACs) (*17*, *18*). The end sequences spanned by known distances provide long-range continuity across the genome. A modification of the BAC end-sequencing (BES) method was applied successfully to complete chromosome 2 from the *Arabidopsis thaliana* genome (*19*).

In 1997, Weber and Myers (*20*) proposed whole-genome shotgun sequencing of the human genome. Their proposal was not well received (*21*). However, by early 1998, as less than 5% of the genome had been sequenced, it was clear that the rate of progress in human genome sequencing worldwide was very slow (*22*), and the prospects for finishing the genome by the 2005 goal were uncertain.

In early 1998, PE Biosystems (now Applied Biosystems) developed an automated, high-throughput capillary DNA sequencer, subsequently called the ABI PRISM 3700 DNA Analyzer. Discussions between PE Biosystems and TIGR scientists resulted in a plan to undertake the sequencing of the human genome with the 3700 DNA Analyzer and the whole-genome shotgun sequencing techniques developed at TIGR (*23*). Many of the principles of operation of a genome-sequencing facility were established in the TIGR facility (*24*). However, the facility envisioned for Celera would have a capacity roughly 50 times that of TIGR, and thus new developments were required for sample preparation and tracking and for whole-genome assembly. Some argued that the required 150-fold scale-up from the *H. influenzae* genome to the human genome with its complex repeat sequences was not feasible (*25*). The *Drosophila melanogaster* genome was thus chosen as a test case for whole-genome assembly on a large and complex eukaryotic genome. In collaboration with Gerald Rubin and the Berkeley *Drosophila* Genome Project, the nucleotide sequence of the 120-Mbp euchromatic portion of the *Drosophila* genome was determined over a 1-year period (*26*–*28*). The *Drosophila* genome-sequencing effort resulted in two key findings: (i) that the assembly algorithms could generate chromosome assemblies with highly accurate order and orientation with substantially less than 10-fold coverage, and (ii) that undertaking multiple interim assemblies in place of one comprehensive final assembly was not of value.

These findings, together with the dramatic changes in the public genome effort subsequent to the formation of Celera (*29*), led to a modi-

genome over a 3-year period and to make interim assembled sequence data available quarterly. The modifications included a plan to perform random shotgun sequencing to ~5-fold coverage and to use the unordered and unoriented BAC sequence fragments and chromosomes published in GenBank by the publicly funded genome effort (*30*) to accelerate the project. We also abandoned the quarterly announcements in the absence of interim assemblies to report.

Although this strategy provided a reasonable result very early that was consistent with a whole-genome shotgun assembly with eight-fold coverage, the human genome sequence is not as finished as the *Drosophila* genome was with an effective 13-fold coverage. However, it became clear that even with this reduced coverage strategy, Celera could generate an accurately ordered and oriented scaffold sequence of the human genome in less than 1 year. Human genome sequencing was initiated 8 September 1999 and completed 17 June 2000. The first assembly was completed 25 June 2000, and the assembly reported here was completed 1 October 2000. Here we describe the whole-genome random shotgun sequencing effort applied to the human genome. We developed two different assembly approaches for assembling the ~3 billion bp that make up the 23 pairs of chromosomes of the *Homo sapiens* genome. Any GenBank-derived data were shredded to remove potential bias to the final sequence from chimeric clones, foreign DNA contamination, or misassembled contigs. Insofar as a correctly and accurately assembled genome sequence with faithful order and orientation of contigs is essential for an accurate analysis of the human genetic code, we have devoted a considerable portion of this manuscript to the documentation of the quality of our reconstruction of the genome. We also describe our preliminary analysis of the human genetic code on the basis of computational methods. Figure 1 (see fold-out chart associated with this issue; files for each chromosome can be found in Web fig. 1 on *Science* Online at www.sciencemag.org/cgi/content/full/291/5507/1304/DC1) provides a graphical overview of the genome and the features encoded in it. The detailed manual curation and interpretation of the genome are just beginning.

To aid the reader in locating specific analytical sections, we have divided the paper into seven broad sections. A summary of the major results appears at the beginning of each section.

1 Sources of DNA and Sequencing Methods

Summary. This section discusses the rationale and ethical rules governing donor selection to ensure ethnic and gender diversity along with the methodologies for DNA extraction and library construction. The plasmid library construction is the first critical step in shotgun sequencing. If the DNA libraries are not uniform in size, nonchimeric, and do not randomly represent the genome, then the subsequent steps cannot accurately reconstruct the genome sequence. We used automated high-throughput DNA sequencing and the computational infrastructure to enable efficient tracking of enormous amounts of sequence information (27.3 million sequence reads; 14.9 billion bp of sequence). Sequencing and tracking from both ends of plasmid clones from 2-, 10-, and 50-kbp libraries were essential to the computational reconstruction of the genome. Our evidence indicates that the accurate pairing rate of end sequences was greater than 98%.

Various policies of the United States and the World Medical Association, specifically the Declaration of Helsinki, offer recommendations for conducting experiments with human subjects. We convened an Institutional Review Board (IRB) (*31*) that helped us establish the protocol for obtaining and using human DNA and the informed consent process used to enroll research volunteers for the DNA-sequencing studies reported here. We adopted several steps and procedures to protect the privacy rights and confidentiality of the research subjects (donors). These included a two-stage consent process, a secure random alphanumeric coding system for specimens and records, circumscribed contact with the subjects by researchers, and options for off-site contact of donors. In addition, Celera applied for and received a Certificate of Confidentiality from the Department of Health and Human Services. This Certificate authorized Celera to protect the privacy of the individuals who volunteered to be donors as provided in Section 301(d) of the Public Health Service Act 42 U.S.C. 241(d).

Celera and the IRB believed that the initial version of a completed human genome should be a composite derived from multiple donors of diverse ethnic backgrounds Prospective donors were asked, on a voluntary basis, to self-designate an ethnogeographic category (e.g., African-American, Chinese, Hispanic, Caucasian, etc.). We enrolled 21 donors (*32*).

... and self-designated ethnogeographic group. From females, ~130 ml of whole, heparinized blood was collected. From males, ~130 ml of whole, heparinized blood was

nome, and even a modest error rate can affect the ordering of clones and the assembly of genomic sequence. In addition, maintaining the validity of mate-pair information is absolutely critical for the algorithms described below. Procedural controls were established for maintaining the validity of sequence mate-pairs as sequencing reactions proceeded through the process, including strict rules built into the LIMS. The accuracy of sequence data produced by the Celera process was validated in the course of the *Drosophila* genome project (*26*). By collecting data for the entire human genome in a single facility, standards and the cost advantages associated with automation, an economy of scale, and process consistency.

2 Genome Assembly Strategy and Characterization

Summary. We describe in this section the two approaches that we used to assemble the genome. One method involves the computational combination of all sequence reads with shredded data from GenBank to generate an independent, nonbiased view of the genome. The second method provided slightly greater sequence coverage (fewer gaps) and was the principal sequence used for the analysis phase. In addition, we document the completeness and correctness of this assembly process

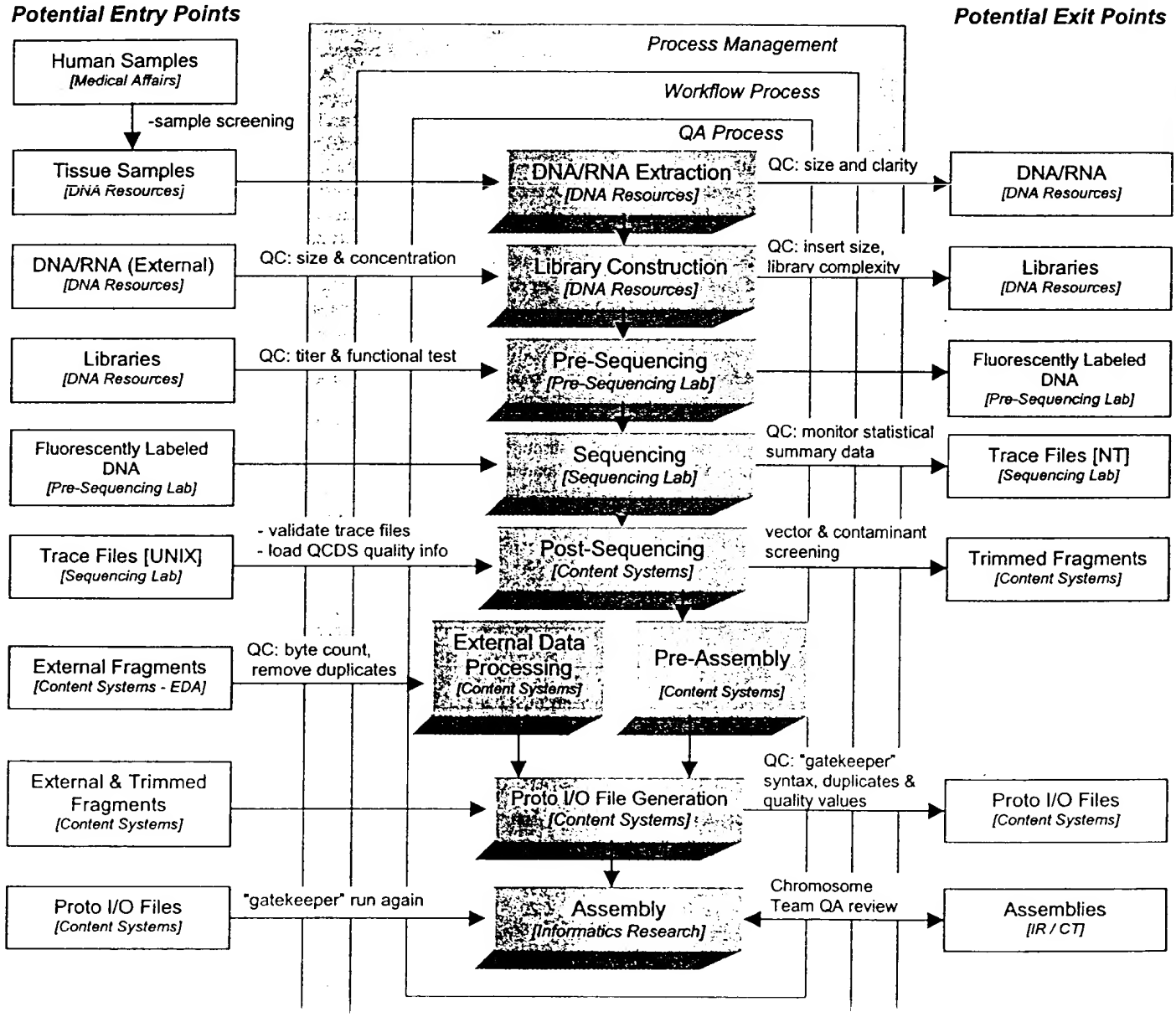

Fig. 2. Flow diagram for sequencing pipeline. Samples are received, selected, and processed in compliance with standard operating procedures, with a focus on quality within and across departments. Each process has defined inputs and outputs with the capability to exchange samples and data with both internal and external entities according to defined quality guidelines. Manufacturing pipeline processes, products, quality control measures, and responsible parties are indicated and are described further in the text.

and provide a comparison to the public gen sequence, which was reconstructed largely an independent BAC-by-BAC approach. Our assemblies effectively covered the euchromatic regions of the human chromosomes. More than 90% of the genome was in scaffold assemblies of 100,000 bp or greater, and 25% of the ge- larger.

Shotgun sequence assembly is a classic example of an inverse problem: given a set of reads randomly sampled from a target sequence, reconstruct the order and the position of those reads in the target. Genome assembly algorithms developed for *Drosophila* have now been extended to assemble the ~25-fold larger human genome. Celera assemblies consist of a set of contigs that are ordered and oriented into scaffolds that are then mapped to chromosomal locations by using known markers. The contigs consist of a collection of overlapping sequence reads that provide a consensus reconstruction for a contiguous interval of the genome. Mate pairs are a central component of the assembly strategy. They are used to produce scaffolds in which the size of gaps between consecutive contigs is known with reasonable precision. This is accomplished by observing that a pair of reads, one of which is in one contig, and the other of which is in another, implies an orientation and distance between the two contigs (Fig. 3). Finally, our assemblies did not incorporate all reads into the final set of reported scaffolds. This set of unincorporated reads is termed "chaff," and typically consisted of reads from within highly repetitive regions, data from other organisms introduced through various routes as found in many genome projects, and data of poor quality or with untrimmed vector.

2.1 Assembly data sets

We used two independent sets of data for our assemblies. The first was a random shotgun data set of 27.27 million reads of average length 543 bp produced at Celera. This consisted largely of mate-pair reads from 16 libraries constructed from DNA samples taken from five

10, and 50 kbp were used. By looking at how mate pairs from a library were positioned in known sequenced stretches of the genome, we were able to characterize the range of insert sizes in each library and determine a mean and standard deviation. Table 1 details the number of reads, sequencing coverage, and clone coverage achieved by the data set. The clone coverage is the coverage of the genome in cloned DNA, considering the entire insert of each clone that has sequence from both ends. The clone coverage provides a measure of the amount of physical DNA coverage of the genome. Assuming a genome size of 2.9 Gbp, the Celera trimmed sequences gave a 5.1× coverage of the genome, and clone coverage was 3.42×, 16.40×, and 18.84× for the 2-, 10-, and 50-kbp libraries, respectively, for a total of 38.7× clone coverage.

The second data set was from the publicly funded Human Genome Project (PFP) and is primarily derived from BAC clones (*30*). The BAC data input to the assemblies came from a download of GenBank on 1 September 2000 (Table 2) totaling 4443.3 Mbp of sequence. The data for each BAC is deposited at one of four levels of completion. Phase 0 data are a set of generally unassembled sequencing reads from a very light shotgun of the BAC, typically less than 1×. Phase 1 data are unordered assemblies of contigs, which we call BAC contigs or bactigs. Phase 2 data are ordered assemblies of bactigs. Phase 3 data are complete BAC

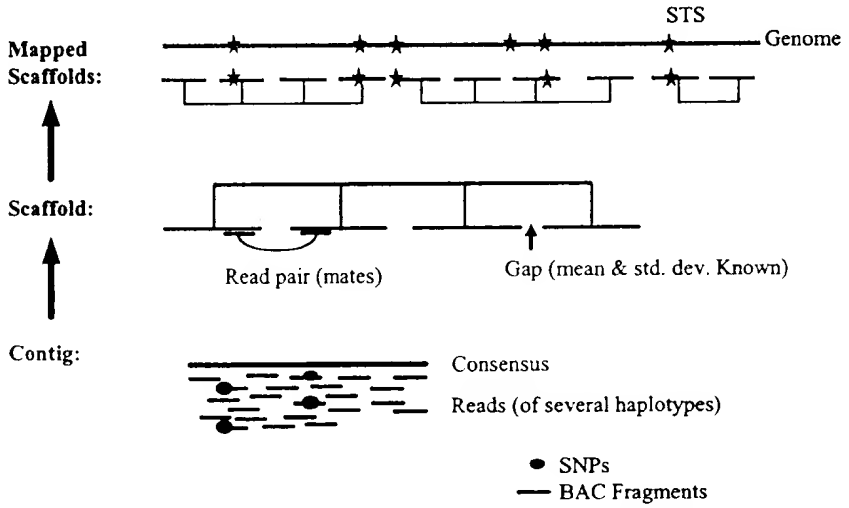

Fig. 3. Anatomy of whole-genome assembly. Overlapping shredded bactig fragments (red lines) and internally derived reads from five different individuals (black lines) are combined to produce a contig and a consensus sequence (green line). Contigs are connected into scaffolds (red) by using

uences. In the past 2 years the PFP has focused on a product of lower quality and completeness, but on a faster time-course, by concentrating on the production of Phase 1 data from a 3× to 4× light-shotgun of each BAC clone.

We screened the bactig sequences for con-

against three data sets: (i) vector sequences in Univec core (*38*), filtered for a 25-bp match at 98% sequence identity at the ends of the sequence and a 30-bp match internal to the sequence; (ii) the nonhuman portion of the High Throughput Genomic (HTG) Seqences division of GenBank (*39*), filtered at 200 bp at 98%; and (iii) the nonredundant nucleotide sequences from GenBank without primate and human virus entries, filtered at 200 bp at 98%. Whenever 25 bp or more of vector was found within 50 bp of the end of a contig, the tip up to the matching vector was excised. Under these criteria we removed 2.6 Mbp of possible contaminant and vector from the Phase 3 data, 61.0 Mbp from the Phase 1 and 2 data, and 16.1 Mbp from the Phase 0 data (Table 2). This left us with a total of 4363.7 Mbp of PFP sequence data 20% finished, 75% rough-draft (Phase 1 and 2), and 5% single sequencing reads (Phase 0). An additional 104,018 BAC end-sequence mate pairs were also downloaded and included in the data sets for both assembly processes (*18*).

2.2 Assembly strategies

Two different approaches to assembly were pursued. The first was a whole-genome assembly process that used Celera data and the PFP data in the form of additional synthetic shotgun data, and the second was a compartmentalized assembly process that first partitioned the Celera and PFP data into sets localized to large chromosomal segments and then performed ab initio shotgun assembly on each set. Figure 4 gives a schematic of the overall process flow.

For the whole-genome assembly, the PFP data was first disassembled or "shredded" into a synthetic shotgun data set of 550-bp reads that form a perfect 2× covering of the bactigs. This resulted in 16.05 million "faux" reads that were sufficient to cover the genome 2.96× because of redundancy in the BAC data set, without incorporating the biases inherent in the PFP assembly process. The combined data set of 43.32 million reads (8×), and all associated mate-pair information, were then subjected to our whole-genome assembly algorithm to produce a reconstruction of the genome. Neither the location of a BAC in the genome nor its assembly of bactigs was used in this process. Bactigs were shredded into reads because we found strong evidence that ? 13% of them were

information was ignored because some BACs were not correctly placed on the PFP physical at least 2.2% of the BACs contained sequence data that were not part of the given BAC (*41*), (see below). In short, we performed a true, a initio whole-genome assembly in which

Table 2. GenBank data input into assembly.

Center	Statistics	Completion phase sequence		
		0	1 and 2	3
Whitehead Institute/ MIT Center for Genome Research, USA	Number of accession records	2,825	6,533	363
	Number of contigs	243,786	138,023	363
	Total base pairs	194,490,158	1,083,848,245	48,829,358
	Total vector masked (bp)	1,553,597	875,618	2,202
	Total contaminant masked (bp)	13,654,482	4,417,055	98,028
	Average contig length (bp)	798	7,853	134,516
Washington University, USA	Number of accession records	19	3,232	1,300
	Number of contigs	2,127	61,812	1,300
	Total base pairs	1,195,732	561,171,788	164,214,395
	Total vector masked (bp)	21,604	270,942	8,287
	Total contaminant masked (bp)	22,469	1,476,141	469,487
	Average contig length (bp)	562	9,079	126,319
Baylor College of Medicine, USA	Number of accession records	0	1,626	363
	Number of contigs	0	44,861	363
	Total base pairs	0	265,547,066	49,017,104
	Total vector masked (bp)	0	218,769	4,960
	Total contaminant masked (bp)	0	1,784,700	485,137
	Average contig length (bp)	0	5,919	135,033
Production Sequencing Facility, DOE Joint Genome Institute, USA	Number of accession records	135	2,043	754
	Number of contigs	7,052	34,938	754
	Total base pairs	8,680,214	294,249,631	60,975,328
	Total vector masked (bp)	22,644	162,651	7,274
	Total contaminant masked (bp)	665,818	4,642,372	118,387
	Average contig length (bp)	1,231	8,422	80,867
The Institute of Physical and Chemical Research (RIKEN), Japan	Number of accession records	0	1,149	300
	Number of contigs	0	25,772	300
	Total base pairs	0	182,812,275	20,093,926
	Total vector masked (bp)	0	203,792	2,371
	Total contaminant masked (bp)	0	308,426	27,781
	Average contig length (bp)	0	7,093	66,978
Sanger Centre, UK	Number of accession records	0	4,538	2,599
	Number of contigs	0	74,324	2,599
	Total base pairs	0	689,059,692	246,118,000
	Total vector masked (bp)	0	427,326	25,054
	Total contaminant masked (bp)	0	2,066,305	374,561
	Average contig length (bp)	0	9,271	94,697
Others*	Number of accession records	42	1,894	3,458
	Number of contigs	5,978	29,898	3,458
	Total base pairs	5,564,879	283,358,877	246,474,157
	Total vector masked (bp)	57,448	279,477	32,136
	Total contaminant masked (bp)	575,366	1,616,665	1,791,849
	Average contig length (bp)	931	9,478	71,277
All centers combined†	Number of accession records	3,021	21,015	9,137
	Number of contigs	258,943	409,628	9,137
	Total base pairs	209,930,983	3,360,047,574	835,722,268
	Total vector masked (bp)	1,655,293	2,438,575	82,284
	Total contaminant masked (bp)	14,918,135	16,311,664	3,365,230
	Average contig length (bp)	811	8,203	91,466

[illegible] Research; The Institute of Physical and Chemical Research, Gene Bank; The University of Oklahoma; University of Texas Southwestern Medical Center, University of Washington. †The 4,405,700,825 bases contributed by all centers were shredded into faux reads resulting in 2.96× coverage of the genome.

quence coverage, but not mate pairs, assemble bactigs, or genome locality, from some external nally generated data.

In the compartmentalized shotgun assembl (CSA), Celera and PFP data were partitione into the largest possible chromosomal segmen or "components" that could be determined wit confidence, and then shotgun assembly was ap plied to each partitioned subset wherein th bactig data were again shredded into faux read to ensure an independent ab initio assembly o the component. By subsetting the data in thi way, the overall computational effort was re duced and the effect of interchromosomal dupl cations was ameliorated. This also resulted in reconstruction of the genome that was relativel independent of the whole-genome assembly re sults so that the two assemblies could be com pared for consistency. The quality of the part tioning into components was crucial so tha different genome regions were not mixed to gether. We constructed components from (i) th longest scaffolds of the sequence from eac BAC and (ii) assembled scaffolds of data uniqu to Celera's data set. The BAC assemblies wer obtained by a combining assembler that used th bactigs and the 5× Celera data mapped to thos bactigs as input. This effort was undertaken a an interim step solely because the more accurat and complete the scaffold for a given sequenc stretch, the more accurately one can tile thes scaffolds into contiguous components on th basis of sequence overlap and mate-pair info mation. We further visually inspected and cu rated the scaffold tiling of the components t further increase its accuracy. For the final CS. assembly, all but the partitioning was ignored and an independent, ab initio reconstruction o the sequence in each component was obtained by applying our whole-genome assembly algo rithm to the partitioned, relevant Celera data an the shredded, faux reads of the partitioned, re evant bactig data.

2.3 Whole-genome assembly

The algorithms used for whole-genome as sembly (WGA) of the human genome wer enhancements to those used to produce th sequence of the *Drosophila* genome reporte in detail in (*28*).

The WGA assembler consists of a pipelin composed of five principal stages: Screene Overlapper, Unitigger, Scaffolder, and Repe Resolver, respectively. The Screener find and marks all microsatellite repeats with le than a 6-bp element, and screens out a

[illegible] screened regions do not get scaffolded. Full o be part of an overlap that involves unscreen matching segments.

The Overlapper compares every read against every other read in search of complete end-to-end overlaps of at least 40 bp and with no more than 6% differences in the match. Because all data are scrupulously vector-trimmed, the Overlapper can insist on com-

all overlaps took roughly 10,000 CPU hours with a suite of four-processor Alpha SMPs with 4 gigabytes of RAM. This took 4 to 5 days in elapsed time with 40 such machines operating in parallel.

Every overlap computed above is statistically a 1-in-10^{17} event and thus not a coincidental event. What makes assembly combinatorially difficult is that while many overlaps are actually sampled from overlapping regions of the genome, and thus imply that the sequence reads should be assembled together, even more overlaps are actually from two distinct copies of a low-copy repeated element not screened above, thus constituting an error if put together. We call the former "true overlaps" and the latter "repeat-induced overlaps." The assembler must avoid choosing repeat-induced overlaps, especially early in the process.

We achieve this objective in the Unitigger. We first find all assemblies of reads that appear to be uncontested with respect to all other reads. We call the contigs formed from these subassemblies unitigs (for uniquely assembled contigs). Formally, these unitigs are the uncontested interval subgraphs of the graph of all overlaps (*42*). Unfortunately, although empirically many of these assemblies are correct (and thus involve only true overlaps), some are in fact collections of reads from several copies of a repetitive element that have been overcollapsed into a single subassembly. However, the overcollapsed unitigs are easily identified because their average coverage depth is too high to be consistent with the overall level of sequence coverage. We developed a simple statistical discriminator that gives the logarithm of the odds ratio that a unitig is composed of unique DNA or of a repeat consisting of two or more copies. The discriminator, set to a sufficiently stringent threshold, identifies a subset of the unitigs that we are certain are correct. In addition, a second, less stringent threshold identifies a subset of remaining unitigs very likely to be correctly assembled, of which we select those that will consistently scaffold (see below), and thus are again almost certain to be correct. We call the union of these two sets U-unitigs. Empirically, we found from a 6× simulated shotgun of human chromosome 22 that we get U-unitigs covering 98% of the stretches of unique DNA that are >2 kbp long. We are further able to identify the boundary of the start of a repetitive element singly interspersed Alu elements and other 100-to 400-bp repetitive segments.

The result of running the Unitigger was thus a set of correctly assembled subcontigs covering an estimated 73.6% of the human genome. The Scaffolder then proceeded to

gether into scaffolds. When there are two or more mate pairs that imply that a given pair of U-unitigs are at a certain distance and orientation with respect to each other, the probability of this being wrong is again roughly 1 in 10^{10}, assuming that mate pairs are false less than 2% of the time. Thus, one can with high confidence link together all U-unitigs that are linked by at least two 2- or 10-kbp mate pairs producing intermediate-sized scaffolds that are then recursively linked together by confirming 50-kbp mate pairs and BAC end sequences. This process yielded scaffolds that are on the order of megabase pairs in size with gaps between their contigs that generally correspond to repetitive elements and occasionally to small sequencing gaps. These scaffolds reconstruct the majority of the unique sequence within a genome.

For the *Drosophila* assembly, we engaged in a three-stage repeat resolution strategy where each stage was progressively more aggressive and thus more likely to make a mistake. For the human assembly, we continued to use the first "Rocks" substage where all unitigs with a good, but not definitive, discriminator score are placed in a scaffold

two or more mate pairs with one of their reads already in the scaffold unambiguously place the unitig in the given gap. We estimate the probability of inserting a unitig into an incorrect gap with this strategy to be less than 10^{-7} based on a probabilistic analysis.

We revised the ensuing "Stones" substage of the human assembly, making it more like the mechanism suggested in our earlier work (*43*). For each gap, every read R that is placed in the gap by virtue of its mated pair M being in a contig of the scaffold and implying R's placement is collected. Celera's mate-pairing information is correct more than 99% of the time. Thus, almost every, but not all, of the reads in the set belong in the gap, and when a read does not belong it rarely agrees with the remainder of the reads. Therefore, we simply assemble this set of reads within the gap, eliminating any reads that conflict with the assembly. This operation proved much more reliable than the one it replaced for the *Drosophila* assembly; in the assembly of a simulated shotgun data set of human chromo-

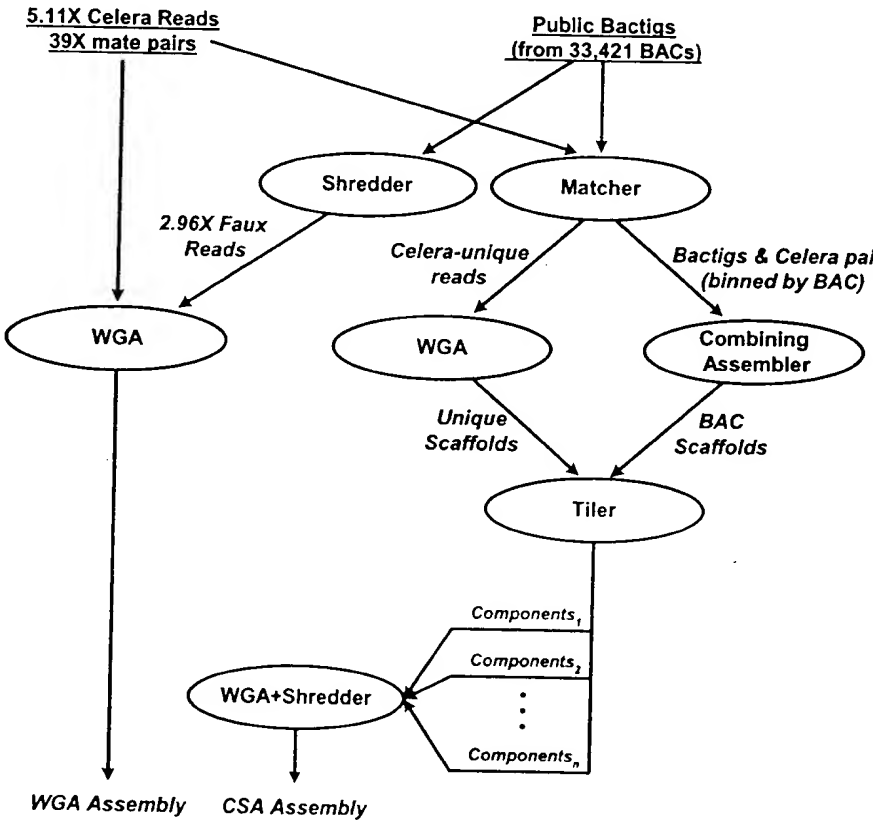

Fig. 4. Architecture of Celera's two-pronged assembly strategy. Each oval denotes a computation

some 22, all stones were placed correctly.

The final method of resolving gaps is to fill them with assembled BAC data that cover [illegible] gap walking. We did not include the very aggressive "Pebbles" substage described in our *Drosophila* work, which made enough mistakes so as to produce repeat reconstructions for long interspersed elements whose quality was only 99.62% correct. We decided that for the human genome it was philosophically better not to introduce a step that was certain to produce less than 99.99% accuracy. The cost was a somewhat larger number of gaps of somewhat larger size.

At the final stage of the assembly process, and also at several intermediate points, a consensus sequence of every contig is produced. Our algorithm is driven by the principle of maximum parsimony, with quality-value–weighted measures for evaluating each base. The net effect is a Bayesian estimate of the correct base to report at each position. Consensus generation uses Celera data whenever it is present. In the event that no Celera data cover a given region, the BAC data sequence is used.

A key element of achieving a WGA of the human genome was to parallelize the Overlapper and the central consensus sequence–constructing subroutines. In addition, memory was a real issue—a straightforward application of the software we had built for *Drosophila* would have required a computer with a 600-gigabyte RAM. By making the Overlapper and Unitigger incremental [illegible] computation with a maximum of instantaneous usage of 28 gigabytes of RAM. Moreover, the incremental nature of the first three stages allowed us to continually update the state of this part of the computation as data were delivered and then perform a 7-day run to complete Scaffolding and Repeat Resolution whenever desired. For our assembly operations, the total compute infrastructure consists of 10 four-processor SMPs with 4 gigabytes of memory per cluster (Compaq's ES40, Regatta) and a 16-processor NUMA machine with 64 gigabytes of memory (Compaq's GS160, Wildfire). The total compute for a run of the assembler was roughly 20,000 CPU hours.

The assembly of Celera's data, together with the shredded bactig data, produced a set of scaffolds totaling 2.848 Gbp in span and consisting of 2.586 Gbp of sequence. The chaff, or set of reads not incorporated in the assembly, numbered 11.27 million (26%), which is consistent with our experience for *Drosophila*. More than 84% of the genome was covered by scaffolds >100 kbp long, and these averaged 91% sequence and 9% gaps with a total of 2.297 Gbp of sequence. There were a total of 93,857 gaps among the 1637 scaffolds >100 kbp. The average scaffold size was 1.5 Mbp, the average contig size was 24.06 kbp, and the average gap size was 2.43 kbp, where the distribution of each was essentially exponer More than 50% of all gaps were less than [illegible] long, and no gap was >100 kbp long. Sim ly, more than 65% of the sequence is in cor >30 kbp, more than 31% is in contigs > kbp, and the largest contig was 1.22 Mbp l Table 3 gives detailed summary statistics the structure of this assembly with a di comparison to the compartmentalized shot assembly.

2.4 Compartmentalized shotgun assembly

In addition to the WGA approach, we p sued a localized assembly approach that v intended to subdivide the genome into s ments, each of which could be shotgun sembled individually. We expected that t would help in resolution of large interch mosomal duplications and improve the stat tics for calculating U-unitigs. The compa mentalized assembly process involved cl tering Celera reads and bactigs into lar multiple megabase regions of the genom and then running the WGA assembler on t Celera data and shredded, faux reads o tained from the bactig data.

The first phase of the CSA strategy was separate Celera reads into those that matche the BAC contigs for a particular PFP BA entry, and those that did not match any publ data. Such matches must be guaranteed t

Table 3. Scaffold statistics for whole-genome and compartmentalized shotgun assemblies.

	Scaffold size				
	All	>30 kbp	>100 kbp	>500 kbp	>1000 kbp
	Compartmentalized shotgun assembly				
No. of bp in scaffolds (including intrascaffold gaps)	2,905,568,203	2,748,892,430	2,700,489,906	2,489,357,260	2,248,689,12
No. of bp in contigs	2,653,979,733	2,524,251,302	2,491,538,372	2,320,648,201	2,106,521,90
No. of scaffolds	53,591	2,845	1,935	1,060	72
No. of contigs	170,033	112,207	107,199	93,138	82,00
No. of gaps	116,442	109,362	105,264	92,078	81,28
No. of gaps ≤1 kbp	72,091	69,175	67,289	59,915	53,354
Average scaffold size (bp)	54,217	966,219	1,395,602	2,348,450	3,118,84
Average contig size (bp)	15,609	22,496	23,242	24,916	25,686
Average intrascaffold gap size (bp)	2,161	2,054	1,985	1,832	1,749
Largest contig (bp)	1,988,321	1,988,321	1,988,321	1,988,321	1,988,321
% of total contigs	100	95	94	87	79
	Whole-genome assembly				
No. of bp in scaffolds (including intrascaffold gaps)	2,847,890,390	2,574,792,618	2,525,334,447	2,328,535,466	2,140,943,032
No. of bp in contigs	2,586,634,108	2,334,343,339	2,297,678,935	2,143,002,184	1,983,305,432
No. of scaffolds	118,968	2,507	1,637	818	554
No. of contigs	221,036	99,189	95,494	84,641	76,285
No. of gaps	102,068	96,682	93,857	83,823	75,731
No. of gaps ≤1 kbp	62,356	60,343	59,156	[illegible]	
Average scaffold size (bp)	[illegible]				
[illegible]	[illegible]				
Largest contig (bp)	[illegible]	[illegible]	1,224,073	1,224,073	1,224,073
% of total contigs	100	90	89	83	77

properly place a Celera read, so all reads were first masked against a library of common repetitive elements, and only matches of at least 40 bp to unmasked portions of the read constituted a hit. Of Celera's 27.27 million reads, 20.76 million matched a bactig and another 0.62 million reads, which did not have any matches, were nonetheless identified as belonging in the region of the bactig's BAC because their mate matched the bactig. Of the remaining reads, 2.92 million were completely screened out and so could not be matched, but the other 2.97 million reads had unmasked sequence totaling 1.189 Gbp that were not found in the GenBank data set. Because the Celera data are 5.11× redundant, we estimate that 240 Mbp of unique Celera sequence is not in the GenBank data set.

In the next step of the CSA process, a combining assembler took the relevant 5× Celera reads and bactigs for a BAC entry, and produced an assembly of the combined data for that locale. These high-quality sequence reconstructions were a transient result whose utility was simply to provide more reliable information for the purposes of their tiling into sets of overlapping and adjacent scaffold sequences in the next step. In outline, the combining assembler first examines the set of matching Celera reads to determine if there are excessive pileups indicative of unscreened repetitive elements. Wherever these occur, reads in the repeat region whose mates have not been mapped to consistent positions are removed. Then all sets of mate pairs that consistently imply the same relative position of two bactigs are bundled into a link and weighted according to the number of mates in the bundle. A "greedy" strategy then attempts to order the bactigs by selecting bundles of mate-pairs in order of their weight. A selected mate-pair bundle can tie together two formative scaffolds. It is incorporated to form a single scaffold only if it is consistent with the majority of links between contigs of the scaffold. Once scaffolding is complete, gaps are filled by the "Stones" strategy described above for the WGA assembler.

The GenBank data for the Phase 1 and 2 BACs consisted of an average of 19.8 bactigs per BAC of average size 8099 bp. Application of the combining assembler resulted in individual Celera BAC assemblies being put together into an average of 1.83 scaffolds (median of 1 scaffold) consisting of an average of 8.57 contigs of average size 18,973 bp. In addition to defining order and orientation of the sequence fragments, there were 57% fewer gaps in the combined result. For Phase 0 data, the average GenBank entry consisted of 91.52 reads of average length 784 bp. Application of the combining assembler resulted in an average of 54.8 scaffolds consist-

assembly took place, but not enough Celera data were matched to truly assemble the 0.5× to 1× data set represented by the typical Phase 0 BACs. The combining assembler was also applied to the Phase 3 BACs for SNP identification, confirmation of assembly, and localization of the Celera reads. The phase 0 data suggest that a combined whole-genome shotgun data set and 1× light-shotgun of BACs will not yield good assembly of BAC regions; at least 3× light-shotgun of each BAC is needed.

The 5.89 million Celera fragments not matching the GenBank data were assembled with our whole-genome assembler. The assembly resulted in a set of scaffolds totaling 442 Mbp in span and consisting of 326 Mbp of sequence. More than 20% of the scaffolds were >5 kbp long, and these averaged 63% sequence and 27% gaps with a total of 302 Mbp of sequence. All scaffolds >5 kbp were forwarded along with all scaffolds produced by the combining assembler to the subsequent tiling phase.

At this stage, we typically had one or two scaffolds for every BAC region constituting at least 95% of the relevant sequence, and a collection of disjoint Celera-unique scaffolds. The next step in developing the genome components was to determine the order and overlap tiling of these BAC and Celera-unique scaffolds across the genome. For this, we used Celera's 50-kbp mate-pairs information, and BAC-end pairs (*18*) and sequence tagged site (STS) markers (*44*) to provide long-range guidance and chromosome separation. Given the relatively manageable number of scaffolds, we chose not to produce this tiling in a fully automated manner, but to compute an initial tiling with a good heuristic and then use human curators to resolve discrepancies or missed join opportunities. To this end, we developed a graphical user interface that displayed the graph of tiling overlaps and the evidence for each. A human curator could then explore the implication of mapped STS data, dot-plots of sequence overlap, and a visual display of the mate-pair evidence supporting a given choice. The result of this process was a collection of "components," where each component was a tiled set of BAC and Celera-unique scaffolds that had been curator-approved. The process resulted in 3845 components with an estimated span of 2.922 Gbp.

In order to generate the final CSA, we assembled each component with the WGA algorithm. As was done in the WGA process, the bactig data were shredded into a synthetic 2× shotgun data set in order to give the assembler the freedom to independently assemble the data. By using faux reads rather than bactigs, the assembly algorithm could

C ric or contaminating sequence (from another part of the genome) would not be incorporated into the reassembly of the component because it did not belong there. In effect, the previous steps in the CSA process served only to bring together Celera fragments and PFP data relevant to a large contiguous segment of the genome, whereupon we applied the assembler used for WGA to produce an ab initio assembly of the region.

WGA assembly of the components resulted in a set of scaffolds totaling 2.906 Gbp in span and consisting of 2.654 Gbp of sequence. The chaff, or set of reads not incorporated into the assembly, numbered 6.17 million, or 22%. More than 90.0% of the genome was covered by scaffolds spanning >100 kbp long, and these averaged 92.2% sequence and 7.8% gaps with a total of 2.492 Gbp of sequence. There were a total of 105,264 gaps among the 107,199 contigs that belong to the 1940 scaffolds spanning >100 kbp. The average scaffold size was 1.4 Mbp, the average contig size was 23.24 kbp, and the average gap size was 2.0 kbp where each distribution of sizes was exponential. As such, averages tend to be underrepresentative of the majority of the data. Figure 5 shows a histogram of the bases in scaffolds of various size ranges. Consider also that more than 49% of all gaps were <500 bp long, more than 62% of all gaps were <1 kbp, and all gaps are <100 kbp long. Similarly, more than 73% of the sequence is in contigs > 30 kbp, more than 49% is in contigs >100 kbp, and the largest contig was 1.99 Mbp long. Table 3 provides summary statistics for the structure of this assembly with a direct comparison to the WGA assembly.

2.5 Comparison of the WGA and CSA scaffolds

Having obtained two assemblies of the human genome via independent computational processes (WGA and CSA), we compared scaffolds from the two assemblies as another means of investigating their completeness, consistency, and contiguity. From each assembly, a set of reference scaffolds containing at least 1000 fragments (Celera sequencing reads or bactig shreds) was obtained; this amounted to 2218 WGA scaffolds and 1717 CSA scaffolds, for a total of 2.087 Gbp and 2.474 Gbp. The sequence of each reference scaffold was compared to the sequence of all scaffolds from the other assembly with which it shared at least 20 fragments or at least 20% of the fragments of the smaller scaffold. For each such comparison, all matches of at least 200 bp with at most 2% mismatch were tabulated.

From this tabulation, we estimated the amount of unique sequence in each assembly in two ways. The first was to determine the

not covered by a matching segment in the other assembly. Some 82.5 Mbp of the WGA (3.95%) was not covered by the CSA, where- [illegible] covered by the WGA. This estimate did not require any consistency of the assemblies or any uniqueness of the matching segments. Thus, another analysis was conducted in which matches of less than 1 kbp between a pair of scaffolds were excluded unless they were confirmed by other matches having a consistent order and orientation. This gives some measure of consistent coverage: 1.982 Gbp (95.00%) of the WGA is covered by the CSA, and 2.169 Gbp (87.69%) of the CSA is covered by the WGA by this more stringent measure.

The comparison of WGA to CSA also permitted evaluation of scaffolds for structural inconsistencies. We looked for instances in which a large section of a scaffold from one assembly matched only one scaffold from the other assembly, but failed to match over the full length of the overlap implied by the matching segments. An initial set of candidates was identified automatically, and then each candidate was inspected by hand. From this process, we identified 31 instances in which the assemblies appear to disagree in a nonlocal fashion. These cases are being further evaluated to determine which assembly is in error and why.

In addition, we evaluated local inconsistencies of order or orientation. The following results exclude cases in which one contig in one assembly corresponds to more than one overlapping contig in the other assembly (as long as the order and orientation of the latter agrees with the positions they match in the former). Most of these small rearrangements involved segments on the order of hundreds of base pairs and rarely >1 kbp. We found a total of 295 kbp (0.012%) in the CSA assemblies that were locally inconsistent with the WGA assemblies, whereas 2.108 Mbp (0.11%) in the WGA assembly were inconsistent with the CSA assembly.

The CSA assembly was a few percentage points better in terms of coverage and slightly more consistent than the WGA, because it [illegible] gun assemblies of megabase-sized problems, whereas the WGA is performing a shotgun assembly of a gigabase-sized problem. When one considers the increase of two-and-a-half orders of magnitude in problem size, the information loss between the two is remarkably small. Because CSA was logistically easier to deliver and the better of the two results available at the time when downstream analyses needed to be begun, all subsequent analysis was performed on this assembly.

2.6 Mapping scaffolds to the genome

The final step in assembling the genome was to order and orient the scaffolds on the chromosomes. We first grouped scaffolds together on the basis of their order in the components from CSA. These grouped scaffolds were reordered by examining residual mate-pairing data between the scaffolds. We next mapped the scaffold groups onto the chromosome using physical mapping data. This step depends on having reliable high-resolution map information such that each scaffold will overlap multiple markers. There are two genome-wide types of map information available: high-density STS maps and fingerprint maps of BAC clones developed at Washington University (*45*). Among the genome-wide STS maps, GeneMap99 (GM99) has the most markers and therefore was most useful for mapping scaffolds. The two different mapping approaches are complementary to one another. The fingerprint maps should have better local order because they were built by comparison of overlapping BAC clones. On the other hand, GM99 should have a more reliable long-range order, because the framework markers were derived from well-validated genetic maps. Both types of maps were used as a reference for human curation of the components that were the input to the regional assembly, but they did not determine the order of sequences produced by the assembler.

In order to determine the effectiveness of the fingerprint maps and GM99 for mapping scaffolds, we first examined the validity of these maps by comparison with large scaffolds. Only 1% of the STS markers on the 10 largest scaffolds (those >9 Mbp) were mapped on a different chromosome on GM99. Two percent of the STS markers disagreed in position by more than five framework bins. However, for the fingerprint maps, a 2% chromosome discrepancy was observed, and on average 23.8% of BAC locations in the scaffold sequence disagreed with fingerprint map placement by more than five BACs. When further examining the source of discrepancy, it was found that most of the discrepancy came from 4 of the 10 scaffolds, indicating this there is variation in the quality of either the map or the scaffolds. All four scaffolds were assembled, as well as the other six, as judged by clone coverage analysis, and showed the same low discrepancy rate to GM99, and thus we concluded that the fingerprint map global order in these cases was not reliable. Smaller scaffolds had a higher discordance rate with GM99 (4.21% of STSs were discordant by more than five framework bins), but a lower discordance rate with the fingerprint maps (11% of BACs disagreed with fingerprint maps by more than five BACs). This observation agrees with the clone coverage analysis (*46*) that Celera scaffold construction was better supported by long-range mate pairs in larger scaffolds than in small scaffolds.

We created two orderings of Celera scaffolds on the basis of the markers (BAC or STS) on these maps. Where the order of scaffolds agreed between GM99 and the WashU BAC map, we had a high degree of confidence that that order was correct; these scaffolds were termed "anchor scaffolds." Only scaffolds with a low overall discrepancy rate with both maps were considered anchor scaffolds. Scaffolds in GM99 bins were allowed to permute in their order to match WashU ordering, provided they did not violate their framework orders. Orientation of individual scaffolds was determined by the presence of multiple mapped markers with consistent order. Scaffolds with only one marker have insufficient information to assign orientation. We found 70.1% of the genome in anchored scaffolds, more than 99% of which are also oriented (Table 4). Because GM99 is of lower resolution than the WashU map, a number of scaffolds without STS matches could be ordered relative to the anchored scaffolds because they included se- [illegible] repancies, a number of scaffolds determined to be "unmappable" on the WashU map could be ordered relative to the anchored scaffolds

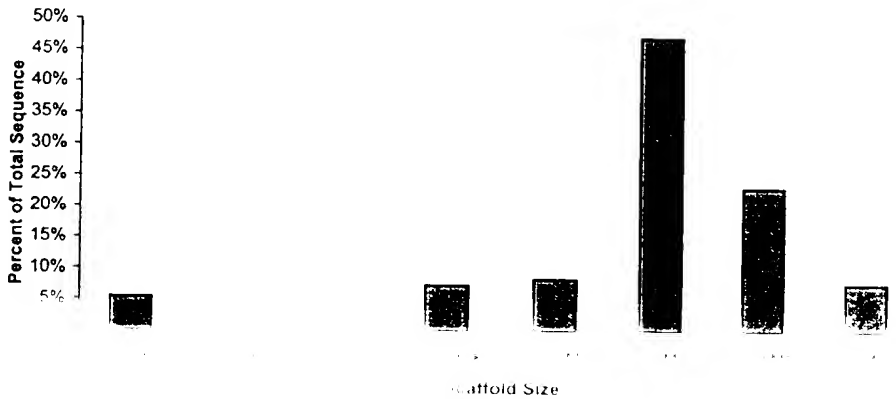

Fig. 5. Distribution of scaffold sizes of the CSA. For each range of scaffold sizes, the percent of total sequence is indicated.

with GM99. These scaffolds were termed "ordered scaffolds." We found that 13.9% of the assembly could be ordered by these additional methods, and thus 84.0% of the genome was ordered unambiguously.

Next, all scaffolds that could be placed, but not ordered, between anchors were assigned to the interval between the anchored scaffolds and were deemed to be "bounded" between them. For example, small scaffolds having STS hits from the same GeneMap bin or hitting the same BAC cannot be ordered relative to each other, but can be assigned a placement boundary relative to other anchored or ordered scaffolds. The remaining scaffolds either had no localization information, conflicting information, or could only be assigned to a generic chromosome location. Using the above approaches, ~98% of the genome was anchored, ordered, or bounded.

Finally, we assigned a location for each scaffold placed on the chromosome by spreading out the scaffolds per chromosome. We assumed that the remaining unmapped scaffolds, constituting 2% of the genome, were distributed evenly across the genome. By dividing the sum of unmapped scaffold lengths with the sum of the number of mapped scaffolds, we arrived at an estimate of interscaffold gap of 1483 bp. This gap was used to separate all the scaffolds on each chromosome and to assign an offset in the chromosome.

During the scaffold-mapping effort, we encountered many problems that resulted in additional quality assessment and validation analysis. At least 978 (3% of 33,173) BACs were believed to have sequence data from more than one location in the genome (*47*). This is consistent with the bactig chimerism analysis reported above in the Assembly Strategies section. These BACs could not be assigned to unique positions within the CSA assembly and thus could not be used for ordering scaffolds. Likewise, it was not always possible to assign STSs to unique locations in the assembly because of genome duplications, repetitive elements, and pseudogenes.

Because of the time required for an exhaustive search for a perfect overlap, CSA generated 21,607 intrascaffold gaps where the mate-pair data suggested that the contigs should overlap, but no overlap was found. These gaps were defined as a fixed 50 bp in length and make up 18.6% of the total 116,442 gaps in the CSA assembly.

We chose not to use the order of exons implied in cDNA or EST data as a way of ordering scaffolds. The rationale for not using this data was that doing so would have biased certain regions of the assembly by rearranging scaffolds to fit the transcript data

7 Assembly and validation analysis

We analyzed the assembly of the genome from the perspectives of completeness (amount of coverage of the genome) and correctness (the structural accuracy of the order and orientation and the consensus sequence of the assembly).

Completeness. Completeness is defined as the percentage of the euchromatic sequence represented in the assembly. This cannot be known with absolute certainty until the euchromatin sequence has been completed. However, it is possible to estimate completeness on the basis of (i) the estimated sizes of intrascaffold gaps; (ii) coverage of the two published chromosomes, 21 and 22 (*48*, *49*); and (iii) analysis of the percentage of an independent set of random sequences (STS markers) contained in the assembly. The whole-genome libraries contain heterochromatic sequence and, although no attempt has been made to assemble it, there may be instances of unique sequence embedded in regions of heterochromatin as were observed in *Drosophila* (*50*, *51*).

The sequences of human chromosomes 21 and 22 have been completed to high quality and published (*48*, *49*). Although this sequence served as input to the assembler, the finished sequence was shredded into a shotgun data set so that the assembler had the opportunity to assemble it differently from the original sequence in the case of structural polymorphisms or assembly errors in the BAC data. In particular, the assembler must be able to resolve repetitive elements at the scale of components (generally multimegabase in size), and so this comparison reveals the level to which the assembler resolves repeats. In certain areas, the assembly structure differs from the published versions of chromosomes 21 and 22 (see below). The consequence of the flexibility to assemble "finished" sequence differently on the basis of Celera data resulted in an assembly with more segments than the chromosome 21 and 22 sequences. We examined the reasons why there are more gaps in the Celera sequence than in chromosomes 21 and 22 and expect that they may be typical of gaps in other regions of the genome. In the Celera assembly, there are 25 scaffolds, each containing at least 10 kb of sequence, that collectively span 94.3% of chromosome 21. Sixty-two scaffolds span 95.7% of chromosome 22. The total length of the gaps remaining in the Celera assembly for these two chromosomes is 3.4 Mbp. These gap sequences were analyzed by RepeatMasker and by searching against the entire genome assembly (*52*). About 50% of the gap sequence consisted of common repetitive elements identified by RepeatMasker; more than half of the remainder

ness. To measure the content of an independent set of sequence data in the assembly. We compared 48,938 STS markers from Genemap99 (*51*) to the scaffolds. Because these markers were not used in the assembly processes, they provided a truly independent measure of completeness. [redacted] used to locate STSs on the assembled genome. We found 44,524 (91%) of the STSs in the mapped genome. An additional 2648 markers (5.4%) were found by searching the unassembled data or "chaff." We identified 1283 STS markers (2.6%) not found in either Celera sequence or BAC data as of September 2000, raising the possibility that these markers may not be of human origin. If that were the case, the Celera assembled sequence would represent 93.4% of the human genome and the unassembled data 5.5%, for a total of 98.9% coverage. Similarly, we compared CSA against 36,678 TNG radiation hybrid markers (*55a*) using the same method. We found that 32,371 markers (88%) were located in the mapped CSA scaffolds, with 2055 markers (5.6%) found in the remainder. This gave a 94% coverage of the genome through another genome-wide survey.

Correctness. Correctness is defined as the structural and sequence accuracy of the assembly. Because the source sequences for the Celera data and the GenBank data are from different individuals, we could not directly compare the consensus sequence of the as-

Table 4. Summary of scaffold mapping. Scaffolds were mapped to the genome with different levels of confidence (anchored scaffolds have the highest confidence; unmapped scaffolds have the lowest). Anchored scaffolds were consistently ordered by the WashU BAC map and GM99. Ordered scaffolds were consistently ordered by at least one of the following: the WashU BAC map, GM99, or component tiling path. Bounded scaffolds had order conflicts between at least two of the external maps, but their placements were adjacent to a neighboring anchored or ordered scaffold. Unmapped scaffolds had, at most, a chromosome assignment. The scaffold subcategories are given below each category.

Mapped scaffold category	Number	Length (bp)	% Total length
Anchored	1,526	1,860,676,676	70
Oriented	1,246	1,852,088,645	70
Unoriented	280	8,588,031	0.3
Ordered	2,001	369,235,857	14
Oriented	839	329,633,166	12
Unoriented	1,162	39,602,691	2
Bounded	38,241	368,753,463	14
Oriented	7,453	274,536,424	10
Unoriented	30,788	94,217,039	4
Unmapped	11,823	55,313,737	2
Known chromosome	281	2,505,844	0.1

sembly against other finished sequence for determining sequencing accuracy at the nucleotide level, although this has been done for identifying polymorphisms as described in Section 6. The accuracy of the consensus sequence is at least 99.96% on the basis of a statistical estimate derived from the quality values of the underlying reads.

The structural consistency of the assembly can be measured by mate-pair analysis. In a correct assembly, every mated pair of sequencing reads should be located on the consensus sequence with the correct separation and orientation between the pairs. A pair is termed "valid" when the reads are in the correct orientation and the distance between them is within the mean ± 3 standard deviations of the distribution of insert sizes of the library from which the pair was sampled. A pair is termed "misoriented" when the reads are not correctly oriented, and is termed "misseparated" when the distance between the reads is not in the correct range but the reads are correctly oriented. The mean ± the standard deviation of each library used by the assembler was determined as described above. To validate these, we examined all reads mapped to the finished sequence of chromosome 21 (*48*) and determined how many incorrect mate pairs there were as a result of laboratory tracking errors and chimerism (two different segments of the genome cloned into the same plasmid), and how tight the distribution of insert sizes was for those that were correct (Table 5). The standard deviations for all Celera libraries were [illegible] length, with the exception of a few 50-kbp libraries. The 2- and 10-kbp libraries contained less than 2% invalid mate pairs, whereas the 50-kbp libraries were somewhat higher (~10%). Thus, although the mate-pair information was not perfect, its accuracy was such that measuring valid, misoriented, and misseparated pairs with respect to a given assembly was deemed to be a reliable instrument for validation purposes, especially when several mate pairs confirm or deny an ordering.

The clone coverage of the genome was 39×, meaning that any given base pair was, on average, contained in 39 clones or, equivalently, spanned by 39 mate-paired reads. Areas of low clone coverage or areas with a high proportion of invalid mate pairs would indicate potential assembly problems. We computed the coverage of each base in the assembly by valid mate pairs (Table 6). In summary, for scaffolds >30 kbp in length, less than 1% of the Celera assembly was in regions of less than 3× clone coverage. Thus, more than 99% of the assembly, including order and orientation, is strongly supported by this measure alone.

We examined the locations and number of all misoriented and misseparated mates. In addition to doing this analysis on the CSA assembly (as of 1 October 2000), we also performed a study of the PFP assembly as of 5 September 2000 (*30*, *55b*). In this latter case, Celera mate pairs had to be mapped to [illegible] due to high-fidelity repeats, the only pairs mapped were those for which both reads matched at only one location with less than 6% differences. A threshold was set such that sets of five or more simultaneously invalid mate pairs indicated a potential breakpoint, where the construction of the two assemblies differed. The graphic comparison of the CSA chromosome 21 assembly with the published sequence (Fig. 6A) serves as a validation of this methodology. Blue tick marks in the panels indicate breakpoints. There were a similar (small) number of breakpoints on both chromosome sequences. The exception was 12 sets of scaffolds in the Celera assembly (a total of 3% of the chromosome length in 212 single-contig scaffolds) that were mapped to the wrong positions because they were too small to be mapped reliably. Figures 6 and 7 and Table 6 illustrate the mate-pair differences and breakpoints between the two assemblies. There was a higher percentage of misoriented and misseparated mate pairs in the large-insert libraries (50 kbp and BAC ends) than in the small-insert libraries in both assemblies (Table 6). The large-insert libraries are more likely to identify discrepancies simply because they span a larger segment of the genome. The graphic comparison between the two assemblies for chromosome 8 (Fig. 6, B and C) shows that there are many

Table 5. Mate-pair validation. Celera fragment sequences were mapped to the published sequence of chromosome 21. Each mate pair uniquely mapped was evaluated for correct orientation and placement (number of mate pairs tested). If the two mates had incorrect relative orientation or placement, they were considered invalid (number of invalid mate pairs).

Library type	Library no.	Chromosome 21						Genome		
		Mean insert size (bp)	SD (bp)	SD/ mean (%)	No. of mate pairs tested	No. of invalid mate pairs	% invalid	Mean insert size (bp)	SD (bp)	SD/ mean (%)
2 kbp	1	2,081	106	5.1	3,642	38	1.0	2,082	90	4.3
	2	1,913	152	7.9	28,029	413	1.5	1,923	118	6.1
	3	2,166	175	8.1	4,405	57	1.3	2,162	158	7.3
10 kbp	4	11,385	851	7.5	4,319	80	1.9	11,370	696	6.1
	5	14,523	1,875	12.9	7,355	156	2.1	14,142	1,402	9.9
	6	9,635	1,035	10.7	5,573	109	2.0	9,606	934	9.7
	7	10,223	928	9.1	34,079	399	1.2	10,190	777	7.6
50 kbp	8	64,888	2,747	4.2	16	1	6.3	65,500	5,504	8.4
	9	53,410	5,834	10.9	914	170	18.6	53,311	5,546	10.4
	10	52,034	7,312	14.1	5,871	569	9.7	51,498	6,588	12.8
	11	52,282	7,454	14.3	2,629	213	8.1	52,282	7,454	14.3
	12	46,616	7,378	15.8	2,153	215	10.0	45,418	9,068	20.0
	13	55,788	10,099	18.1	2,244	249	11.1	53,062	10,893	20.5
	14	39,894	5,019	12.6	199	7	3.5	36,838	9,988	27.1
BES	15	48,931	9,813	20.1	144	10	6.9	47,845	4,774	10.0
		[illegible]	[illegible]	[illegible]	[illegible]	[illegible]	[illegible]	[illegible]	[illegible]	[illegible]
					[illegible]	[illegible]	[illegible]	46,500	[illegible]	[illegible]
					102,894	2,768 (mean = 2.7)	2.7			

more breakpoints for the PFP assembly than [illegible]. Figure 7 shows the breakpoint map (blue tick marks) assemblies of each chromosome in a side-by-side fashion. The order and orientation of Celera's assembly shows substantially fewer breakpoints except on the two finished chromosomes. Figure 7 also depicts large gaps (>10 kbp) in both assemblies as red tick marks. In the CSA assembly, the size of all gaps have been estimated on the basis of the mate-pair data. Breakpoints can be caused by structural polymorphisms, because the two assemblies were derived from different human genomes. They also reflect the unfinished nature of both genome assemblies.

3 Gene Prediction and Annotation

Summary. To enumerate the gene inventory, we developed an integrated, evidence-based approach named Otto. The evidence used to increase the likelihood of identifying genes includes regions conserved between the mouse and human genomes, similarity to ESTs or other mRNA-derived data, or similarity to other proteins. A comparison of Otto (combined Otto-RefSeq and Otto homology) with Genscan, a standard gene-prediction algorithm, showed greater sensitivity (0.78 versus 0.50) and specificity (0.93 versus 0.63) of Otto in the ability to define gene structure. Otto-predicted genes were complemented with a set of genes from three gene-prediction programs that exhibited weaker, but still significant, evidence that they may be expressed. Conservative criteria, requiring at least two lines of evidence, were used to define a set of 26,383 genes with good confidence that were used for more detailed analysis presented in the subsequent sections. Extensive manual curation to establish precise characterization of gene structure will be necessary to improve the results from this initial computational approach.

3.1 Automated gene annotation

A gene is a locus of cotranscribed exons. A single gene may give rise to multiple transcripts, and thus multiple distinct proteins with multiple functions, by means of alternative splicing and alternative transcription initiation and termination sites. Our cells are [illegible] within the billions of base pairs of the genomic DNA [illegible] initiating transcription and for splicing together exons separated by a few or hundreds of thousands of base pairs. The first step in characterizing the genome is to define the structure of each gene and each transcription unit.

The number of protein-coding genes in mammals has been controversial from the outset. Initial estimates based on reassociation data placed it between 30,000 to 40,000, whereas later estimates from the brain were >100,000 (*56*). More recent data from both the corporate and public sectors, based on extrapolations from EST, CpG island, and transcript density–based extrapolations, have not reduced this variance. The highest recent number of 142,634 genes emanates from a report from Incyte Pharmaceuticals, and is based on a combination of EST data and the association of ESTs with CpG islands (*57*). In stark contrast are three quite different, and much lower estimates: one of ~35,000 genes derived with genome-wide EST data and sampling procedures in conjunction with chromosome 22 data (*58*); another of 28,000 to 34,000 genes derived with a comparative methodology involving sequence conservation between humans and the puffer fish *Tetraodon nigroviridis* (*59*); and a figure of 35,000 genes, which was derived simply by extrapolating from the density of 770 known and predicted genes in the 67 Mbp of chromosomes 21 and 22, to the approximately 3-Gbp euchromatic genome.

The problem of computational identification of transcriptional units in genomic DNA sequence can be divided into two phases. The first is to partition the sequence into segments that are likely to correspond to individual genes. This is not trivial and is a weakness of most de novo gene-finding algorithms. It is also critical to determining the number of genes in the human gene inventory. The second challenge is to construct a gene model that reflects the probable structure of the transcript(s) encoded in the region. This can be done with reasonable accuracy when a full-length cDNA has been sequenced or a highly homologous protein sequence is [illegible]. De novo gene prediction, although [illegible] less accurate, is also [illegible] that are not represented by homologous proteins or ESTs. The following section describes the methods we have developed to address these problems for the prediction of protein-coding genes.

We have developed a rule-based expert system, called Otto, to identify and characterize genes in the human genome (*60*). Otto attempts to simulate in software the process that a human annotator uses to identify a gene and refine its structure. In the process of annotating a region of the genome, a human curator examines the evidence provided by the computational pipeline (described below) and examines how various types of evidence relate to one another. A curator puts different levels of confidence in different types of evidence and looks for certain patterns of evidence to support gene annotation. For example, a curator may examine homology to a number of ESTs and evaluate whether or not they can be connected into a longer, virtual mRNA. The curator would also evaluate the strength of the similarity and the contiguity of the match, in essence asking whether any ESTs cross splice-junctions and whether the edges of putative exons have consensus splice sites. This kind of manual annotation process was used to annotate the *Drosophila* genome.

The Otto system can promote observed evidence to a gene annotation in one of two ways. First, if the evidence includes a high-quality match to the sequence of a known gene [here defined as a human gene represented in a curated subset of the RefSeq database (*61*)], then Otto can promote this to a gene annotation. In the second method, Otto evaluates a broad spectrum of evidence and determines if this evidence is adequate to support promotion to a gene annotation. These processes are described below.

Initially, gene boundaries are predicted on the basis of examination of sets of overlapping protein and EST matches generated by a computational pipeline (*62*). This pipeline searches the scaffold sequences against protein, EST, and genome-sequence databases to define regions of sequence similarity and runs three de novo gene-prediction programs.

To identify likely gene boundaries, regions of the genome were partitioned by Otto on the basis of sequence matches identified by BLAST. Each of the database sequences matched in the region under analysis was compared by an algorithm that takes into [illegible] coordinates of the matching sequences that may define a gene and identi-

Table 6. Genome-wide mate pair analysis of compartmentalized shotgun (CSA) and PFP assemblies.*

Genome library	CSA			PFP		
	% valid	% mis-oriented	% mis-separated†	% valid	% mis-oriented	% mis-separated†
[illegible]	[illegible]	[illegible]	[illegible]	95.7	2.0	2.3
Mean	97.4					

*Data for individual chromosomes can be found in Web fig. 3 on Science Online at www.sciencemag.org/cgi/content/full/291/5507/1304/DC1. †Mates are misseparated if their distance is >3 SD from the mean library size

gene boundaries. During this process, multiple hits to the same region were collapsed to a coherent set of data by tracking the coverage of a region. For example, if a group of bases was represented by multiple overlapping ESTs, the union of these regions matched by the set of ESTs on the scaffold was marked as being supported by EST evidence. This resulted in a series of "gene bins," each of which was believed to contain a single gene. One weakness of this initial implementation of the algorithm was in predicting gene boundaries in regions of tandemly duplicated genes. Gene clusters frequently resulted in homologous neighboring genes being joined together, resulting in an annotation that artificially concatenated these gene models. Next, known genes (those with an exact match of a full-length cDNA sequence to the genome) were identified, and the region corresponding to the cDNA was annotated as a predicted transcript. A subset of the curated human gene set RefSeq from the National Center for Biotechnology Information (NCBI) was included as a data set searched in the computational pipeline. If a RefSeq transcript matched the genome assembly for at least 50% of its length at >92% identity, then the SIM4 (*63*) alignment of the RefSeq transcript to the region of the genome under analysis was promoted to the status of an Otto annotation. Because sequence errors such as frameshifts, it was not always possible to predict a transcript that agrees precisely with the experimentally determined cDNA sequence. A total of 6538 genes in our inventory were identified and transcripts predicted in this way.

Regions that have a substantial amount of sequence similarity, but do not match known genes, were analyzed by that part of the Otto system that uses the sequence similarity information to predict a transcript. Here, Otto

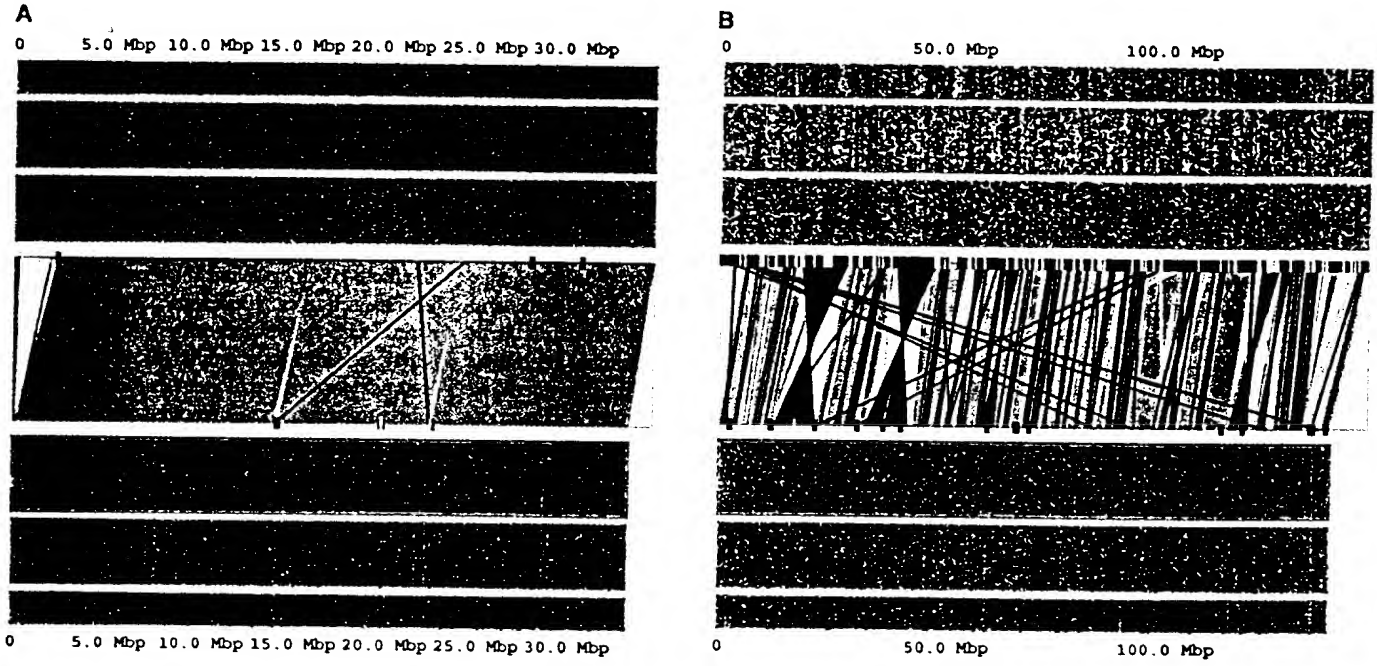

Fig. 6. Comparison of the CSA and the PFP assembly. (**A**) All of chromosome 21, (**B**) all of chromosome 8, and (**C**) a 1-Mb region of chromosome 8 representing a single Celera scaffold. To generate the figure, Celera fragment sequences were mapped onto each assembly. The PFP assembly is indicated in the upper third of each panel; the Celera assembly is indicated in the lower third. In the center of the panel, green lines show Celera sequences that are in the same order and orientation in both assemblies and form the longest consistently ordered run of sequences. Yellow lines indicate sequence blocks that are in the same orientation, but out of order. Red lines indicate sequence blocks that are not in the same orientation. For clarity, in the latter two cases, lines are only drawn between segments of matching sequence that are at least 50 kbp long. The top and bottom thirds of each panel show the extent of Celera mate-pair violations (red, misoriented; yellow, incorrect distance between the mates) for each assembly grouped by library size. (Mate pairs that are within the correct distance, as expected from the mean library insert size, are omitted from the figure.) [illegible] Plots of all 24 chromosomes [illegible] fig. 3 on *Science* Online at www.sciencemag.org/cgi/content/full/291/5507/1304/DC1

evaluates evidence generated by the computational pipeline, corresponding to conservation between mouse and human genomic DNA, similarity to human transcripts (ESTs and cDNAs), similarity to rodent transcripts (ESTs and cDNAs), and similarity of the translation of human genomic DNA to known proteins to predict potential genes in the human genome. The sequence from the region of genomic DNA contained in a gene bin was extracted, and the subsequences supported by any homology evidence were marked (plus 100

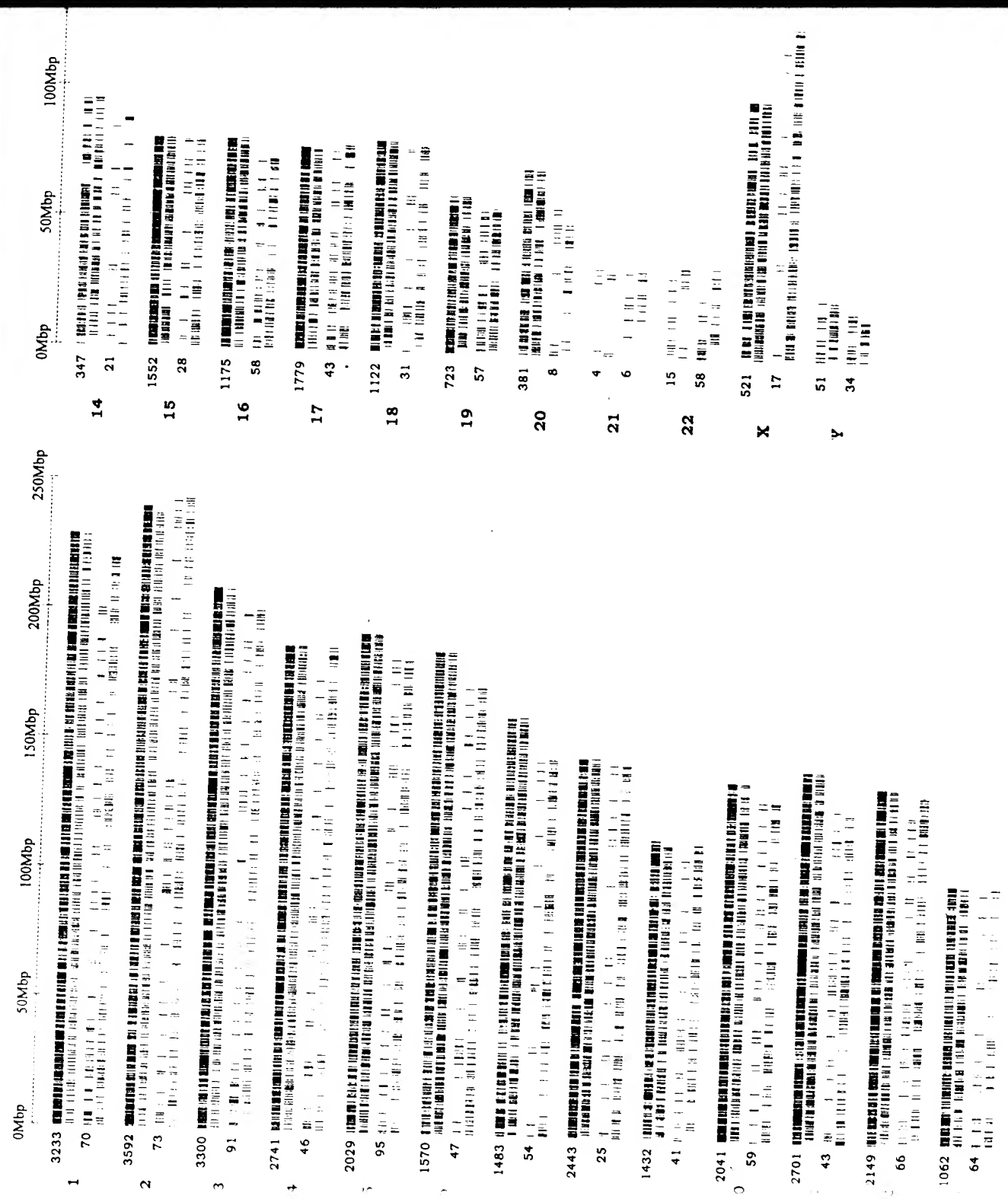

...chromosome. ... and the lower pair of lines represent Celera s... ...bp. The number of breakpoints per chromosome is indicated in black, and the chromosome numbers in red

bases flanking these regions). The other bases in the region, those not covered by any homology evidence, were replaced by N's. This sequence, represented by the consensus genomic sequence and the remainder represented by N's, was then evaluated by Genscan to see if a consistent gene model could be generated. This procedure simplified the gene-prediction task by first establishing the boundary for the gene (not a strength of most gene-finding algorithms), and by eliminating regions with no supporting evidence. If Genscan returned a plausible gene model, it was further evaluated before being promoted to an "Otto" annotation. The final Genscan predictions were often quite different from the prediction that Genscan returned on the same region of native genomic sequence. A weakness of using Genscan to refine the gene model is the loss of valid, small exons from the final annotation.

The next step in defining gene structures based on sequence similarity was to compare each predicted transcript with the homology-based evidence that was used in previous steps to evaluate the depth of evidence for each exon in the prediction. Internal exons were considered to be supported if they were covered by homology evidence to within ±10 bases of their edges. For first and last exons, the internal edge was required to be within 10 bases, but the external edge was allowed greater latitude to allow for 5′ and 3′ untranslated regions (UTRs). To be retained, a prediction for a multi-exon gene must have evidence such that the total number of "hits," as defined above, divided by the number of exons in the prediction must be >0.66 or must correspond to a RefSeq sequence. A single-exon gene must be covered by at least three supporting hits (±10 bases on each side), and these must cover the complete predicted open reading frame. For a single-exon gene, we also required that the Genscan prediction include both a start and a stop codon. Gene models that did not meet these criteria were disregarded, and those that passed were promoted to Otto predictions. Homology-based Otto predictions do not contain 3′ and 5′ untranslated [illegible] programs [GRAIL, Genscan, and FgenesH (*63*)] were run as part of the computational analysis, the results of these programs were not directly used in making the Otto predictions. Otto predicted 11,226 additional genes by means of sequence similarity.

Table 7. Sensitivity and specificity of Otto and Genscan. Sensitivity and specificity were calculated by first aligning the prediction to the published RefSeq transcript, tallying the number (*N*) of uniquely aligned RefSeq bases. Sensitivity is the ratio of *N* to the length of the published RefSeq transcript. Specificity is the ratio of *N* to the length of the prediction. All differences are significant (Tukey HSD; $P < 0.001$).

Method	Sensitivity	Specificity
Otto (RefSeq only)*	0.939	0.973
Otto (homology)†	0.604	0.884

[illegible] ence-based Genscan predictions. †Refers to those annotations produced by supplying all available evidence to Genscan.

3.2 Otto validation

To validate the Otto homology-based process and the method that Otto uses to define the structures of known genes, we compared transcripts predicted by Otto with their corresponding (and presumably correct) transcript from a set of 4512 RefSeq transcripts for which there was a unique SIM4 alignment (Table 7). In order to evaluate the relative performance of Otto and Genscan, we made three comparisons. The first involved a determination of the accuracy of gene models predicted by Otto with only homology data other than the corresponding RefSeq sequence (Otto homology in Table 7). We measured the sensitivity (correctly predicted bases divided by the total length of the cDNA) and specificity (correctly predicted bases divided by the sum of the correctly and incorrectly predicted bases). Second, we examined the sensitivity and specificity of the Otto predictions that were made solely with the RefSeq sequence, which is the process that Otto uses to annotate known genes (Otto-RefSeq). And third, we determined the accuracy of the Genscan predictions corresponding to these RefSeq sequences. As expected, the alignment method (Otto-RefSeq) was the most accurate, and Otto-homology performed better than Genscan by both criteria. Thus, 6.1% of true RefSeq nucleotides were not represented in the Otto-refseq annotations and 2.7% of the nucleotides in the Otto-RefSeq transcripts were not contained in the original RefSeq transcripts. The discrepancies could come from legitimate differences between the Celera assembly and the RefSeq transcript due to polymorphisms, incomplete or incorrect data in the Celera assembly, errors introduced by Sim4 during the alignment process, or the presence of alternatively spliced forms in the data set used for the comparisons.

Because Otto uses an evidence-based approach to reconstruct genes, the absence of experimental evidence for intervening exons may inadvertantly result in a set of exons that cannot be spliced together to give rise to a transcript. In such cases, Otto may "split genes" when in fact all the evidence should be com- [illegible] into a single transcript. We observed [illegible] both RefSeq and homology-based predictions by Otto split known genes into fewer segments than Genscan alone.

3.3 Gene number

Recognizing that the Otto system is quite conservative, we used a different gene-prediction strategy in regions where the homology evidence was less strong. Here the results of de novo gene predictions were used. For these genes, we insisted that a predicted transcript have at least two of the following types of evidence to be included in the gene set for further analysis: protein, human EST, rodent EST, or mouse genome fragment matches. This final class of predicted genes is a subset of the predictions made by the three gene-finding programs that were used in the computational pipeline. For these, there was not sufficient sequence similarity information for Otto to attempt to predict a gene structure. The three de novo gene-finding programs resulted in about 155,695 predictions, of which ~76,410 were nonredundant (nonoverlapping with one another). Of these, 57,935 did not overlap known genes or predictions made by Otto. Only 21,350 of the gene predictions that did not overlap Otto predictions were partially supported by at least one type of sequence similarity evidence, and 8619 were partially supported by two types of evidence (Table 8).

The sum of this number (21,350) and the number of Otto annotations (17,764), 39,114, is near the upper limit for the human gene complement. As seen in Table 8, if the requirement for other supporting evidence is made more stringent, this number drops rapidly so that demanding two types of evidence reduces the total gene number to 26,383 and demanding three types reduces it to ~23,000. Requiring that a prediction be supported by all four categories of evidence is too stringent because it would eliminate genes that encode novel proteins (members of currently undescribed protein families). No correction for pseudogenes has been made at this point in the analysis.

In a further attempt to identify genes that were not found by the autoannotation process or any of the de novo gene finders, we examined regions outside of gene predictions that were similar to the EST sequence, and where the EST matched the genomic sequence across a splice junction. After correcting for potential 3′ UTRs of predicted genes, about 2500 such regions remained. Addition of a requirement for at least one of the following evidence types—homology to mouse genomic sequence fragments, rodent ESTs, or cDNAs—or similarity to a known protein reduced this number to 1010. Adding this to [illegible] paragraph

[illegible] human genome, depending on the stringency of evidence considered. Table 8 illustrates the number of genes and presents the degree of

confidence based on the supporting evidence. Transcripts encoded by a set of 26,383 genes were assembled for further analysis. This set includes the 6538 genes predicted by Otto on the basis of matches to known genes, 11,226 [illegible] ogy evidence, and 8619 from the subset of transcripts from de novo gene-prediction programs that have two types of supporting evidence. The 26,383 genes are illustrated along chromosome diagrams in Fig. 1. These are a very preliminary set of annotations and are subject to all the limitations of an automated process. Considerable refinement is still necessary to improve the accuracy of these transcript predictions. All the predictions and descriptions of genes and the associated evidence that we present are the product of completely computational processes, not expert curation. We have attempted to enumerate the genes in the human genome in such a way that we have different levels of confidence based on the amount of supporting evidence: known genes, genes with good protein or EST homology evidence, and de novo gene predictions confirmed by modest homology evidence.

3.4 Features of human gene transcripts

We estimate the average span for a "typical" gene in the human DNA sequence to be about 27,894 bases. This is based on the average span covered by RefSeq transcripts, used because it represents our highest confidence set.

The set of transcripts promoted to gene annotations varies in a number of ways. As can be seen from Table 8 and Fig. 9, transcripts predicted by Otto tend to be longer, having on average about 7.8 exons, whereas those promoted from gene-prediction programs average about 3.7 exons. The largest number of exons that we have identified in a transcript is 234 in the titin mRNA. Table 8 compares the amounts of evidence that support the Otto and other predicted transcripts. For example, one can see that a typical Otto transcript has 6.99 of its 7.81 exons supported by protein homology evidence. As would be expected, the Otto transcripts generally have more support than do transcripts predicted by the de novo methods.

4 Genome Structure

Summary. This section describes several of the noncoding attributes of the assembled genome sequence and their correlations with the predicted gene set. These include an analysis of G+C content and gene density in the context of cytogenetic maps of the genome, an enumerative analysis of CpG islands, and a brief description of the genome-wide repetitive elements.

4.1 Cytogenetic maps

Perhaps the most obvious, and certainly the most visible, element of the structure of the genome is the banding pattern produced by [illegible] studies have revealed that about 17% to 20% of the human chromosome complement consists of C-bands, or constitutive heterochromatin (*64*). Much of this heterochromatin is highly polymorphic and consists of different families of alpha satellite DNAs with various higher order repeat structures (*65*). Many chromosomes have complex inter- and intrachromosomal duplications present in pericentromeric regions (*66*). About 5% of the sequence reads were identified as alpha satellite sequences; these were not included in the assembly.

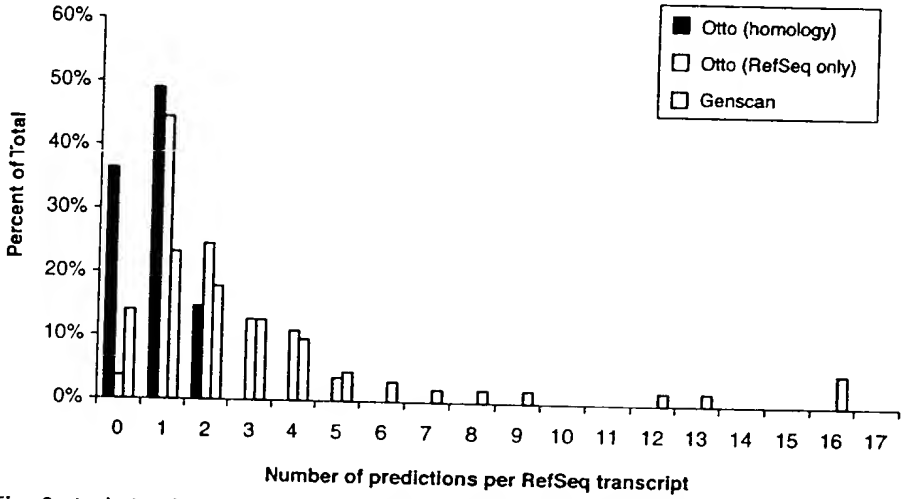

Fig. 8. Analysis of split genes resulting from different annotation methods. A set of 4512 Sim4-based alignments of RefSeq transcripts to the genomic assembly were chosen (see the text for criteria), and the numbers of overlapping Genscan, Otto (RefSeq only) annotations based solely on Sim4-polished RefSeq alignments, and Otto (homology) annotations (annotations produced by supplying all available evidence to Genscan) were tallied. These data show the degree to which multiple Genscan predictions and/or Otto annotations were associated with a single RefSeq transcript. The zero class for the Otto-homology predictions shown here indicates that the Otto-homology calls were made without recourse to the RefSeq transcript, and thus no Otto call was made because of insufficient evidence.

Table 8. Numbers of exons and transcripts supported by various types of evidence for Otto and de novo gene prediction methods. Highlighted cells indicate the gene sets analyzed in this paper (boldface, set of genes selected for protein analysis; italic, total set of accepted de novo predictions).

		Total	Types of evidence				No. of lines of evidence*			
			Mouse	Rodent	Protein	Human	≥1	≥2	≥3	≥4
Otto	Number of transcripts	17,969	17,065	14,881	15,477	16,374	**17,968**†	17,501	15,877	12,451
	Number of exons	141,218	111,174	89,569	108,431	118,869	140,710	127,955	99,574	59,804
De novo	Number of transcripts	58,032	14,463	5,094	8,043	9,220	*21,350*	**8,619**	4,947	1,904
	Number of exons	319,935	48,594	19,344	26,264	40,104	79,148	31,130	17,508	6,520
No. of exons per transcript	Otto	7.84	5.77	6.01	6.99	7.24	7.81	7.19	6.00	4.28
	De novo	[illegible]								

[illegible] [illegible] elsewhere in the text.

Examination of pericentromeric regions is ongoing.

The remaining ~80% of the genome, the [illegible] R-, and T-bands (*67*). These cytogenetic bands have been presumed to differ in their nucleotide composition and gene density, although we have been unable to determine precise band boundaries at the molecular level. T-bands are the most G+C- and gene-rich, and G-bands are G+C-poor (*68*). Bernardi has also offered a description of the euchromatin at the molecular level as long stretches of DNA of differing base composition, termed isochores (denoted L, H1, H2, and H3), which are >300 kbp in length (*69*). Bernardi defined the L (light) isochores as G+C-poor (<43%), whereas the H (heavy) isochores fall into three G+C-rich classes representing 24, 8, and 5% of the genome. Gene concentration has been claimed to be very low in the L isochores and 20-fold more enriched in the H2 and H3 isochores (*70*). By examining contiguous 50-kbp windows of G+C content across the assembly, we found that regions of G+C content >48% (H3 isochores) averaged 273.9 kbp in length, those with G+C content between 43 and 48% (H1+H2 isochores) averaged 202.8 kbp in length, and the average span of regions with <43% (L isochores) was 1078.6 kbp. The correlation between G+C content and gene density was also examined in 50-kbp windows along the assembled sequence (Table 9 and Figs. 10 and 11). We found that the density of genes was greater in regions of high G+C than in regions of low G+C content, as expected. However, the correlation between G+C content and gene density was not as skewed as previously predicted (*69*). A higher proportion of genes were located in the G+C-poor regions than had been expected.

Chromosomes 17, 19, and 22, which have a disproportionate number of H3-containing bands, had the highest gene density (Table 10). Conversely, of the chromosomes that we found to have the lowest gene density, X, 4, 18, 13, and Y, also have the fewest H3 bands. Chromosome 16, which also has [illegible] bands, did not have a particularly low gene density in our analysis. In addition, chromosome 8, which we found to have a low gene density, does not appear to be unusual in its H3 banding.

How valid is Ohno's postulate (*71*) that mammalian genomes consist of oases of genes in otherwise essentially empty deserts? It appears that the human genome does indeed contain deserts, or large, gene-poor regions. If we define a desert as a region >500 kbp without a gene, then we see that 605 Mbp, or about 20% of the genome, is in deserts. These are not uniformly distributed over the various chromosomes. Gene-rich chromosomes 17, 19, and 22 have only about 12% of their collective 171 Mbp in deserts, whereas gene-poor chromosomes 4, 13, 18, and X have 27.5% of their 492 Mbp in deserts (Table 11). The apparent lack of predicted genes in these regions does not necessarily imply that they are devoid of biological function.

4.2 Linkage map

Linkage maps provide the basis for genetic analysis and are widely used in the study of the inheritance of traits and in the positional cloning of genes. The distance metric, centimorgans (cM), is based on the recombination rate between homologous chromosomes during meiosis. In general, the rate of recombination in females is greater than that in males, and this [illegible] the genome (*72*). One of the opportunities enabled by a nearly complete genome sequence is to produce the ultimate physical map, and to fully analyze its correspondence with two other maps that have been widely used in genome and genetic analysis: the linkage map and the cytogenetic map. This would close the loop between the mapping and sequencing phases of the genome project.

We mapped the location of the markers that constitute the Genethon linkage map to the genome. The rate of recombination, expressed as cM per Mbp, was calculated for 3-Mbp windows as shown in Table 12. Higher rates of recombination in the telomeric region of the chromosomes have been previously documented (*73*). From this mapping result, there is a difference of 4.99 between lowest rates and highest rates and the largest difference of 4.4 between males and females (4.99 to 0.47 on chromosome 16). This indicates that the variability in recombination rates among regions of the genome exceeds the differences in recombination rates between males and females. The human genome has recombination hotspots, where recombination rates vary fivefold or more over a space of 1 kbp, so the picture one gets of the magnitude of variability in recombination rate will depend on the size of the window

Table 9. Characteristics of G+C in isochores.

Isochore	G+C (%)	Fraction of genome		Fraction of genes	
		Predicted*	Observed	Predicted*	Observed
H3	>48	5	9.5	37	24.8
H1/H2	43–48	25	21.2	32	26.6
L	<43	67	69.2	31	48.5

*The predictions were based on Bernardi's definitions (*70*) of the isochore structure of the human genome.

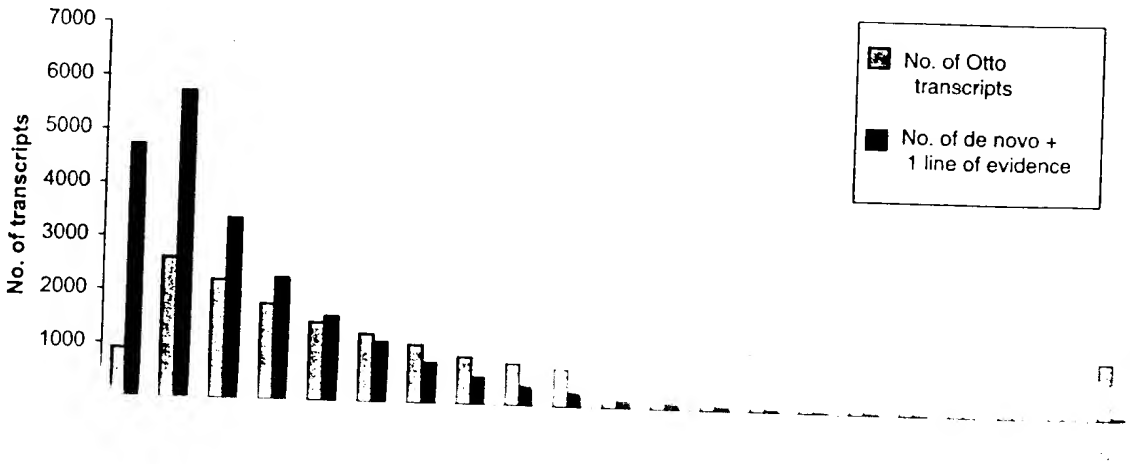

Fig. 9. Comparison of the number of exons per transcript between the 17,968 Otto transcripts and 21,350 de novo transcript predictions with at least one line of evidence that do not overlap with an Otto prediction. Both sets have the highest number of transcripts in the two-exon category, but the de novo gene predictions are skewed much more [illegible] have one or two exons, and 5.7% have more than 20. In the de novo set, 49.3% of the transcripts have one or two exons, and 0.2% have more than 20.

examined. Unfortunately, too few meiotic crossovers have occurred in Centre d'Étude du Polymorphism Humain (CEPH) and other reference families to provide a resolution any finer than about 3 Mbp. The next challenge will be to determine a sequence basis of [illegible] accurate predictor for the rate for variation in recombination rates between any pair of markers would be extremely useful in designing markers to narrow a region of linkage, such as in positional cloning projects.

4.3 Correlation between CpG islands and genes

CpG islands are stretches of unmethylated DNA with a higher frequency of CpG dinucleotides when compared with the entire genome (*74*). CpG islands are believed to preferentially occur at the transcriptional start of genes, and it has been observed that most housekeeping genes have CpG islands at the 5′ end of the transcript (*75, 76*). In addition, experimental evidence indicates that CpG island methylation is correlated with gene inactivation (*77*) and has been shown to be important during gene imprinting (*78*) and tissue-specific gene expression (*79*)

Experimental methods have been used that resulted in an estimate of 30,000 to 45,000 CpG islands in the human genome (*74, 80*) and an estimate of 499 CpG islands on human chromosome 22 (*81*). Larsen *et al.* (*76*) and Gardiner-Garden and Frommer (*75*) used a computational method to identify CpG islands and defined them as regions of DNA of >200 bp that have a G+C content of >50% and a ratio of observed versus expected frequency of CG dinucleotide ≥0.6.

It is difficult to make a direct comparison of experimental definitions of CpG islands with computational definitions because [illegible] consider the methylation state of cytosine and experimental methods do not directly select regions of high G+C content. However, we can determine the correlation of CpG island with gene starts, given a set of annotated genomic transcripts and the whole genome sequence. We have analyzed the publicly available annotation of chromosome 22, as well as using the entire human genome in our assembly and the computationally annotated genes. A variation of the CpG island computation was compared with Larsen *et al.* (*76*). The main differences are that we use a sliding window of 200 bp, consecutive windows are merged only if they overlap, and we recompute the CpG value upon merging, thus rejecting any potential island if it scores less than the threshold.

To compute various CpG statistics, we used two different thresholds of CG dinucleotide likelihood ratio. Besides using the original threshold of 0.6 (method 1), we used a higher threshold of CG dinucleotide likelihood ratio of 0.8 (method 2), which results in the number of CpG islands on chromosome 22 close to the number of annotated genes on this chromosome. The main results are summarized in Table 13. CpG islands computed with method 1 predicted only 2.6% of the CSA sequence as CpG, but 40% of the gene starts (start codons) are contained inside a CpG island. This is comparable to ratios reported by others (*82*). The last two rows of the table show the observed and expected average distance, respectively, of the closest CpG island from the first exon. The observed average distances to the closest CpG islands are smaller than the corresponding expected distances, confirming an association between CpG island and the first exon.

We also looked at the distribution of CpG island nucleotides among various sequence classes such as intergenic regions, introns, exons, and first exons. We computed the likelihood score for each sequence class as the ratio of the observed fraction of CpG island nucleotides in that sequence class and the expected fraction of CpG island nucleotides in that sequence class. The result of applying method 1 on CSA were scores of 0.89 for intergenic region, 1.2 for intron, 5.86 for exon, and 13.2 for first exon. The same trend was also found for chromosome 22 and after the application of a higher threshold (method 2) on both data sets. In sum, genome-wide analysis has extended earlier analysis and suggests a strong correlation between CpG islands and first coding exons.

4.4 Genome-wide repetitive elements

The proportion of the genome covered by various classes of repetitive DNA is presented in Table 14. We observed about 35% of the genome in these repeat classes, very similar to values reported previously (*83*). Repetitive sequence may be underrepresented in the Celera assembly as a result of incomplete repeat resolution, as discussed above. About 8% of the scaffold length is in gaps, and we expect that much of this is repetitive sequence. Chromosome 19 has the highest repeat density (57%), as well as the highest gene density (Table 10). Of interest, among the different classes of repeat elements, we observe a clear association of Alu elements and gene density, which was not observed between LINEs and gene density.

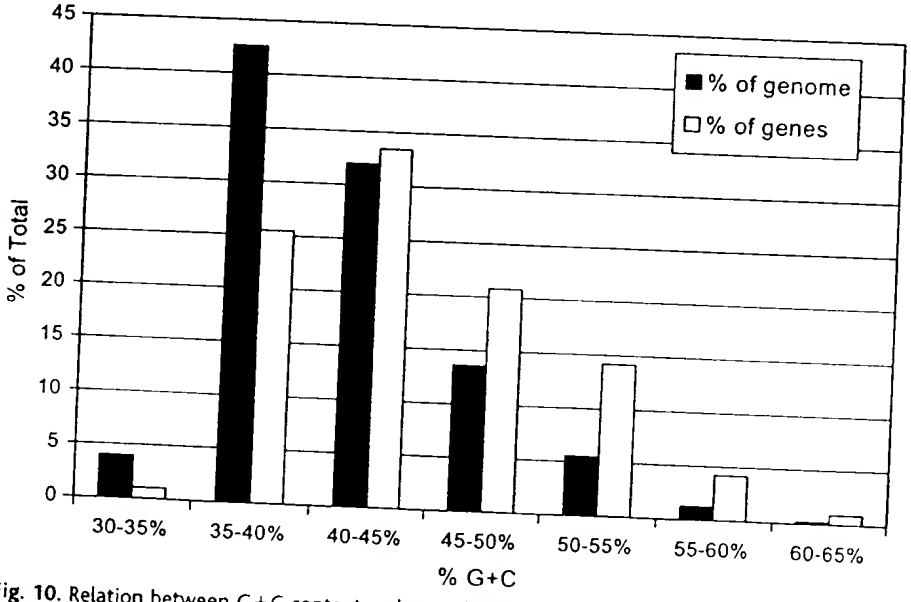

Fig. 10. Relation between G+C content and gene density. The blue bars show the percent of the genome (in 50-kbp windows) with the indicated G+C content. The percent of the [illegible]

5 Genome Evolution

Summary. The dynamic nature of genome evolution can be captured at several levels. These include gene duplications mediated by RNA intermediates (retrotransposition) and segmental genomic duplications. In this section, we document the genome-wide occurrence of retrotransposition events generating functional (intronless paralogs) or inactive genes (pseudogenes). Genes involved in translational processes and nuclear regulation account for nearly 50% of all intronless paralogs and processed pseudogenes detected in our survey. We [illegible]

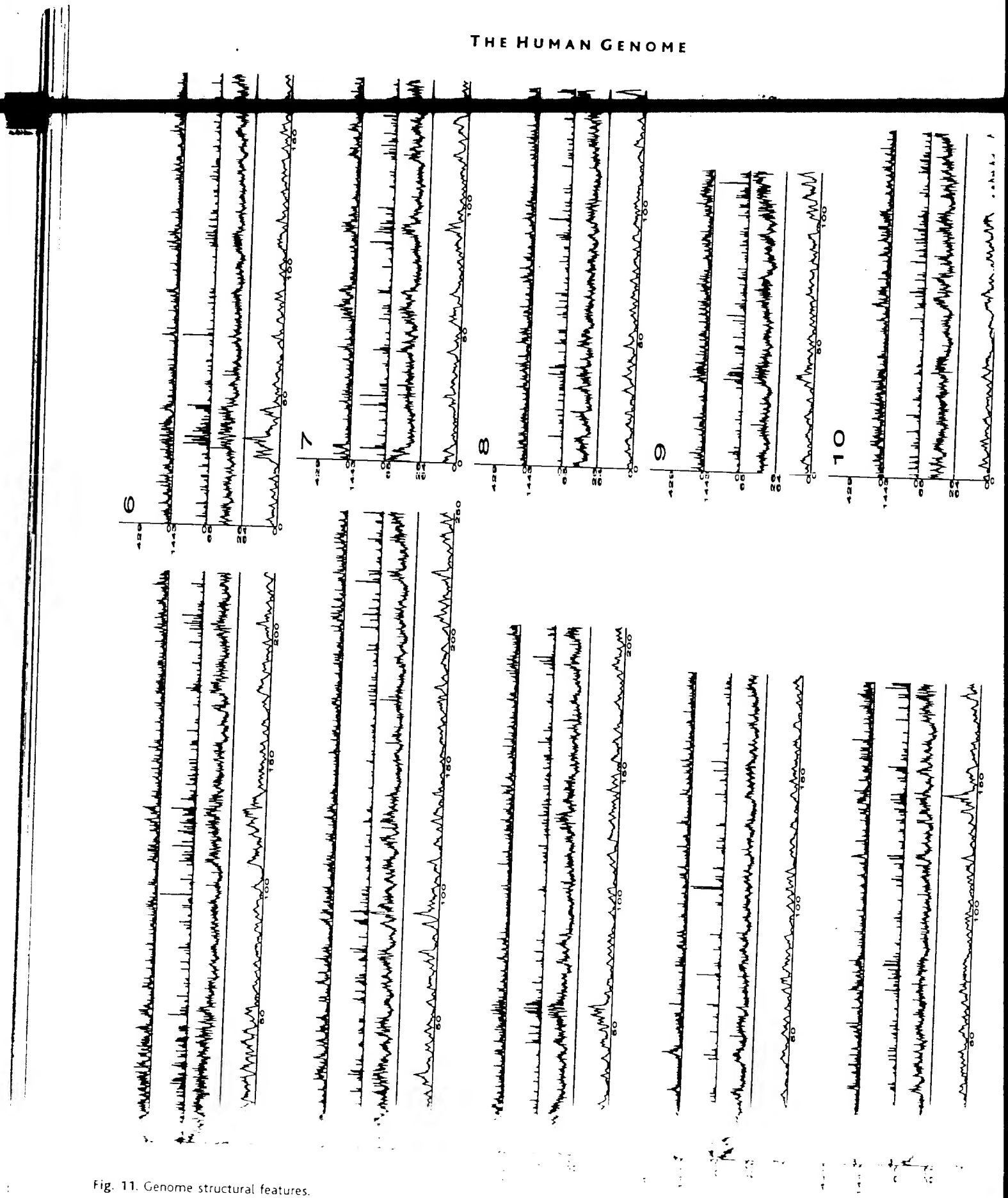

Fig. 11. Genome structural features.

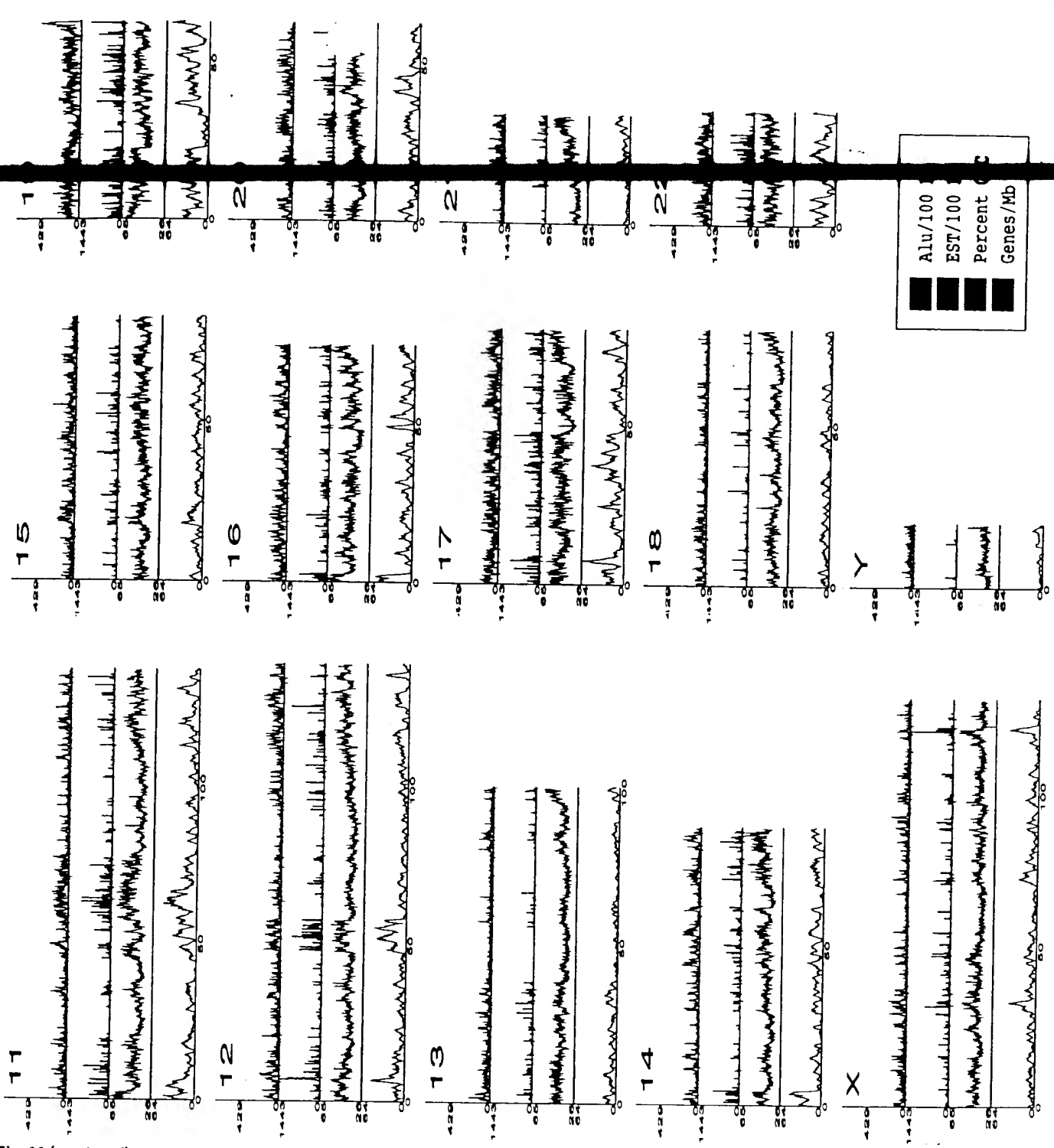

Fig. 11 (continued). Relation among gene density (orange), G+C content (green), EST density (blue), and Alu density (pink) along the lengths of each of the chromosomes. Gene density was calculated in 1-Mbp windows. The percent of G+C nucleotides was calculated in 100-kbp windows. The number of ESTs and Alu elements is shown per 100-kbp window.

5.1 Retrotransposition in the human genome

Retrotransposition of processed mRNA transcripts into the genome results in functional genes, called intronless paralogs, or inactivated genes (pseudogenes). A paralog refers to a gene that appears in more than a duplication event. The existence of both intron-containing and intronless forms of genes encoding functionally similar or identical proteins has been previously described (*84*, *85*). Cataloging these evolutionary events on the genomic landscape is of value in understanding the functional events in cellular biology. Identification of conserved intronless paralogs in the mouse or other mammalian genomes should provide the basis for capturing the evolutionary chronology of these transposition events and provide insights into gene loss

Table 1. ... refers to ... of the chromosomes. De novo/any refers to the union of de novo predictions that do not overlap Otto predictions and have at least one other type of supporting evidence; de novo/2x refers to the union of de novo predictions that do not overlap Otto predictions and have at least two types of evidence. Deserts are regions of sequence with no annotated genes.

Chr.	Sequence coverage (CS assembly)					Base composition			Gene prediction*					Gene density (genes/Mbp)					
	...of scaffolds	Largest scaffold (Mbp)	No. of scaffolds >500 kbp	Sequence covered by scaffolds >500 kbp	% of total sequence in scaffolds >500 kbp	% repeat	% GC	No of CpG islands	Otto	De novo/ any	De novo/ 2×	Total (Otto + de novo/ any)	Total (Otto + de novo/ any)	Sequence in deserts >500/ kbp	Sequence in deserts >1 Mbp	Otto	De novo/ any	De novo/ 2×	Otto + de novo/ any	Otto + de novo/ 2×
1	549	11	82	192	88	37	42	2,335	1,743	1,710	710	3,453	2,453	29	6	8	8	3	16	11
2	263	13	78	217	91	36	40	1,703	1,183	1,771	633	2,954	1,816	55	19	5	7	2	12	7
3	532	7	78	173	87	37	40	1,271	1,013	1,414	598	2,427	1,611	50	12	5	7	3	12	8
4	180	10	70	169	91	37	38	1,081	696	1,165	449	1,861	1,145	55	18	4	6	2	10	6
5	231	11	63	163	89	37	40	1,302	892	1,244	474	2,136	1,366	46	15	5	7	2	11	7
6	713	13	58	160	93	37	40	1,384	943	1,314	524	2,257	1,467	38	9	6	7	3	13	8
7	326	14	53	130	89	38	40	1,406	759	1,072	460	1,831	1,219	26	12	5	7	3	12	8
8	772	11	54	135	92	36	40	948	583	977	357	1,560	940	33	6	4	7	2	11	6
9	616	8	40	101	89	38	41	1,315	689	848	329	1,537	1,018	22	9	6	7	3	13	8
10	605	9	55	116	89	36	42	1,087	685	968	342	1,653	1,027	21	8	5	7	2	12	7
11	614	9	44	116	88	39	42	1,461	1,051	1,134	535	2,185	1,586	27	9	8	8	4	16	12
12	614	8	51	117	87	38	41	1,131	925	936	417	1,861	1,342	24	9	7	7	3	14	10
13	438	13	34	91	91	36	38	644	341	691	241	1,032	582	31	16	4	7	2	10	5
14	376	11	16	83	95	40	41	913	583	700	290	1,283	873	34	20	7	8	3	14	10
15	347	8	31	70	87	37	42	722	558	640	246	1,198	804	8	1	7	8	3	15	10
16	320	8	27	62	82	40	44	1,533	748	673	247	1,421	995	13	3	10	9	3	19	12
17	283	6	40	61	78	39	45	1,489	897	648	313	1,545	1,210	15	6	12	8	4	19	15
18	333	13	18	72	92	36	40	510	283	543	189	826	472	21	10	4	7	2	10	6
19	282	3	31	38	67	57	49	2,804	1,141	534	268	1,675	1 409	3	0	20	9	4	29	8
20	280	14	17	58	94	41	44	997	517	469	180	986	697	7	1	8	7	3	16	7
21	158	10	6	32	96	38	41	519	184	265	102	449	286	15	9	6	8	3	13	8
22	133	11	12	32	88	44	48	1,173	494	341	147	835	641	3	0	14	9	4	23	7
X	146	4	91	93	73	46	39	726	605	860	387	1,465	992	29	8	5	6	3	11	7
Y	138	2	10	12	65	50	39	65	55	155	49	210	104	4	2	3	8	2	11	5
U*	42	1						479	196	278	132	474	328							
Total	291		1,059	2,490				28,519	17,764	21,350	8,619	39,114	26,383	606	208					
Avg.	244	9	44	104	87	40	41	1,160	714	812	333	1,526	1,047	25	9	7	7	3	14	9

*Chromosome ... unknown.

Otto-predicted, single-exon genes were ... jected to BLAST analysis against the proteins encoded by the remaining multiexon predicted transcripts. Using homology criteria of 70% sequence identity over 90% of the length, we identified 298 instances of single-... sequences, 97 were represented in the GenBank data set of experimentally validated full-length genes at the stringency specified and were verified by manual inspection.

We believe that these 97 cases may represent intronless paralogs (see Web table 1 on *Science* Online at www.sciencemag.org/cgi/content/full/291/5507/1304/DC1) of known genes. Most of these are flanked by direct repeat sequences, although the precise nature of these repeats remains to be determined. All of the cases for which we have high confidence contain polyadenylated [poly(A)] tails characteristic of retrotransposition.

Recent publications describing the phenomenon of functional intronless paralogs speculate that retrotransposition may serve as a mechanism used to escape X-chromosomal inactivation (*84*, *86*). We do not find a bias toward X chromosome origination of these retrotransposed genes; rather, the results show a random chromosome distribution of both the intron-containing and corresponding intronless paralogs. We also have found several cases of retrotransposition from a single source chromosome to multiple target chromosomes. Interesting examples include the retrotransposition of a five exon–containing ribosomal protein L21 gene on chromosome 13 onto chromosomes 1, 3, 4, 7, 10, and 14, respectively. The size of the source genes can also show variability. The largest example is the 31-exon diacylglycerol kinase zeta gene on chromosome 11 that has an intronless paralog on chromosome 13. Regardless of route, retrotransposition with subsequent gene changes in coding or noncoding regions that lead to different functions or expression patterns, represents a key route to providing an enhanced functional repertoire in mammals (*87*).

Our preliminary set of retrotransposed intronless paralogs contains a clear overrepresentation of genes involved in translational processes (40% ribosomal proteins and 10% translation elongation factors) and nuclear regulation (HMG nonhistone proteins, 4%), as well as metabolic and regulatory enzymes. EST matches specific to a subset of intronless paralogs suggest expression of these intronless paralogs. Differences in the upstream regulatory sequences between the source genes and their intronless paralogs could account for differences in tissue-specific gene expression. Defining which, if any, of these processed genes are fun...

5.2 Pseudogenes

A pseudogene is a nonfunctional copy that is very similar to a normal gene but that has been altered slightly so that it is not expressed. We developed a method for the preliminary analysis of processed pseudogenes in the human genome as a starting point in elucidating the ongoing evolutionary forces ...

Size of the genome (including gaps)	2.91 Gbp
Size of the genome (excluding gaps)	2.66 Gbp
Longest contig	1.99 Mbp
Longest scaffold	14.4 Mbp
Percent of A+T in the genome	54
Percent of G+C in the genome	38
Percent of undetermined bases in the genome	9
Most GC-rich 50 kb	Chr. 2 (66%)
Least GC-rich 50 kb	Chr. X (25%)
Percent of genome classified as repeats	35
Number of annotated genes	26,383
Percent of annotated genes with unknown function	42
Number of genes (hypothetical and annotated)	39,114
Percent of hypothetical and annotated genes with unknown function	59
Gene with the most exons	Titin (234 exons)
Average gene size	27 kbp
Most gene-rich chromosome	Chr. 19 (23 genes/Mb)
Least gene-rich chromosomes	Chr. 13 (5 genes/Mb), Chr. Y (5 genes/Mb)
Total size of gene deserts (>500 kb with no annotated genes)	605 Mbp
Percent of base pairs spanned by genes	25.5 to 37.8*
Percent of base pairs spanned by exons	1.1 to 1.4*
Percent of base pairs spanned by introns	24.4 to 36.4*
Percent of base pairs in intergenic DNA	74.5 to 63.6*
Chromosome with highest proportion of DNA in annotated exons	Chr. 19 (9.33)
Chromosome with lowest proportion of DNA in annotated exons	Chr. Y (0.36)
Longest intergenic region (between annotated + hypothetical genes)	Chr. 13 (3,038,416 bp)
Rate of SNP variation	1/1250 bp

*In these ranges, the percentages correspond to the annotated gene set (26, 383 genes) and the hypothetical + annotated gene set (39,114 genes), respectively.

Table 12. Rate of recombination per physical distance (cM/Mb) across the genome. Genethon markers were placed on CSA-mapped assemblies, and then relative physical distances and rates were calculated in 3-Mb windows for each chromosome. NA, not applicable.

Chrom.	Male			Sex-average			Female		
	Max.	Avg.	Min.	Max.	Avg.	Min.	Max.	Avg.	Min.
1	2.60	1.12	0.23	2.81	1.42	0.52	3.39	1.76	0.68
2	2.23	0.78	0.33	2.65	1.12	0.54	3.17	1.40	0.61
3	2.55	0.86	0.23	2.40	1.07	0.42	2.71	1.30	0.33
4	1.66	0.67	0.15	2.06	1.04	0.60	2.50	1.40	0.77
5	2.00	0.67	0.18	1.87	1.08	0.42	2.26	1.43	0.62
6	1.97	0.71	0.28	2.57	1.12	0.37	3.47	1.67	0.64
7	2.34	1.16	0.48	1.67	1.17	0.47	2.27	1.21	0.34
8	1.83	0.73	0.14	2.40	1.05	0.46	3.44	1.36	0.43
9	2.01	0.99	0.53	1.95	1.32	0.77	2.63	1.66	0.82
10	3.73	1.03	0.22	3.05	1.29	0.66	2.84	1.51	0.76
11	1.43	0.72	0.31	2.13	0.99	0.47	3.10	1.32	0.49
12	4.12	0.76	0.26	3.35	1.16	0.49	2.93	1.55	0.59
13	1.60	0.75	0.01	1.87	0.95	0.17	2.49	1.19	0.32
14	3.15	0.98	0.18	2.65	1.30	0.62	3.14	1.63	0.75
15	2.28	0.94	0.34	2.31	1.22	0.42	2.53	1.56	0.54
16	1.83	1.00	0.47	2.70	1.55	0.63	4.99	2.32	1.12
17	3.87	0.87	0.00	3.54	1.35	0.54	4.19	1.83	0.94
18	3.12	1.37	0.86	3.75	1.66	0.43	4.35	2.24	0.72
19	3.02	0.97	0.10	2.57	1.41	0.49	2.89	1.75	0.87
20	3.64	0.89	0.00	2.79	1.50	0.83	3.31	2.15	1.34
21	3.23	1.26	0.69	2.37	1.62	1.08	2.58	1.90	1.18
22	1.25	1.10	0.84	1.88	1.41	1.08	3.73	2.08	0.93
X	NA	NA	NA	...	...	...	...	...	...

that account for gene inactivation. The general structural characteristics of these pro-

lack of intervening sequences found in the functional counterparts, a poly(A) tract at the 3′ end, and direct repeats flanking the pseudogene sequence. Processed pseudogenes occur as a result of retrotransposition, whereas unprocessed pseudogenes arise from segmental genome duplication.

We searched the complete set of Otto-predicted transcripts against the genomic sequence by means of BLAST. Genomic regions corresponding to all Otto-predicted transcripts were excluded from this analysis. We identified 2909 regions matching with greater than 70% identity over at least 70% of the length of the transcripts that likely represent processed pseudogenes. This number is probably an underestimate because specific methods to search for pseudogenes were not used.

We looked for correlations between structural elements and the propensity for retrotransposition in the human genome. GC content and transcript length were compared between the genes with processed pseudogenes (1177 source genes) versus the remainder of the predicted gene set

dogenes have shorter average transcript length (1027 bp versus 1594 bp for the Otto set) as compared with genes for which no pseudogene was detected. The overall GC content did not show any significant difference, contrary to a recent report (*88*). There is a clear trend in gene families that are present as processed pseudogenes. These include ribosomal proteins (67%), lamin receptors (10%), translation elongation factor alpha (5%), and HMG–non-histone proteins (2%). The increased occurrence of retrotransposition (both intronless paralogs and processed pseudogenes) among genes involved in translation and nuclear regulation may reflect an increased transcriptional activity of these genes.

5.3 Gene duplication in the human genome

Building on a previously published procedure (*27*), we developed a graph-theoretic algorithm, called Lek, for grouping the predicted human protein set into protein families (*89*).

Table 13. Characteristics of CpG islands identified in chromosome 22 (34-Mbp sequence length) and the whole genome (2.9-Gbp sequence length) by means of two different methods. Method 1 uses a CG likelihood ratio of ≥0.6. Method 2 uses a CG likelihood ratio of ≥0.8.

	Chromosome 22		Whole genome (CS assembly)	
	Method 1	Method 2	Method 1	Method 2
Number of CpG islands detected	5,211	522	195,706	26,876
Average length of island (bp)	390	535	395	497
Percent of sequence predicted as CpG	5.9	0.8	2.6	0.4
Percent of first exons that overlap a CpG island	44	25	42	22
Percent of first exons with first position of exon contained inside a CpG island	37	22	40	21
Average distance between first exon and closest CpG island (bp)	1,013	10,486	2,182	17,021
Expected distance between first exon and closest CpG island (bp)	3,262	32,567	7,164	55,811

Table 14. Distribution of repetitive DNA in the compartmentalized shotgun assembly sequence.

Repetitive elements	Megabases in assembled sequences	Percent of assembly	Previously predicted (%) (*83*)
Alu	288		
Total	1025	35.3	35.6

The complete clusters that result from the Lek clustering provide a basis for

ing the role of whole-genome or chromosomal duplication in protein family expansion as opposed to other means, such as tandem duplication. Because each complete cluster represents a closed and certain island of homology, and because Lek is capable of simultaneously clustering protein complements of several organisms, the number of proteins contributed by each organism to a complete cluster can be predicted with confidence depending on the quality of the annotation of each genome. The variance of each organism's contribution to each cluster can then be calculated, allowing an assessment of the relative importance of large-scale duplication versus smaller-scale, organism-specific expansion and contraction of protein families, presumably as a result of natural selection operating on individual protein families within an organism. As can be seen in Fig. 12, the large variance in the relative numbers of human as compared with *D. melanogaster* and *Caenorhabditis elegans* proteins in complete clusters may be explained by multiple events of relative expansions in gene families in each of the three animal genomes. Such expansions would give rise to the distribution that shows a peak at 1:1 in the ratio for human-worm or human-fly clusters with the slope spread covering both human and fly/worm predominance, as we observed (Fig. 12). Furthermore, there are nearly as many clusters where worm and fly proteins predominate despite the larger numbers of proteins in the human. At face value, this analysis suggests that natural selection acting on individual protein families has been a major force driving the expansion of at least some elements of the human protein set. However, in our analysis, the difference between an ancient whole-genome duplication followed by loss, versus piecemeal duplication, cannot be easily distinguished. In order to differentiate these scenarios, more extended analyses were performed.

5.4 Large-scale duplications

Using two independent methods, we searched for large-scale duplications in the human genome. First, we describe a protein family–based method that identified highly conserved blocks of duplication. We then describe our comprehensive method for identifying all interchromosomal block duplications. The latter method identified a large number of duplicated chromosomal segments covering

served homologous proteins that occur in more than one location on the genome. For this comparison, two genes were considered equivalent if their protein products were de-

termined to be in the same family and same complete Lek cluster (essentially paralogous genes) (*89*). Initially, each chromosome was represented as a string of genes ordered by the start codons for predicted genes along the chromosome. We considered local inversions are relatively common events relative to large-scale duplications. Each gene was indexed according to the protein family and Lek complete cluster (*89*). All pairs of indexed gene strings were then aligned in both the forward and reverse directions with the Smith-Waterman algorithm (*90*). A match between two proteins of the same Lek complete cluster was given a score of 10 and a mismatch −10, with gap open and extend penalties of −4 and −1. With these parameters, 19 conserved interchromosomal blocks of duplication were observed, all of which were also detected and expanded by the comprehensive method described below. The detection of only a relatively small number of block duplications was a consequence of using an intrinsically conservative method grounded in the conservative constraints of the complete Lek clusters.

In the second, more comprehensive approach, we aligned all chromosomes directly with one another using an algorithm based on the MUMmer system (*91*). This alignment method uses a suffix tree data structure and a linear-time algorithm to align long sequences very rapidly; for example, two chromosomes of 100 Mbp can be aligned in less than 20 min (on a Compaq Alpha computer) with 4 gigabytes of memory. This procedure was used recently to identify numerous large-scale segmental duplications among the five chromosomes of *A. thaliana* (*92*); in that organism, the method revealed that 60% of the genome (66 Mbp) is covered by 24 very large duplicated segments. For *Arabidopsis*, a DNA-based alignment was sufficient to reveal the segmental duplications between chromosomes; in the human genome, DNA alignments at the whole-chromosome level are insufficiently sensitive. Therefore, a modified procedure was developed and applied, as follows. First, all 26,588 proteins (9,675,713 million amino acids) were concatenated end-to-end in order as they occur along each of the 24 chromosomes, irrespective of strand location. The concatenated protein set was then aligned against each chromosome by the MUMmer algorithm. The resulting matches were clustered to extract all sets of three or more protein matches that occur in close proximity on two different chromosomes (*93*); these represent the candidate segmental duplications. A series of filters were developed and applied to remove likely false-positives from this set: for exam-

filtering methods, a shuffled protein set was first created by taking the 26,588 proteins, randomizing their order, and then partitioning them into 24 shuffled chromosomes, each containing the same number of proteins as the true genome. This shuffled protein set has the [illegible] particular, every protein and every domain appears the same number of times. The complete algorithm was then applied to both the real and the shuffled data, with the results on the shuffled data being used to estimate the false-positive rate. The algorithm after filtering yielded 10,310 gene pairs in 1077 duplicated blocks containing 3522 distinct genes; tandemly duplicated expansions in many of the blocks explain the excess of gene pairs to distinct genes. In the shuffled data, by contrast, only 370 gene pairs were found, giving a false-positive estimate of 3.6%. The most likely explanation for the 1077 block duplications is ancient segmental duplications. In many cases, the order of the proteins has been shuffled, although proximity is preserved. Out of the 1077 blocks, 159 contain only three genes, 137 contain four genes, and 781 contain five or more genes.

To illustrate the extent of the detected duplications, Fig. 13 shows all 1077 block duplications indexed to each chromosome in 24 panels in which only duplications mapped to the indexed chromosome are displayed. The figure makes it clear that the duplications are ubiquitous in the genome. One feature that it displays is many relatively small chromosomal stretches, with one-to-many duplication relationships that are graphically striking. One such example captured by the analysis is the well-documented olfactory receptor (OR) family, which is scattered in blocks throughout the genome and which has been analyzed for genome-deployment reconstruc-

[illegible]s at several evolutionary stages (*94*). The figure also illustrates that some chromosomes, such as chromosome 2, contain many more detected large-scale duplications than others. Indeed, one of the largest duplicated segments in a large block of 33 [illegible] chromosome 2, spread among eight smaller blocks in 2p, that aligns to a paralogous set on chromosome 14, with one rearrangement (see chromosomes 2 and 14 panels in Fig. 13). The proteins are not contiguous but span a region containing 97 proteins on chromosome 2 and 332 proteins on chromosome 14. The likelihood of observing this many duplicated proteins by chance, even over a span of this length, is 2.3×10^{-68} (*93*). This duplicated set spans 20 Mbp on chromosome 2 and 63 Mbp on chromosome 14, over 70% of the latter chromosome. Chromosome 2 also contains a block duplication that is nearly as large, which is shared by chromosome arm 2q and chromosome 12. This duplication incorporates two of the four known Hox gene clusters, but considerably expands the extent of the duplications proximally and distally on the pair of chromosome arms. This breadth of duplication is also seen on the two chromosomes carrying the other two Hox clusters.

An additional large duplication, between chromosomes 18 and 20, serves as a good example to illustrate some of the features common to many of the other observed large duplications (Fig. 13, inset). This duplication contains 64 detected ordered intrachromosomal pairs of homologous genes. After discounting a 40-Mb stretch of chromosome 18 free of matches to chromosome 20, which is likely to represent a large insert (between the gene assignments "Krup rel" and "collagen rel" on chromosome 18 in Fig. 13), the full duplication segment covers 36 Mb on chromosome 18 and 28 Mb on chromosome 20.

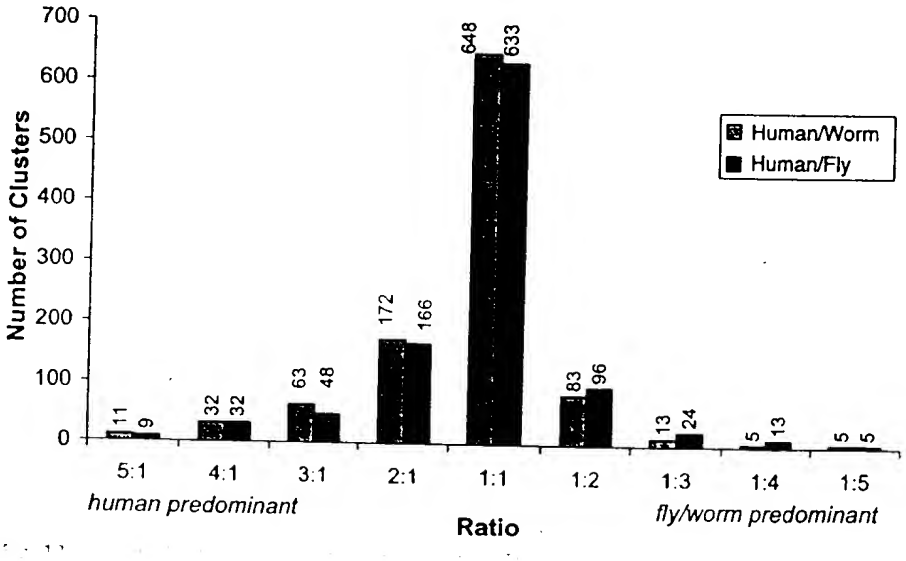

By this measure, the duplication segment [illegible] length. The most likely scenario is that the whole span of this region was duplicated as a single very large block, followed by shuffling owing to smaller scale rearrangements. As such, at least four subsequent rearrangements would need to be invoked to explain the relative insertions and inversions seen in the duplicated segment interval. The 64 protein pairs in this alignment occur among 217 protein assignments on chromosome 18, and among 322 protein assignments on chromosome 20, for a density of involved proteins of 20 to 30%. This is consistent with an ancient large-scale duplication followed by subsequent gene loss on one or both chromosomes. Loss of just one member of a gene pair subsequent to the duplication would result in a failure to score a gene pair in the block; less than 50% gene loss on the chromosomes would lead to the duplication density observed here. As an independent verification of the significance of the alignments detected, it can be seen that a substantial number of the pairs of aligning proteins in this duplication, including some of those annotated (Fig. 13), are those populating small Lek complete clusters (see above). This indicates that they are members of very small families of paralogs; their relative scarcity within the genome validates the uniqueness and robust nature of their alignments.

Two additional qualitative features were observed among many of the large-scale duplications. First, several proteins with disease associations, with OMIM (Online Mendelian Inheritance in Man) assignments, are members of duplicated segments (see web table 2 on *Science* Online at www.sciencemag.org/cgi/content/full/291/5507/1304/DC1). We have also observed a few instances where paralogs on both duplicated segments are associated with similar disease conditions. Notable among these genes are proteins involved in hemostasis (coagulation factors) that are associated with bleeding disorders, transcriptional regulators like the homeobox proteins associated with developmental disorders, and potassium channels associated with cardiovascular conduction abnormalities. For each of these disease genes, closer study of the paralogous genes in the duplicated segment may reveal new insights into disease causation, with further investigation needed to determine whether they might be involved in the same or similar genetic diseases. Second, although there is a conserved number of proteins and coding exons predicted for spe-

[illegible] pair of duplicated chromosome regions was [illegible] ses to explain which mechanisms foster these processes must be tested.

Evaluation of the alignment results gives some perspective on dating of the duplications. As noted above, large-scale ancient segmental duplication in fact best explains many of the blocks detected by this genome-wide analysis. The regions of human chromosomes involved in the large-scale duplications expanded upon above (chromosomes 2 to 14, 2 to 12, and 18 to 20) are each syntenic to a distinct mouse chromosomal region. The corresponding mouse chromosomal regions are much more similar in sequence conservation, and even in order, to their human synteny partners than the human duplication regions are to each other. Further, the corresponding mouse chromosomal regions each bear a significant proportion of genes orthologous to the human genes on which the human duplication assignments were made. On the basis of these factors, the corresponding mouse chromosomal spans, at coarse resolution, appear to be products of the same large-scale duplications observed in humans. Although further detailed analysis must be carried out once a more complete genome is assembled for mouse, the underlying large duplications appear to predate the two species' divergence. This dates the duplications, at the latest, before divergence of the primate and rodent lineages. This date can be further refined upon examination of the synteny between human chromosomes and those of chicken, pufferfish (*Fugu rubripes*), or zebrafish (*95*). The only substantial syntenic stretches mapped in these species corresponding to both pairs of human duplications are restricted to the Hox cluster regions. When the synteny of these regions (or others) to human chromosomes is extended with further mapping, the ages of the nearly chromosome-length duplications seen in humans are likely to be dated to the root of vertebrate divergence.

The MUMmer-based results demonstrate large block duplications that range in size from a few genes to segments covering most of a chromosome. The extent of segmental duplications raises the question of whether an ancient whole-genome duplication event is the underlying explanation for the numerous duplicated regions (*96*). The duplications have undergone many deletions and subsequent rearrangements; these events make it difficult to distinguish between a whole-genome duplication and multiple smaller events. Further analysis, focused especially on comparing the estimated ages of

[illegible] veal the stagewise history of our genome [illegible] the key functions that distinguish us from oth living things.

6 A Genome-Wide Examination of Sequence Variations

Summary. Computational methods were us to identify single-nucleotide polymorphisn (SNPs) by comparison of the Celera sequen to other SNP resources. The SNP rate b tween two chromosomes was ~1 per 1200 1500 bp. SNPs are distributed nonrandoml throughout the genome. Only a very sma proportion of all SNPs (<1%) potentiall impact protein function based on the fun tional analysis of SNPs that affect the pr dicted coding regions. This results in an e timate that only thousands, not millions, c genetic variations may contribute to the struc tural diversity of human proteins.

Having a complete genome sequence enable researchers to achieve a dramatic acceleration in the rate of gene discovery, but only through analysis of sequence variation in DNA can we discover the genetic basis for variation in health among human beings. Whole-genome shotgun sequencing is a particularly effective method for detecting sequence variation in tandem with whole-genome assembly. In addition, we compared the distribution and attributes of SNPs ascertained by three other methods: (i) alignment of the Celera consensus sequence to the PFP assembly, (ii) overlap of high-quality reads of genomic sequence (referred to as "Kwok"; 1,120,195 SNPs) (*97*), and (iii) reduced representation shotgun sequencing (referred to as "TSC"; 632,640 SNPs) (*98*). These data were consistent in showing an overall nucleotide diversity of ~8×10^{-4}, marked heterogeneity across the genome in SNP density, and an overwhelming preponderance of noncoding variation that produces no change in expressed proteins.

6.1 SNPs found by aligning the Celera consensus to the PFP assembly

Ideally, methods of SNP discovery make full use of sequence depth and quality at every site, and quantitatively control the rate of false-positive and false-negative calls with an explicit sampling model (*99*). Comparison of consensus sequences in the absence of these details necessitated a more ad hoc approach (quality scores could not readily be obtained for the PFP assembly). First, all sequence differences between the two consensus sequences were identified;

[illegible] the cases more than 10-fold longer than the corresponding chromosome 20 DNA. This selective accretion of noncoding DNA (or conversely, loss of noncoding DNA) on one of a

[illegible] hypotheses is more likely. Comparisons of genomes of different vertebrates, and even cross-phyla genome comparisons, will allow for the deconvolution of duplications to eventually re-

[illegible] steps, we monitored the ratio of transition and transversion substitutions, because a 2:1 ratio has been well documented as typical in mammalian evolution (*100*) and in human SNPs

(*101*, *102*). The filtering steps consisted of moving variants where the quality score in the Celera consensus was less than 30 and where the density of variants was greater than 5 in 400 bp. These filters resulted in shifting the transition-to-transversion ratio from 1.57:1 to [illegible] between the Celera and PFP consensus sequences, these filters resulted in identification of 2,104,820 putative SNPs from a total of 2,778,474 substitution differences. Overlaps between this set of SNPs and those found by other methods are described below.

6.2 Comparisons to public SNP databases

Additional SNPs, including 2,536,021 from dbSNP (www.ncbi.nlm.nih.gov/SNP) and 13,150 from HGMD (Human Gene Mutation Database, from the University of Wales, UK), were mapped on the Celera consensus sequence by a sequence similarity search with the program PowerBlast (*103*). The two largest data sets in dbSNP are the Kwok and TSC sets, with 47% and 25% of the dbSNP records. Low-quality alignments with partial coverage of the dbSNP sequence and alignments that had less than 98% sequence identity between the Celera sequence and the dbSNP flanking sequence were eliminated. dbSNP sequences mapping to multiple locations on the Celera genome were discarded. A total of 2,336,935 dbSNP variants were mapped to 1,223,038 unique locations on the Celera sequence, implying considerable redundancy in dbSNP. SNPs in the TSC set mapped to 585,811 unique genomic locations, and SNPs in the Kwok set mapped to 438,032 unique locations. The combined unique SNPs counts used in this analysis, including Celera-PFP, TSC, and Kwok, is 2,737,668. Table 15 shows that a substantial fraction of SNPs identified by one of these methods was also found by another method. The very high overlap (36.2%) between the Kwok and Celera-PFP SNPs may be due in part to the use by Kwok of sequences that went into the PFP assembly. The unusually low overlap (16.4%) between the Kwok and TSC sets is due to their being the smallest two sets. In addition, 24.5% of the Celera-PFP SNPs overlap with SNPs derived from the Celera genome sequences (*46*). SNP validation in population samples is an expensive and laborious process, so confirmation on multiple data sets may [illegible] (by computational analysis).

One means of assessing whether the three sets of SNPs provide the same picture of human variation is to tally the frequencies of the six possible base changes in each set of SNPs (Table 16). Previous measures of nucleotide diversity were mostly derived from small-scale analysis on candidate genes (*101*), and our analysis with all three data sets validates the previous observations at the whole-genome scale. There is remarkable homogeneity between the SNPs found in the Kwok set, the TSC set, and in our whole-genome shotgun (*46*) in this substitution pattern. Compared with the rest of the data sets, Celera-PFP deviates slightly from the 2:1 transition-to-transversion ratio observed in the other SNP sets. This result is not unexpected, because some fraction of the computationally identified SNPs in the Celera-PFP comparison may in fact be sequence errors. A 2:1 transition:transversion ratio for the bona fide SNPs would be obtained if one assumed that 15% of the sequence differences in the Celera-PFP set were a result of (presumably random) sequence errors.

6.3 Estimation of nucleotide diversity from ascertained SNPs

The number of SNPs identified varied widely across chromosomes. In order to normalize these values to the chromosome size and sequence coverage, we used π, the standard statistic for nucleotide diversity (*104*). Nucleotide diversity is a measure of per-site heterozygosity, quantifying the probability that a pair of chromosomes drawn from the population will differ at a nucleotide site. In order to calculate nucleotide diversity for each chromosome, we need to know the number of nucleotide sites that were surveyed for variation, and in methods like reduced respresentation sequencing, we need to know the sequence quality and the depth of coverage at each site. These data are not readily available, so we could not estimate nucleotide diversity from the TSC effort. Estimation of nucleotide diversity from high-quality sequence overlaps should be possible, but again, [illegible] of all the alignments.

Estimation of nucleotide diversity from a shotgun assembly entails calculating for each column of the multialignment, the probability that two or more distinct alleles are present, and the probability of detecting a SNP if in fact the alleles have different sequence (i.e., the probability of correct sequence calls). The greater the depth of coverage and the higher the sequence quality, the higher is the chance of successfully detecting a SNP (*105*). Even after correcting for variation in coverage, the nucleotide diversity appeared to vary across autosomes. The significance of this heterogeneity was tested by analysis of variance, with estimates of π for 100-kbp windows to estimate variability within chromosomes (for the Celera-PFP comparison, $F = 29.73$, $P < 0.0001$).

Average diversity for the autosomes estimated from the Celera-PFP comparison was 8.94×10^{-4}. Nucleotide diversity on the X chromosome was 6.54×10^{-4}. The X is expected to be less variable than autosomes, because for every four copies of autosomes in the population, there are only three X chromosomes, and this smaller effective population size means that random drift will more rapidly remove variation from the X (*106*).

Having ascertained nucleotide variation genome-wide, it appears that previous estimates of nucleotide diversity in humans based on samples of genes were reasonably accurate (*101*, *102*, *106*, *107*). Genome-wide, our estimate of nucleotide diversity was 8.98×10^{-4} for the Celera-PFP alignment, and a published estimate averaged over 10 densely resequenced human genes was 8.00×10^{-4} (*108*).

6.4 Variation in nucleotide diversity across the human genome

Such an apparently high degree of variability among chromosomes in SNP density raises the question of whether there is heterogeneity at a finer scale within chromo-

Table 15. Overlap of SNPs from genome-wide SNP databases. Table entries are SNP counts for each pair of data sets. Numbers in parentheses are the fraction of overlap, calculated as the count of overlapping SNPs divided by the number of SNPs in the smaller of the two databases compared. Total SNP counts for the databases are: Celera-PFP, 2,104,820; TSC, 585,811; and Kwok 438,032. Only unique SNPs in the TSC and Kwok data sets were included.

	TSC	Kwok
Celera-PFP	188,694 (0.322)	158,532 (0.362)
[illegible]		

Table 16. Summary of nucleotide changes in different SNP data sets.

SNP data set	A/G (%)	C/T (%)	A/C (%)	A/T (%)	C/G (%)	T/G (%)	Transition: transversion
Celera-PFP	30.7	30.7	10.3	8.6	9.2	10.3	1.59:1
Kwok*	33.7	33.8	8.5	7.0	8.6	8.4	2.07:1
TSC†	33.3	33.4	8.8	7.3	8.6	8.6	1.99:1

*November 2000 release of the NCBI database dbSNP [illegible]

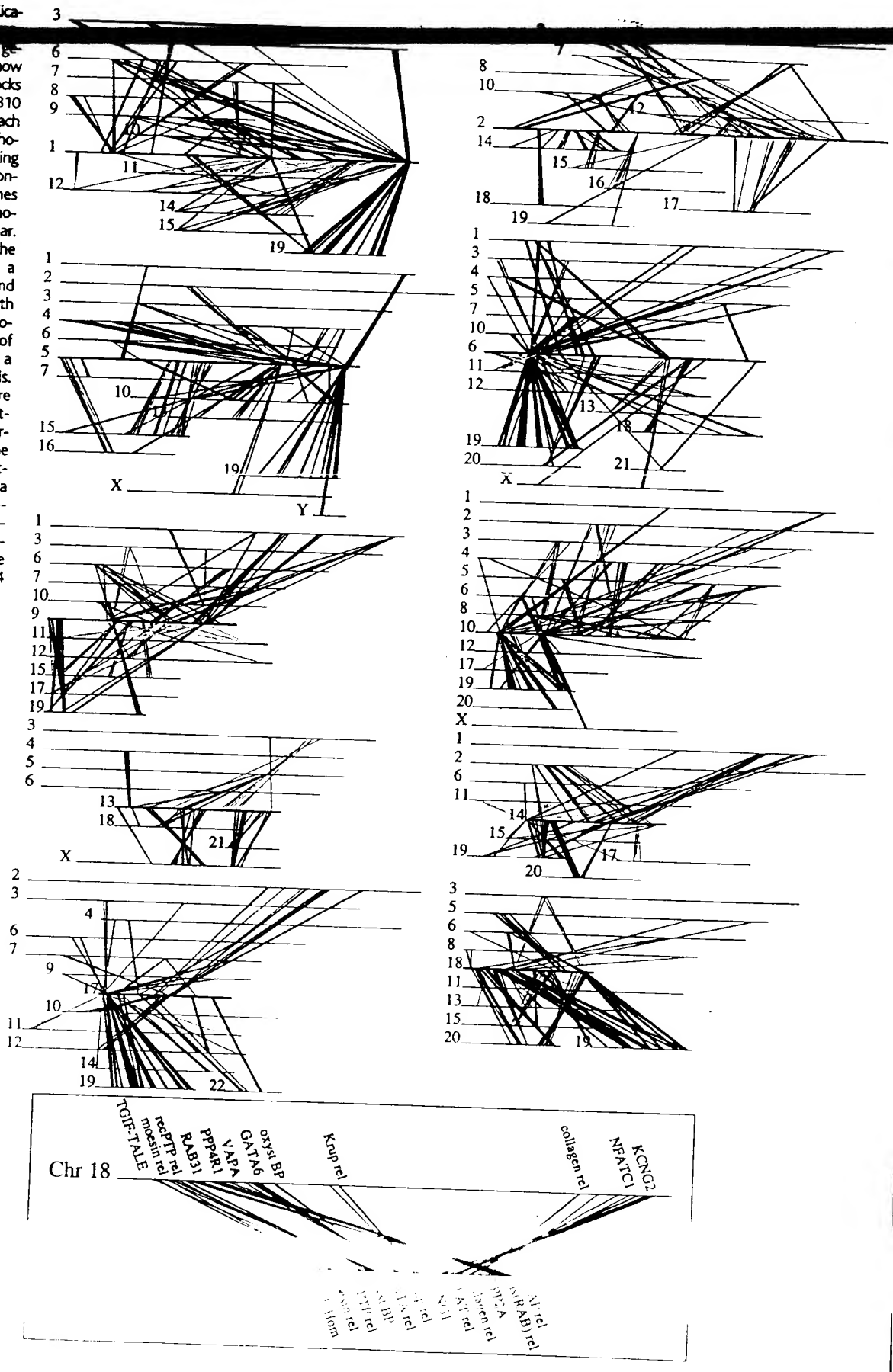

Fig. 13. Segmental duplications in the human genome. The 24 panels show the 1077 duplicated blocks of genes, containing 10,310 pairs of genes in total. Each line represents a pair of homologous genes belonging to a block; all blocks contain at least three genes on each of the chromosomes where they appear. Each panel shows all the duplications between a single chromosome and other chromosomes with shared blocks. The chromosome at the center of each panel is shown as a thick red line for emphasis. Other chromosomes are displayed from top to bottom within each panel ordered by chromosome number. The inset (bottom, center right) shows a close-up of one duplication between chromosomes 18 and 20, expanded to display the gene names of 12 of the 64 gene pairs shown.

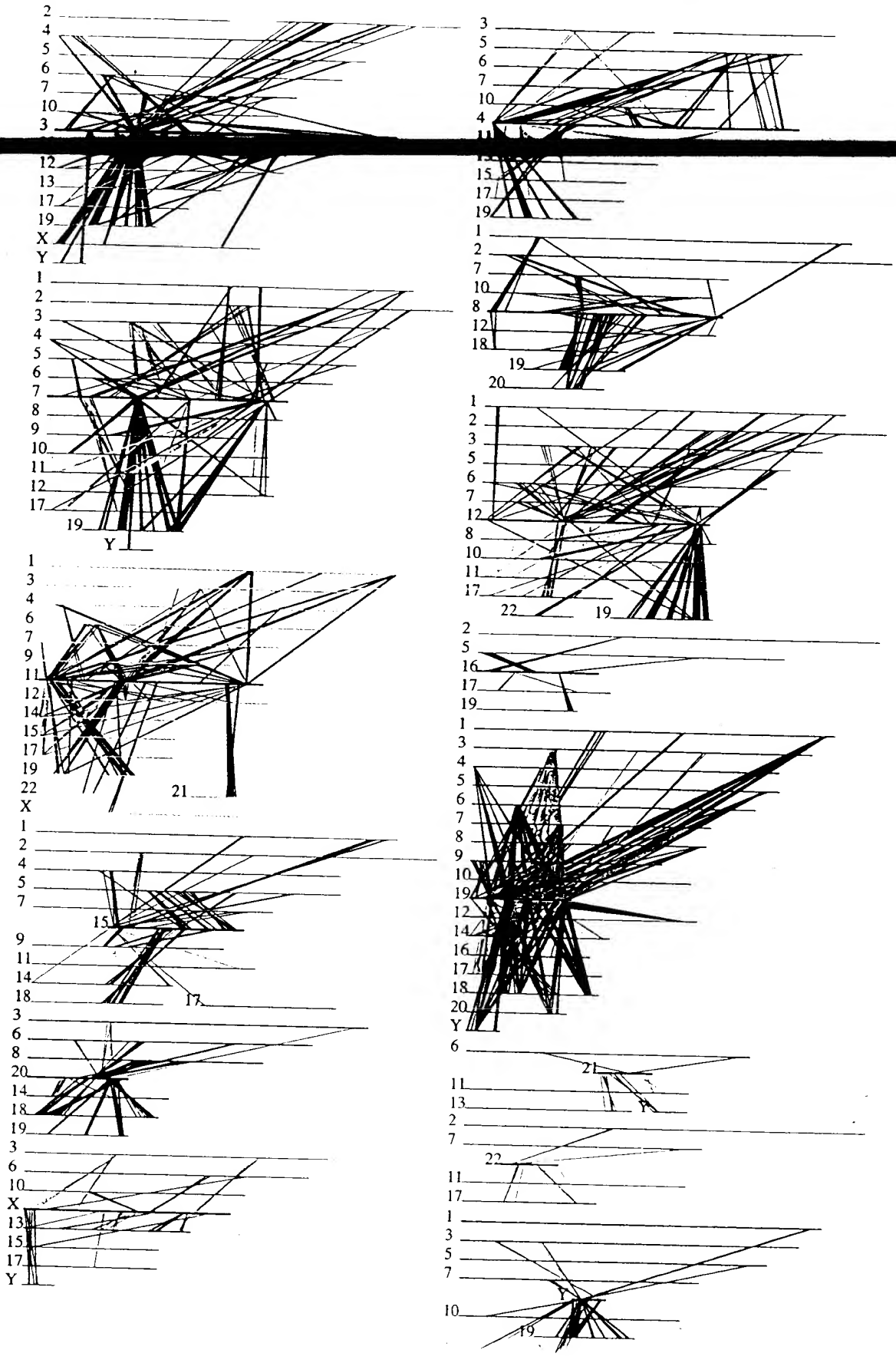

somes, and whether this heterogeneity is occur by random and independent mutations, then it would seem that there ought to be a Poisson distribution of numbers of SNPs in fragments of arbitrary constant size. The observed dispersion in the distribution of SNPs in 100-kbp fragments was far greater than predicted from a Poisson distribution (Fig. 14). However, this simplistic model ignores the different recombination rates and population histories that exist in different regions of the genome. Population genetics theory holds that we can account for this variation with a mathematical formulation called the neutral coalescent (*109*). Applying well-tested algorithms for simulating the neutral coalescent with recombination (*110*), and using an effective population size of 10,000 and a per-base recombination rate equal to the mutation rate (*111*), we generated a distribution of numbers of SNPs by this model as well (*112*). The observed distribution of SNPs has a much larger variance than either the Poisson model or the coalescent model, and the difference is highly significant. This implies that there is significant variability across the genome in SNP density, an observation that begs an explanation.

Several attributes of the DNA sequence may affect the local density of SNPs, including the rate at which DNA polymerase makes errors and the efficacy of mismatch repair. One key factor that is likely to be associated with SNP density is the G+C content, in part because methylated cytosines in CpG dinucleotides tend to undergo deamination to form thymine, accounting for a nearly 10-fold increase in the mutation rate of CpGs over other dinucleotides. We tallied the GC content and nu-

across the entire genome and found that the correlation between them was positive (r = 0.21) and highly significant ($P < 0.0001$), but G+C content accounted for only a small part of the variation.

6.5 SNPs by genomic class

To test homogeneity of SNP densities across functional classes, we partitioned sites into intergenic (defined as >5 kbp from any predicted transcription unit), 5′-UTR, exonic (missense and silent), intronic, and 3′-UTR for 10,239 known genes, derived from the NCBI RefSeq database and all human genes predicted from the Celera Otto annotation. In coding regions, SNPs were categorized as either silent, for those that do not change amino acid sequence, or missense, for those that change the protein product. The ratio of missense to silent coding SNPs in Celera-PFP, TSC, and Kwok sets (1.12, 0.91, and 0.78, respectively) shows a markedly reduced frequency of missense variants compared with the neutral expectation, consistent with the elimination by natural selection of a fraction of the deleterious amino acid changes (*112*). These ratios are comparable to the missense-to-silent ratios of 0.88 and 1.17 found by Cargill *et al.* (*101*) and by Halushka *et al.* (*102*). Similar results were observed in SNPs derived from Celera shotgun sequences (*46*).

It is striking how small is the fraction of SNPs that lead to potentially dysfunctional alterations in proteins. In the 10,239 RefSeq genes, missense SNPs were only about 0.12, 0.14, and 0.17% of the total SNP SNPs, respectively. Nonconservative protein changes constitute an even smaller fraction of missense SNPs (47, 41, and 40% in Celera-PFP, Kwok, and TSC). Intergenic regions have been virtually unstudied (*113*), and we note that 75% of the SNPs we identified were intergenic (Table 17). The SNP rate was highest in introns and lowest in exons. The SNP rate was lower in intergenic regions than in introns, providing one of the first discriminators between these two classes of DNA. These SNP rates were confirmed in the Celera SNPs, which also exhibited a lower rate in exons than in introns, and in extragenic regions than in introns (*46*). Many of these intergenic SNPs will provide valuable information in the form of markers for linkage and association studies, and some fraction is likely to have a regulatory function as well.

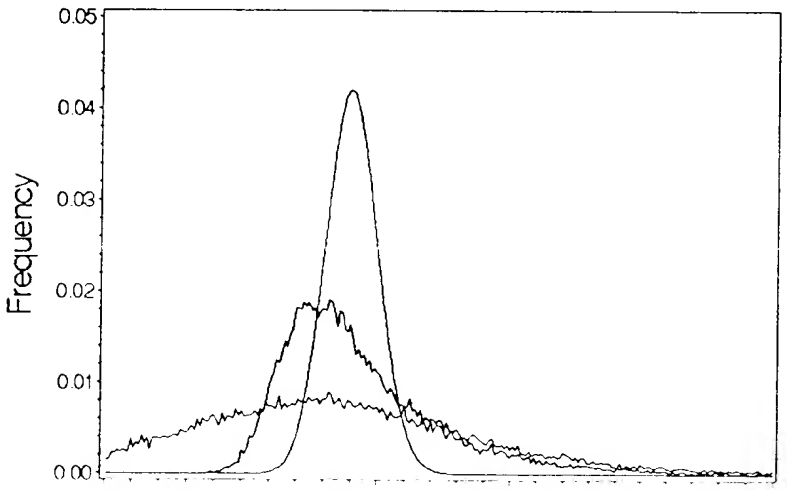

Fig. 14. SNP density in each 100 kbp interval as determined with Celera-PFP SNPs. The color codes are as follows: black, Celera-PFP SNP density; blue, coalescent model; and red, Poisson distribution. The figure shows that the distribution of SNPs along the genome is nonrandom and is not entirely accounted for by a coalescent model of regional history.

7 An Overview of the Predicted Protein-Coding Genes in the Human Genome

Summary. This section provides an initial computational analysis of the predicted protein set with the aim of cataloging prominent differences and similarities when the human genome is compared with other fully sequenced eukaryotic genomes. Over 40% of the predicted protein set in humans cannot be ascribed a molecular function by methods that assign proteins to known families. A protein domain–based analysis provides a detailed catalog of the prominent differences in the human genome when compared with the fly and worm genomes. Prominent among these are domain expansions in proteins involved in developmental regulation and in cellular processes such as neuronal function, hemostasis, acquired immune response, and cytoskeletal complexity. The final enumeration of protein families and details of protein structure will rely on additional experimental work and comprehensive manual curation.

A preliminary analysis of the predicted human protein-coding genes was conducted. Two methods were used to analyze and classify the molecular functions of 26,588 predicted proteins that represent 26,383 gene predictions with at least two lines of evidence as described above. The first method was based on an analysis at the level of protein families, with both the publicly available

[illegible] the level of protein domains, with both the Pfam and SMART databases (*115*, *117*).

The results presented here are preliminary and are subject to several limitations.

Both the gene predictions and functional assignments have been made by using computational tools, although the statistical models in Panther, Pfam, and SMART have been built, annotated, and reviewed by ex-

predicted genes, we expect both false-positive predictions (some of these may in fact be inactive pseudogenes) and false-negative predictions (some human genes will not be computationally predicted). We also expect errors in delimiting the boundaries of exons and genes. Similarly, in the automatic functional assignments, we also expect both false-positive and false-negative predictions. The functional assignment protocol focuses on protein families that tend to be found across several organisms, or on families of known human genes. Therefore, we do not assign a function to many genes that are not in large families, even if the function is known. Unless otherwise specified, all enumeration of the genes in any given family or functional category was taken from the set of 26,588 predicted proteins, which were assigned functions by using statistical score cutoffs defined for models in Panther, Pfam, and SMART.

For this initial examination of the predicted human protein set, three broad questions were asked: (i) What are the likely molecular functions of the predicted gene products, and how are these proteins categorized with current classification methods? (ii) What are the core functions that appear to be common across the animals? (iii) How does the human protein complement differ from that of other sequenced eukaryotes?

7.1 Molecular functions of predicted

Figure 15 shows an overview of the putative molecular functions of the predicted 26,588 human proteins that have at least two lines of supporting evidence. About 41% (12,809) of the gene products could not be classified from this initial analysis and are termed proteins with unknown functions. Because our automatic classification methods treat only relatively large protein families, there are a number of "unclassified" sequences that do, in fact, have a known or predicted function. For the 60% of the protein set that have automatic functional predictions, the specific protein functions have been placed into broad classes. We focus here on molecular function (rather than higher order cellular processes) in order to classify as many proteins as possible. These functional predictions are based on similarity to sequences of known function.

In our analysis of the 12,731 additional low-confidence predicted genes (those with only one piece of supporting evidence), only 636 (5%) of these additional putative genes were assigned molecular functions by the automated methods. One-third of these 636 predicted genes represented endogenous retroviral proteins, further suggesting that the majority of these unknown-function genes are not real genes. Given that most of these additional 12,095 genes appear to be unique among the genomes sequenced to date, many may simply

The most common molecular functions are the transcription factors and those involved in nucleic acid metabolism (nucleic acid enzyme). Other functions that are highly represented in the human genome are the receptors, kinases, and hydrolases. Not surprisingly, most of the hydrolases are proteases. There are also many proteins that are members of proto-oncogene families, as well as families of "select regulatory molecules": (i) proteins involved in specific steps of signal transduction such as heterotrimeric GTP-binding proteins (G proteins) and cell cycle regulators, and (ii) proteins that modulate the activity of kinases, G proteins, and phosphatases.

Table 17. Distribution of SNPs in classes of genomic regions.

Genomic region class	Size of region examined (Mb)	Celera-PFP SNP density (SNP/Mb)
Intergenic	2185	707
Gene (intron + exon)	646	917
Intron	615	921
First intron	164	808
Exon	31	529
First exon	10	592

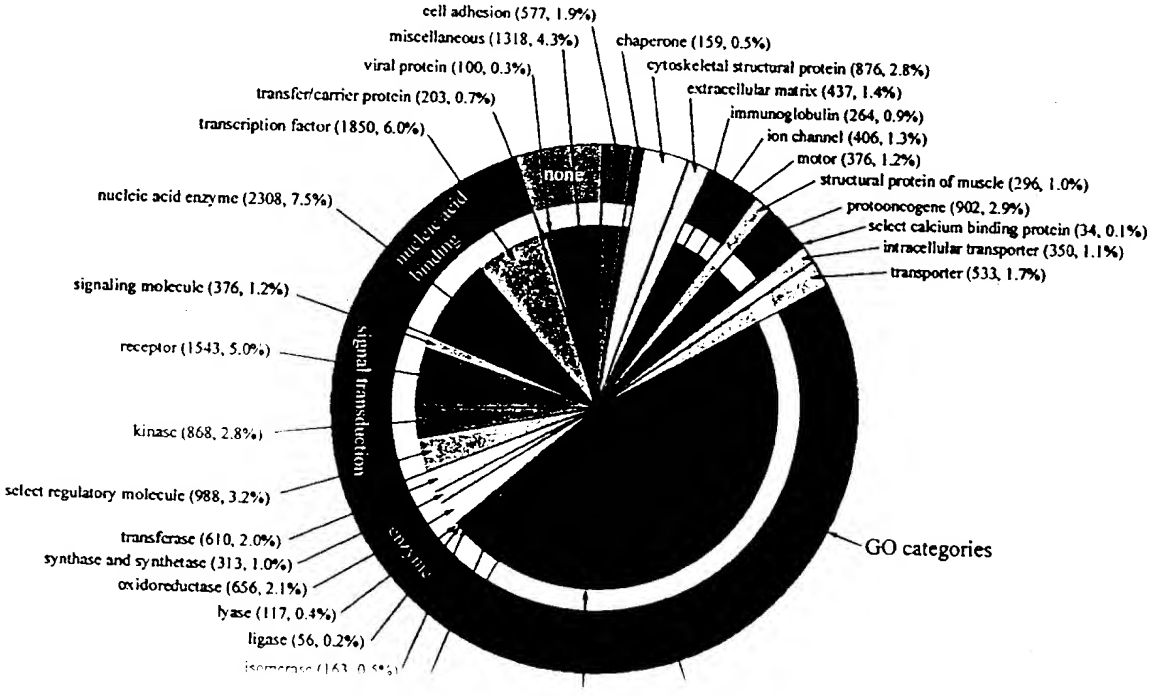

Fig. 15. Distribution of the molecular functions of 26,383 human genes. Each slice lists the numbers and percentages (in parentheses) of human gene functions assigned to a given category of molecular function. The outer circle shows the assignment to molecular function categories in the Gene Ontology (GO) (*179*), and the inner circle shows the assignment to Celera's Panther molecular function categories (*116*).

7.2 Evolutionary conservation of core processes

genome-sequencing projects that have already been completed, reasonable comparative information is available for beginning the analysis of the evolution of the human genome. The genomes of *S. cerevisiae* ("bakers' yeast") (*118*) and two diverse invertebrates, *C. elegans* (a nematode worm) (*119*) and *D. melanogaster* (fly) (*26*), as well as the first plant genome, *A. thaliana*, recently completed (*92*), provide a diverse background for genome comparisons.

We enumerated the "strict orthologs" conserved between human and fly, and between human and worm (Fig. 16) to address the question, What are the core functions that appear to be common across the animals? The concept of orthology is important because if two genes are orthologs, they can be traced by descent to the common ancestor of the two organisms (an "evolutionarily conserved protein set"), and therefore are likely to perform similar conserved functions in the different organisms. It is critical in this analysis to separate orthologs (a gene that appears in two organisms by descent from a common ancestor) from paralogs (a gene that appears in more than one copy in a given organism by a duplication event) because paralogs may subsequently diverge in function. Following the yeast-worm ortholog comparison in (*120*), we identified two different cases for each pairwise comparison (human-fly and [illegible]). This third case was a pair of genes, one from each organism, for which there was no other close homolog in either organism. These are straightforwardly identified as orthologous, because there are no additional members of the families that complicate separating orthologs from paralogs. The second case is a family of genes with more than one member in either or both of the organisms being compared. Chervitz *et al.* (*120*) deal with this case by analyzing a phylogenetic tree that described the relationships between all of the sequences in both organisms, and then looked for pairs of genes that were nearest neighbors in the tree. If the nearest-neighbor pairs were from different organisms, those genes were presumed to be orthologs. We note that these nearest neighbors can often be confidently identified from pairwise sequence comparison without having to examine a phylogenetic tree (see legend to Fig. 16). If the nearest neighbors are not from different organisms, there has been a paralogous expansion in one or both organisms after the speciation event (and/or a gene loss by one organism). When this one-to-one correspondence is lost, defining an ortholog becomes ambiguous. For our initial computational overview of the predicted human protein set, we could not answer this question for every predicted protein. Therefore, we consider only "strict orthologs," i.e., the protein [illegible] (Fig. 16). By these criteria, there are 275 strict human-fly orthologs, 2031 human-worm (1523 in common between these sets). We define the evolutionarily conserved set as those 1523 human proteins that have strict orthologs in both *D. melanogaster* and *C. elegans*.

The distribution of the functions of the conserved protein set is shown in Fig. 16. Comparison with Fig. 15 shows that, not surprisingly, the set of conserved proteins is not distributed among molecular functions in the same way as the whole human protein set. Compared with the whole human set (Fig. 15), there are several categories that are overrepresented in the conserved set by a factor of ~2 or more. The first category is nucleic acid enzymes, primarily the transcriptional machinery (notably DNA/RNA methyltransferases, DNA/RNA polymerases, helicases, DNA ligases, DNA- and RNA-processing factors, nucleases, and ribosomal proteins). The basic transcriptional and translational machinery is well known to have been conserved over evolution, from bacteria through to the most complex eukaryotes. Many ribonucleoproteins involved in RNA splicing also appear to be conserved among the animals. Other enzyme types are also overrepresented (transferases, oxidoreductases, ligases, lyases, and isomerases). Many of these en-

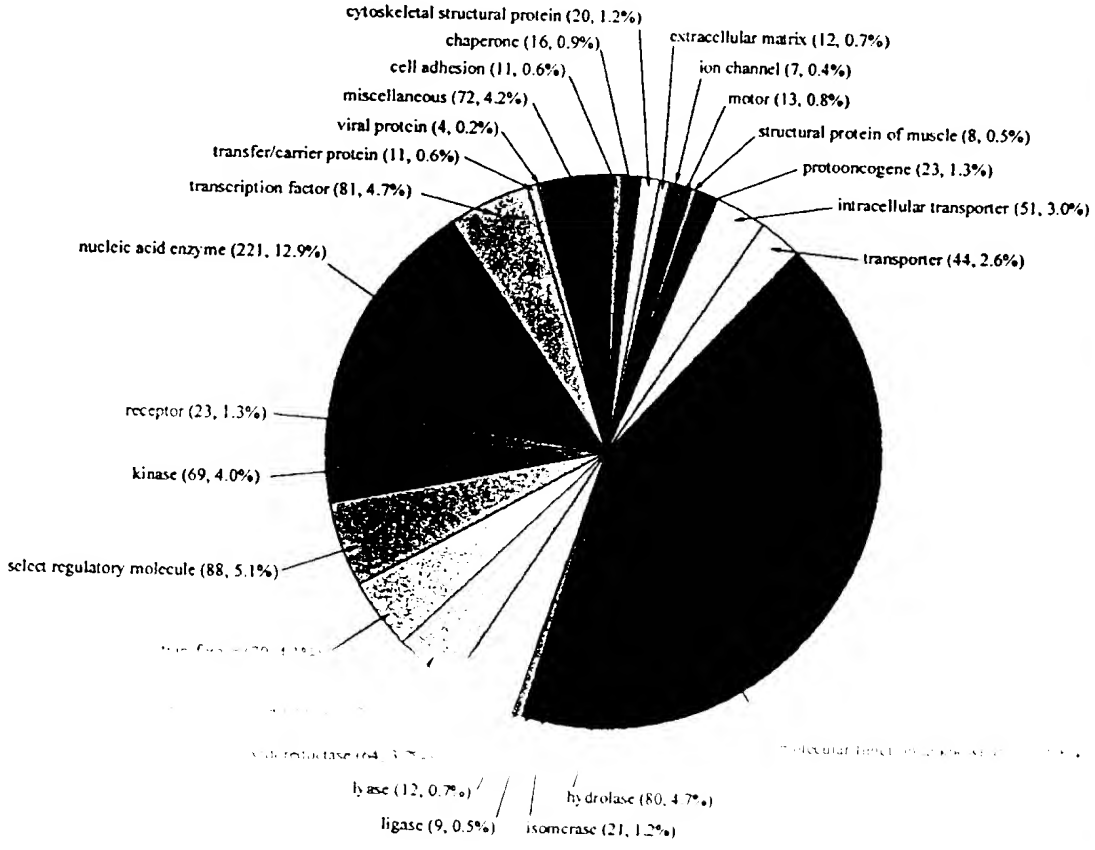

Fig. 16. Functions of putative orthologs across vertebrate and invertebrate genomes. Each slice lists the number and percentages (in parentheses) of "strict orthologs" between the human, fly, and worm genomes involved in a given category of molecular function. "Strict orthologs" are defined here as bi-directional BLAST best hits (*180*) such that each orthologous pair (i) has a BLASTP *P*-value of $\leq 10^{-10}$ (*120*), and (ii) has a more significant BLASTP score than any paralogs in either organism, i.e., there has likely been no duplication subsequent to speciation that might make the orthology ambiguous. This measure is quite strict and is a lower bound on the number of orthologs. By these criteria, there are 2758 strict human-fly orthologs, and 2031 human-worm orthologs (1523 in common between these sets)

zymes are involved in intermediary metabolism. The only exception is the hydrolase category, which is not significantly overrepresented in the shared protein set. Proteases form the largest part of this category, and [redacted] in each of these three organisms after their divergence. The category of select regulatory molecules is also overrepresented in the conserved set. The major conserved families are small guanosine triphosphatases (GTPases) (especially the Ras-related superfamily, including ADP ribosylation factor) and cell cycle regulators (particularly the cullin family, cyclin C family, and several cell division protein kinases). The last two significantly overrepresented categories are protein transport and trafficking, and chaperones. The most conserved groups in these categories are proteins involved in coated vesicle-mediated transport, and chaperones involved in protein folding and heat-shock response [particularly the DNAJ family, and heat-shock protein 60 (HSP60), HSP70, and HSP90 families]. These observations provide only a conservative estimate of the protein families in the context of specific cellular processes that were likely derived from the last common ancestor of the human, fly, and worm. As stated before, this analysis does not provide a complete estimate of conservation across the three animal genomes, as paralogous duplication makes the determination of true orthologs difficult within the members of conserved protein families.

7.3 Differences between the human genome and other sequenced eukaryotic genomes

To explore the molecular building blocks of the vertebrate taxon, we have compared the human genome with the other sequenced eukaryotic genomes at three levels: molecular functions, protein families, and protein domains.

Molecular differences can be correlated with phenotypic differences to begin to reveal the developmental and cellular processes that are unique to the vertebrates. Tables 18 and 19 display a comparison among all sequenced eukaryotic genomes, over selected protein/domain families (defined by sequence similarity, e.g., the serine-threonine protein kinases) and superfamilies (defined by shared molecular function, which may include several sequence-related families, e.g., the cytokines). In these tables we have focused on (super) families that are either very large or that differ significantly in humans compared with the other sequenced eukaryote genomes. We have found that the most prominent human expansions are in proteins involved in (i) [redacted] in development and homeostasis; (iv) hemostasis; and (v) apoptosis.

Acquired immunity. One of the most striking differences between the human genome and the *Drosophila* or *C. elegans* genomes [redacted] acquired immunity (Tables 18 and 19). This is expected, because the acquired immune response is a defense system that only occurs in vertebrates. We observe 22 class I and 22 class II major histocompatibility complex (MHC) antigen genes and 114 other immunoglobulin genes in the human genome. In addition, there are 59 genes in the cognate immunoglobulin receptor family. At the domain level, this is exemplified by an expansion and recruitment of the ancient immunoglobulin fold to constitute molecules such as MHC, and of the integrin fold to form several of the cell adhesion molecules that mediate interactions between immune effector cells and the extracellular matrix. Vertebrate-specific proteins include the paracrine immune regulators family of secreted 4-alpha helical bundle proteins, namely the cytokines and chemokines. Some of the cytoplasmic signal transduction components associated with cytokine receptor signal transduction are also features that are poorly represented in the fly and worm. These include protein domains found in the signal transducer and activator of transcription (STATs), the suppressors of cytokine signaling (SOCS), and protein inhibitors of activated STATs (PIAS). In contrast, many of the animal-specific protein domains that play a role in innate immune response, such as the Toll receptors, do not appear to be significantly expanded in the human genome.

Neural development, structure, and function. In the human genome, as compared with the worm and fly genomes, there is a marked increase in the number of members of protein families that are involved in neural development. Examples include neurotrophic factors such as ependymin, nerve growth factor, and signaling molecules such as semaphorins, as well as the number of proteins involved directly in neural structure and function such as myelin proteins, voltage-gated ion channels, and synaptic proteins such as synaptotagmin. These observations correlate well with the known phenotypic differences between the nervous systems of these taxa, notably (i) the increase in the number and connectivity of neurons; (ii) the increase in number of distinct neural cell types (as many as a thousand or more in human compared with a few hundred in fly and worm) (*121*); (iii) the increased length of individual axons; and (iv) the significant increase in glial cell [redacted] of prominent protein expansions are involved in the processes of neural development. Of the extracellular domains that mediate cell adhesion, the connexin domain– [redacted] mans. These proteins, which are not present in the *Drosophila* or *C. elegans* genomes, appear to provide the constitutive subunits of intercellular channels and the structural basis for electrical coupling. Pathway finding by axons and neuronal network formation is mediated through a subset of ephrins and their cognate receptor tyrosine kinases that act as positional labels to establish topographical projections (*123*). The probable biological role for the semaphorins (22 in human compared with 6 in the fly and 2 in the worm) and their receptors (neuropilins and plexins) is that of axonal guidance molecules (*124*). Signaling molecules such as neurotrophic factors and some cytokines have been shown to regulate neuronal cell survival, proliferation, and axon guidance (*125*). Notch receptors and ligands play important roles in glial cell fate determination and gliogenesis (*126*).

Other human expanded gene families play key roles directly in neural structure and function. One example is synaptotagmin (expanded more than twofold in humans relative to the invertebrates), originally found to regulate synaptic transmission by serving as a Ca^{2+} sensor (or receptor) during synaptic vesicle fusion and release (*127*). Of interest is the increased co-occurrence in humans of PDZ and the SH3 domains in neuronal-specific adaptor molecules; examples include proteins that likely modulate channel activity at synaptic junctions (*128*). We also noted expansions in several ion-channel families (Table 19), including the EAG subfamily (related to cyclic nucleotide gated channels), the voltage-gated calcium/sodium channel family, the inward-rectifier potassium channel family, and the voltage-gated potassium channel, alpha subunit family. Voltage-gated sodium and potassium channels are involved in the generation of action potentials in neurons. Together with voltage-gated calcium channels, they also play a key role in coupling action potentials to neurotransmitter release, in the development of neurites, and in short-term memory. The recent observation of a calcium-regulated association between sodium channels and synaptotagmin may have consequences for the establishment and regulation of neuronal excitability (*129*).

Myelin basic protein and myelin-associated glycoprotein are major classes of protein components in both the central and peripheral nervous system of vertebrates. Myelin P0 is a

Table 18. Domain-based comparative analysis of proteins in *H. sapiens* (H), *D. melanogaster* (F), *C. elegans* (W), *S. cerevisiae* (Y), and *A. thaliana* (A). The predicted protein set of each of the above eukaryotic organisms was analyzed [illegible] Pfam domains as well as the total number of domains (in parentheses) are shown in each column. Domains were categorized into cellular processes for presentation. Some domains (i.e., SH2) are listed in more than one cellular process. Results of the Pfam analysis may differ from results obtained based on human curation of protein families, owing to the [illegible] stringent E value cutoff used for this analysis are marked with a double asterisk (**). Examples include short divergent and predominantly alpha-helical domains, and certain classes of cysteine-rich zinc finger proteins.

Accession number	Domain name	Domain description	H	F	W	Y	A
		Developmental and homeostatic regulators					
PF02039	Adrenomedullin	Adrenomedullin	1	0	0	0	0
PF00212	ANP	Atrial natriuretic peptide	2	0	0	0	0
PF00028	Cadherin	Cadherin domain	100 (550)	14 (157)	16 (66)	0	0
PF00214	Calc_CGRP_IAPP	Calcitonin/CGRP/IAPP family	3	0	0	0	0
PF01110	CNTF	Ciliary neurotrophic factor	1	0	0	0	0
PF01093	Clusterin	Clusterin	3	0	0	0	0
PF00029	Connexin	Connexin	14 (16)	0	0	0	0
PF00976	ACTH_domain	Corticotropin ACTH domain	1	0	0	0	0
PF00473	CRF	Corticotropin-releasing factor family	2	1	0	0	0
PF00007	Cys_knot	Cystine-knot domain	10 (11)	2	0	0	0
PF00778	DIX	Dix domain	5	2	4	0	0
PF00322	Endothelin	Endothelin family	3	0	0	0	0
PF00812	Ephrin	Ephrin	7 (8)	2	4	0	0
PF01404	EPh_lbd	Ephrin receptor ligand binding domain	12	2	1	0	0
PF00167	FGF	Fibroblast growth factor	23	1	1	0	0
PF01534	Frizzled	Frizzled/Smoothened family membrane region	9	7	3	0	0
PF00236	Hormone6	Glycoprotein hormones	1	0	0	0	0
PF01153	Glypican	Glypican	14	2	1	0	0
PF01271	Granin	Grainin (chromogranin or secretogranin)	3	0	0	0	0
PF02058	Guanylin	Guanylin precursor	1	0	0	0	0
PF00049	Insulin	Insulin/IGF/Relaxin family	7	4	0	0	0
PF00219	IGFBP	Insulin-like growth factor binding proteins	10	0	0	0	0
PF02024	Leptin	Leptin	1	0	0	0	0
PF00193	Xlink	LINK (hyaluron binding)	13 (23)	0	1	0	0
PF00243	NGF	Nerve growth factor family	3	0	0	0	0
PF02158	Neuregulin	Neuregulin family	4	0	0	0	0
PF00184	Hormone5	Neurohypophysial hormones	1	0	0	0	0
PF02070	NMU	Neuromedin U	1	0	0	0	0
PF00066	Notch	Notch (DSL) domain	3 (5)	2 (4)	2 (6)	0	0
PF00865	Osteopontin	Osteopontin	1	0	0	0	0
PF00159	Hormone3	Pancreatic hormone peptides	3	0	0	0	0
PF01279	Parathyroid	Parathyroid hormone family	2	0	0	0	0
PF00123	Hormone2	Peptide hormone	5 (9)	0	0	0	0
PF00341	PDGF	Platelet-derived growth factor (PDGF)	5	1	0	0	0
PF01403	Sema	Sema domain	27 (29)	8 (10)	3 (4)	0	0
PF01033	Somatomedin_B	Somatomedin B domain	5 (8)	3	0	0	0
PF00103	Hormone	Somatotropin	1	0	0	0	0
PF02208	Sorb	Sorbin homologous domain	2	0	0	0	0
PF02404	SCF	Stem cell factor	2	0	0	0	0
PF01034	Syndecan	Syndecan domain	3	1	1	0	0
PF00020	TNFR_c6	TNFR/NGFR cysteine-rich region	17 (31)	1	0	0	0
PF00019	TGF-β	Transforming growth factor β-like domain	27 (28)	6	4	0	0
PF01099	Uteroglobin	Uteroglobin family	3	0	0	0	0
PF01160	Opiods_neuropep	Vertebrate endogenous opioids neuropeptide	3	0	0	0	0
PF00110	Wnt	Wnt family of developmental signaling proteins	18	7 (10)	5	0	0
		Hemostasis					
PF01821	ANATO	Anaphylotoxin-like domain	6 (14)	0	0	0	0
PF00386	C1q	C1q domain	24	0	0	0	0
PF00200	Disintegrin	Disintegrin	18	2	3	0	0
PF00754	F5_F8_type_C	F5/8 type C domain	15 (20)	5 (6)	2	0	0
PF01410	COLFI	Fibrillar collagen C-terminal domain	10	0	0	0	0
PF00039	Fn1	Fibronectin type I domain	5 (18)	0	0	0	0
PF00040	Fn2	Fibronectin type II domain	11 (16)	0	0	0	0
PF00051	Kringle	Kringle domain	15 (24)	2	2	0	0
PF01823	MACPF	MAC/Perforin domain	6	0	0	0	0
PF00354	Pentaxin	Pentaxin family	9	0	0	0	0
PF00277	SAA_proteins	Serum amyloid A protein	[illegible]	[illegible]	[illegible]	[illegible]	[illegible]
[illegible]	[illegible]	[illegible]	[illegible]	[illegible]	[illegible]	[illegible]	[illegible]
		[illegible]					
[illegible]	[illegible]	Transglutaminase family	[illegible]	[illegible]	[illegible]	[illegible]	[illegible]
[illegible]	[illegible]	Transglutaminase family	8	1	0	0	0

Table 18 (*Continued*)

Accession number	Domain name	Domain description	H	F	W	Y	A
[illegible]	Gla	[illegible] carboxyglutamic (GLA) domain	[illegible]	[illegible]	[illegible]	[illegible]	[illegible]
		Immune response					
PF00711	Defensin_beta	Beta defensin	1	0	0	0	0
PF00748	Calpain_inhib	Calpain inhibitor repeat	3 (9)	0	0	0	0
PF00666	Cathelicidins	Cathelicidins	2	0	0	0	0
PF00129	MHC_I	Class I histocompatibility antigen, domains alpha 1 and 2	18 (20)	0	0	0	0
PF00993	MHC_II_alpha**	Class II histocompatibility antigen, alpha domain	5 (6)	0	0	0	0
PF00969	MHC_II_beta**	Class II histocompatibility antigen, beta domain	7	0	0	0	0
PF00879	Defensin_propep	Defensin propeptide	3	0	0	0	0
PF01109	GM_CSF	Granulocyte-macrophage colony-stimulating factor	1	0	0	0	0
PF00047	Ig	Immunoglobulin domain	381 (930)	125 (291)	67 (323)	0	0
PF00143	Interferon	Interferon alpha/beta domain	7 (9)	0	0	0	0
PF00714	IFN-gamma	Interferon gamma	1	0	0	0	0
PF00726	IL10	Interleukin-10	1	0	0	0	0
PF02372	IL15	Interleukin-15	1	0	0	0	0
PF00715	IL2	Interleukin-2	1	0	0	0	0
PF00727	IL4	Interleukin-4	1	0	0	0	0
PF02025	IL5	Interleukin-5	1	0	0	0	0
PF01415	IL7	Interleukin-7/9 family	1	0	0	0	0
PF00340	IL1	Interleukin-1	7	0	0	0	0
PF02394	IL1_propep	Interleukin-1 propeptide	1	0	0	0	0
PF02059	IL3	Interleukin-3	1	0	0	0	0
PF00489	IL6	Interleukin-6/G-CSF/MGF family	2	0	0	0	0
PF01291	LIF_OSM	Leukemia inhibitory factor (LIF)/oncostatin (OSM) family	2	0	0	0	0
PF00323	Defensins	Mammalian defensin	2	0	0	0	0
PF01091	PTN_MK	PTN/MK heparin-binding protein	2	0	0	0	0
PF00277	SAA_proteins	Serum amyloid A protein	4	0	0	0	0
PF00048	IL8	Small cytokines (intecrine/chemokine), interleukin-8 like	32	0	0	0	0
PF01582	TIR	TIR domain	18	8	2	0	131 (143)
PF00229	TNF	TNF (tumor necrosis factor) family	12	0	0	0	0
PF00088	Trefoil	Trefoil (P-type) domain	5 (6)	0	2	0	0
		PI-PY-rho GTPase signaling					
PF00779	BTK	BTK motif	5	1	0	0	0
PF00168	C2	C2 domain	73 (101)	32 (44)	24 (35)	6 (9)	66 (90)
PF00609	DAGKa	Diacylglycerol kinase accessory domain (presumed)	9	4	7	0	6
PF00781	DAGKc	Diacylglycerol kinase catalytic domain (presumed)	10	8	8	2	11 (12)
PF00610	DEP	Domain found in Dishevelled, Egl-10, and Pleckstrin (DEP)	12 (13)	4	10	5	2
PF01363	FYVE	FYVE zinc finger	28 (30)	14	15	5	15
PF00996	GDI	GDP dissociation inhibitor	6	2	1	1	3
PF00503	G-alpha	G-protein alpha subunit	27 (30)	10	20 (23)	2	5
PF00631	G-gamma	G-protein gamma like domains	16	5	5	1	0
PF00616	RasGAP	GTPase-activator protein for Ras-like GTPase	11	5	8	3	0
PF00618	RasGEFN	Guanine nucleotide exchange factor for Ras-like GTPases; N-terminal motif	9	2	3	5	0
PF00625	Guanylate_kin	Guanylate kinase	12	8	7	1	4
PF02189	ITAM	Immunoreceptor tyrosine-based activation motif	3	0	0	0	0
PF00169	PH	PH domain	193 (212)	72 (78)	65 (68)	24	23
PF00130	DAG_PE-bind	Phorbol esters/diacylglycerol binding domain (C1 domain)	45 (56)	25 (31)	26 (40)	1 (2)	4
PF00388	PI-PLC-X	Phosphatidylinositol-specific phospholipase C, X domain	12	3	7	1	8
PF00387	PI-PLC-Y	Phosphatidylinositol-specific phospholipase C, Y domain	11	2	7	1	8
PF00640	PID	Phosphotyrosine interaction domain (PTB/PID)	24 (27)	13	11 (12)	0	0
PF02192	PI3K_p85B	PI3-kinase family, p85-binding domain	2	1	1	0	0
PF00794	PI3K_rbd	PI3-kinase family, ras-binding domain	6	3	1	0	0
PF01412	ArfGAP	Putative GTP-ase activating protein for Arf	16	9	8	6	15
PF02196	RBD	Raf-like Ras-binding domain	6 (7)	4	1	0	0
PF02145	Rap_GAP	Rap/ran-GAP	5	4	2	0	0
PF00788	RA	Ras association (RalGDS/AF-6) domain	18 (19)	7 (9)	6	1	0
PF00071	Ras	Ras family	126	[illegible]	[illegible]	[illegible]	[illegible]

Table 18 (*Continued*)

number	Domain name	Domain description	H	F	W	Y	A
PF00620	RhoGAP	RhoGAP domain	59	19	20	9	8
PF00621	RhoGEF	RhoGEF domain	46	23 (24)	18 (19)	3	0
PF00536	SAM	SAM domain (Sterile alpha motif)	29 (31)	15	8	3	6
PF01369	Sec7	Sec7 domain	13	5	5	5	9
PF00017	SH2	Src homology 2 (SH2) domain	87 (95)	33 (39)	44 (48)	1	3
PF00018	SH3	Src homology 3 (SH3) domain	143 (182)	55 (75)	46 (61)	23 (27)	4
PF01017	STAT	STAT protein	7	1	1 (2)	0	0
PF00790	VHS	VHS domain	4	2	4	4	8
PF00568	WH1	WH1 domain	7	2	2 (3)	1	0
		Domains involved in apoptosis					
PF00452	Bcl-2	Bcl-2	9	2	1	0	0
PF02180	BH4	Bcl-2 homology region 4	3	0	1	0	0
PF00619	CARD	Caspase recruitment domain	16	0	2	0	0
PF00531	Death	Death domain	16	5	7	0	0
PF01335	DED	Death effector domain	4 (5)	0	0	0	0
PF02179	BAG	Domain present in Hsp70 regulators	5 (8)	3	2	1	5
PF00656	ICE_p20	ICE-like protease (caspase) p20 domain	11	7	3	0	0
PF00653	BIR	Inhibitor of Apoptosis domain	8 (14)	5 (9)	2 (3)	1 (2)	0
		Cytoskeletal					
PF00022	Actin	Actin	61 (64)	15 (16)	12	9 (11)	24
PF00191	Annexin	Annexin	16 (55)	4 (16)	4 (11)	0	6 (16)
PF00402	Calponin	Calponin family	13 (22)	3	7 (19)	0	0
PF00373	Band_41	FERM domain (Band 4.1 family)	29 (30)	17 (19)	11 (14)	0	0
PF00880	Nebulin_repeat	Nebulin repeat	4 (148)	1 (2)	1	0	0
PF00681	Plectin_repeat	Plectin repeat	2 (11)	0	0	0	0
PF00435	Spectrin	Spectrin repeat	31 (195)	13 (171)	10 (93)	0	0
PF00418	Tubulin-binding	Tau and MAP proteins, tubulin-binding	4 (12)	1 (4)	2 (8)	0	0
PF00992	Troponin	Troponin	4	6	8	0	0
PF02209	VHP	Villin headpiece domain	5	2	2	0	5
PF01044	Vinculin	Vinculin family	4	2	1	0	0
		ECM adhesion					
PF01391	Collagen	Collagen triple helix repeat (20 copies)	65 (279)	10 (46)	174 (384)	0	0
PF01413	C4	C-terminal tandem repeated domain in type 4 procollagen	6 (11)	2 (4)	3 (6)	0	0
PF00431	CUB	CUB domain	47 (69)	9 (47)	43 (67)	0	0
PF00008	EGF	EGF-like domain	108 (420)	45 (186)	54 (157)	0	1
PF00147	Fibrinogen_C	Fibrinogen beta and gamma chains, C-terminal globular domain	26	10 (11)	6	0	0
PF00041	Fn3	Fibronectin type III domain	106 (545)	42 (168)	34 (156)	0	1
PF00757	Furin-like	Furin-like cysteine rich region	5	2	1	0	0
PF00357	Integrin_A	Integrin alpha cytoplasmic region	3	1	2	0	0
PF00362	Integrin_B	Integrins, beta chain	8	2	2	0	0
PF00052	Laminin_B	Laminin B (Domain IV)	8 (12)	4 (7)	6 (10)	0	0
PF00053	Laminin_EGF	Laminin EGF-like (Domains III and V)	24 (126)	9 (62)	11 (65)	0	0
PF00054	Laminin_G	Laminin G domain	30 (57)	18 (42)	14 (26)	0	0
PF00055	Laminin_Nterm	Laminin N-terminal (Domain VI)	10	6	4	0	0
PF00059	Lectin_c	Lectin C-type domain	47 (76)	23 (24)	91 (132)	0	0
PF01463	LRRCT	Leucine rich repeat C-terminal domain	69 (81)	23 (30)	7 (9)	0	0
PF01462	LRRNT	Leucine rich repeat N-terminal domain	40 (44)	7 (13)	3 (6)	0	0
PF00057	Ldl_recept_a	Low-density lipoprotein receptor domain class A	35 (127)	33 (152)	27 (113)	0	0
PF00058	Ldl_recept_b	Low-density lipoprotein receptor repeat class B	15 (96)	9 (56)	7 (22)	0	0
PF00530	SRCR	Scavenger receptor cysteine-rich domain	11 (46)	4 (8)	1 (2)	0	0
PF00084	Sushi	Sushi domain (SCR repeat)	53 (191)	11 (42)	8 (45)	0	0
PF00090	Tsp_1	Thrombospondin type 1 domain	41 (66)	11 (23)	18 (47)	0	0
PF00092	Vwa	von Willebrand factor type A domain	34 (58)	0	17 (19)	0	1
PF00093	Vwc	von Willebrand factor type C domain	19 (28)	6 (11)	2 (5)	0	0
PF00094	Vwd	von Willebrand factor type D domain	15 (35)	3 (7)	9	0	0
		Protein interaction domains					
PF00244	14-3-3	14-3-3 proteins	20	3	3	2	15
PF00023	Ank	Ank repeat	145 (404)	72 (269)	75 (223)	12 (20)	66 (111)
PF00514	Armadillo_seg	Armadillo/beta-catenin-like repeats	22 (56)	11 (38)	3 (11)	2 (10)	25 (67)
PF00168	C2	C2 domain	73 (101)	32 (44)	24 (35)	6 (9)	35 (50)
PF00611	FH2	FH2 domain	9	3	2	4	0
PF01846	FF	FF domain	4 (11)	4 (10)	3 (16)	2 (5)	4 (8)
PF00498	FHA	FHA domain	13	15	7	13 (14)	17

myelin proteins result in severe demyelination, which is a pathological condition in which the myelin is lost and the nerve conduction is severely impaired (*130*). Humans have at least 10 genes belonging to four tion (five myelin P0, three myelin proteolipid, myelin basic protein, and myelin-oligodendrocyte glycoprotein, or MOG), and possibly more-remotely related members of the MOG family. Flies have only a single myelin

Intercellular and intracellular signaling pathways in development and homeostasis. Many protein families that have expanded in humans relative to the invertebrates are involved in signaling processes, particularly in

Table 18 (*Continued*)

Accession number	Domain name	Domain description	H	F	W	Y	A
PF00254	FKBP	FKBP-type peptidyl-prolyl cis-trans isomerases	15 (20)	7 (8)	7 (13)	4	24 (29)
PF01590	GAF	GAF domain	7 (8)	2 (4)	1	0	10
PF01344	Kelch	Kelch motif	54 (157)	12 (48)	13 (41)	3	102 (178)
PF00560	LRR**	Leucine Rich Repeat	25 (30)	24 (30)	7 (11)	1	15 (16)
PF00917	MATH	MATH domain	11	5	88 (161)	1	61 (74)
PF00989	PAS	PAS domain	18 (19)	9 (10)	6	1	13 (18)
PF00595	PDZ	PDZ domain (Also known as DHR or GLGF)	96 (154)	60 (87)	46 (66)	2	5
PF00169	PH	PH domain	193 (212)	72 (78)	65 (68)	24	23
PF01535	PPR**	PPR repeat	5	3 (4)	0	1	474 (2485)
PF00536	SAM	SAM domain (Sterile alpha motif)	29 (31)	15	8	3	6
PF01369	Sec7	Sec7 domain	13	5	5	5	9
PF00017	SH2	Src homology 2 (SH2) domain	87 (95)	33 (39)	44 (48)	1	3
PF00018	SH3	Src homology 3 (SH3) domain	143 (182)	55 (75)	46 (61)	23 (27)	4
PF01740	STAS	STAS domain	5	1	6	2	13
PF00515	TPR**	TPR domain	72 (131)	39 (101)	28 (54)	16 (31)	65 (124)
PF00400	WD40**	WD40 domain	136 (305)	98 (226)	72 (153)	56 (121)	167 (344)
PF00397	WW	WW domain	32 (53)	24 (39)	16 (24)	5 (8)	11 (15)
PF00569	ZZ	ZZ-Zinc finger present in dystrophin, CBP/p300	10 (11)	13	10	2	10
		Nuclear interaction domains					
PF01754	Zf-A20	A20-like zinc finger	2 (8)	2	2	0	8
PF01388	ARID	ARID DNA binding domain	11	6	4	2	7
PF01426	BAH	BAH domain	8 (10)	7 (8)	4 (5)	5	21 (25)
PF00643	Zf-B_box**	B-box zinc finger	32 (35)	1	2	0	0
PF00533	BRCT	BRCA1 C Terminus (BRCT) domain	17 (28)	10 (18)	23 (35)	10 (16)	12 (16)
PF00439	Bromodomain	Bromodomain	37 (48)	16 (22)	18 (26)	10 (15)	28
PF00651	BTB	BTB/POZ domain	97 (98)	62 (64)	86 (91)	1 (2)	30 (31)
PF00145	DNA_methylase	C-5 cytosine-specific DNA methylase	3 (4)	1	0	0	13 (15)
PF00385	Chromo	chromo' (CHRromatin Organization MOdifier) domain	24 (27)	14 (15)	17 (18)	1 (2)	12
PF00125	Histone	Core histone H2A/H2B/H3/H4	75 (81)	5	71 (73)	8	48
PF00134	Cyclin	Cyclin	19	10	10	11	35
PF00270	DEAD	DEAD/DEAH box helicase	63 (66)	48 (50)	55 (57)	50 (52)	84 (87)
PF01529	Zf-DHHC	DHHC zinc finger domain	15	20	16	7	22
PF00646	F-box**	F-box domain	16	15	309 (324)	9	165 (167)
PF00250	Fork_head	Fork head domain	35 (36)	20 (21)	15	4	0
PF00320	GATA	GATA zinc finger	11 (17)	5(6)	8 (10)	9	26
PF01585	G-patch	G-patch domain	18	16	13	4	14 (15)
PF00010	HLH**	Helix-loop-helix DNA-binding domain	60 (61)	44	24	4	39
PF00850	Hist_deacetyl	Histone deacetylase family	12	5 (6)	8 (10)	5	10
PF00046	Homeobox	Homeobox domain	160 (178)	100 (103)	82 (84)	6	66
PF01833	TIG	IPT/TIG domain	29 (53)	11 (13)	5 (7)	2	1
PF02373	JmjC	JmjC domain	10	4	6	4	7
PF02375	JmjN	JmjN domain	7	4	2	3	7
PF00013	KH-domain	KH domain	28 (67)	14 (32)	17 (46)	4 (14)	27 (61)
PF01352	KRAB	KRAB box	204 (243)	0	0	0	0
PF00104	Hormone_rec	Ligand-binding domain of nuclear hormone receptor	47	17	142 (147)	0	0
PF00412	LIM	LIM domain containing proteins	62 (129)	33 (83)	33 (79)	4 (7)	10 (16)
PF00917	MATH	MATH domain	11	5	88 (161)	1	61 (74)
PF00249	Myb_DNA-binding	Myb-like DNA-binding domain	32 (43)	18 (24)	17 (24)	15 (20)	243 (401)
PF02344	Myc-LZ	Myc leucine zipper domain	1	0	0	0	0
PF01753	Zf-MYND	MYND finger	14	14	9	1	7
PF00628	PHD	PHD-finger	68 (86)	40 (53)	32 (44)	14 (15)	96 (105)
PF00157	Pou	Pou domain—N-terminal to homeobox domain	15	5	4	0	0
PF02257	RFX_DNA_binding	RFX DNA-binding domain	7	2	1	1	0
PF00076	Rrm	RNA recognition motif (a.k.a. RRM, RBD, or RNP domain)	224 (324)	127 (199)	94 (145)	43 (73)	232 (369)
PF02037	SAP	SAP domain	15	8	5	5	6 (7)

Table 18 (*Continued*)

number	Domain name	Domain description	H	F	W	Y	A
PF02135	Zf-TAZ	TAZ finger	2 (3)	1 (2)	6 (7)	0	10 (15)
PF01285	TEA	TEA domain	4	1	1	1	0
PF02176	Zf-TRAF	TRAF-type zinc finger	6 (9)	1 (3)	1	0	2
PF00352	TBP	Transcription factor TFIID (or TATA-binding protein, TBP)	2 (4)	4 (8)	2 (4)	1 (2)	2 (4)
PF00567	TUDOR	TUDOR domain	9 (24)	9 (19)	4 (5)	0	2
PF00642	Zf-CCCH	Zinc finger C-x8-C-x5-C-x3-H type (and similar)	17 (22)	6 (8)	22 (42)	3 (5)	31 (46)
PF00096	Zf-C2H2**	Zinc finger, C2H2 type	564 (4500)	234 (771)	68 (155)	34 (56)	21 (24)
PF00097	Zf-C3HC4	Zinc finger, C3HC4 type (RING finger)	135 (137)	57	88 (89)	18	298 (304)
PF00098	Zf-CCHC	Zinc knuckle	9 (17)	6 (10)	17 (33)	7 (13)	68 (91)

(Tables 18 and 19). They include secreted hormones and growth factors, receptors, intracellular signaling molecules, and transcription factors.

Developmental signaling molecules that are enriched in the human genome include growth factors such as wnt, transforming growth factor–β (TGF-β), fibroblast growth factor (FGF), nerve growth factor, platelet derived growth factor (PDGF), and ephrins. These growth factors affect tissue differentiation and a wide range of cellular processes involving actin-cytoskeletal and nuclear regulation. The corresponding receptors of these developmental ligands are also expanded in humans. For example, our analysis suggests at least 8 human ephrin genes (2 in the fly, 4 in the worm) and 12 ephrin receptors (2 in the fly, 1 in the worm). In the wnt signaling pathway, we find 18 wnt family genes (6 in the fly, 5 in the worm) and 12 frizzled receptors (6 in the fly, 5 in the worm). The Groucho family of transcriptional corepressors downstream in the wnt pathway are even more markedly expanded, with 13 predicted members in humans (2 in the fly, 1 in the worm).

Extracellular adhesion molecules involved in signaling are expanded in the human genome (Tables 18 and 19). The interactions of several of these adhesion domains with extracellular matrix proteoglycans play a critical role in host defense, morphogenesis, and tissue repair (*131*). Consistent with the well-defined role of heparan sulfate proteoglycans in modulating these interactions (*132*), we observe an expansion of the heparin sulfate sulfotransferases in the human genome relative to worm and fly. These sulfotransferases modulate tissue differentiation (*133*). A similar expansion in humans is noted in structural proteins that constitute the actin-cytoskeletal architecture. Compared with the fly and worm, we observe an explosive expansion of the nebulin (35 domains per pro-

[illegible] reads are present in proteins involved in modulating the actin-cytoskeleton with predominant expression in neuronal, muscle, and vascular tissues.

Comparison across the five sequenced eukaryotic organisms revealed several expanded protein families and domains involved in cytoplasmic signal transduction (Table 18). In particular, signal transduction pathways playing roles in developmental regulation and acquired immunity were substantially enriched. There is a factor of 2 or greater expansion in humans in the Ras superfamily GTPases and the GTPase activator and GTP exchange factors associated with them. Although there are about the same number of tyrosine kinases in the human and *C. elegans* genomes, in humans there is an increase in the SH2, PTB, and ITAM domains involved in phosphotyrosine signal transduction. Further, there is a twofold expansion of phosphodiesterases in the human genome compared with either the worm or fly genomes.

The downstream effectors of the intracellular signaling molecules include the transcription factors that transduce developmental fates. Significant expansions are noted in the ligand-binding nuclear hormone receptor class of transcription factors compared with the fly genome, although not to the extent observed in the worm (Tables 18 and 19). Perhaps the most striking expansion in humans is in the C2H2 zinc finger transcription factors. Pfam detects a total of 4500 C2H2 zinc finger domains in 564 human proteins, compared with 771 in 234 fly proteins. This means that there has been a dramatic expansion not only in the number of C2H2 transcription factors, but also in the number of these DNA-binding motifs per transcription factor (8 on average in humans, 3.3 on average in the fly, and 2.3 on average in the worm). Furthermore, many of these transcription factors contain either the KRAB or SCAN domains, which are not found in the fly or worm genomes. These domains are involved in the oligomerization of transcription factors and increase the combinatorial partnering of these

[illegible] mains results in organism-specific transcription factor families. The domain combinations found in the human, fly, and worm include the BTB with C2H2 in the fly and humans, and homeodomains alone or in combination with Pou and LIM domains in all of the animal genomes. In plants, however, a different set of transcription factors are expanded, namely, the myb family, and a unique set that includes VP1 and AP2 domain–containing proteins (*134*). The yeast genome has a paucity of transcription factors compared with the multicellular eukaryotes, and its repertoire is limited to the expansion of the yeast-specific C6 transcription factor family involved in metabolic regulation.

While we have illustrated expansions in a subset of signal transduction molecules in the human genome compared with the other eukaryotic genomes, it should be noted that most of the protein domains are highly conserved. An interesting observation is that worms and humans have approximately the same number of both tyrosine kinases and serine/threonine kinases (Table 19). It is important to note, however, that these are merely counts of the catalytic domain; the proteins that contain these domains also display a wide repertoire of interaction domains with significant combinatorial diversity.

Hemostasis. Hemostasis is regulated primarily by plasma proteases of the coagulation pathway and by the interactions that occur between the vascular endothelium and platelets. Consistent with known anatomical and physiological differences between vertebrates and invertebrates, extracellular adhesion domains that constitute proteins integral to hemostasis are expanded in the human relative to the fly and worm (Tables 18 and 19). We note the evolution of domains such as FIMAC, FN1, FN2, and C1q that mediate surface interactions between hematopoeitic cells and the vascular matrix. In addition, there has been extensive recruitment of more-ancient animal-specific domains such as VWA, VWC, VWD, kringle, and FN3 into multidomain proteins that are involved in hemostatic regulation. Although we

[illegible] these multidomain proteins for proteolytic regulation in the vascular compartment. These are represented in plasma proteins that belong to the kinin and complement pathways. There is a

significant expansion in two families of matrix metalloproteases: ADAM (a disintegrin and metalloprotease) and MMPs (matrix metalloproteases) (Table 19). Proteolysis of extracellular matrix (ECM) proteins is critical for tissue

eases such as cancer, arthritis, Alzheimer's disease, and a variety of inflammatory conditions (*135*, *136*). ADAMs are a family of integral membrane proteins with a pivotal role in fibrinogenolysis and modulating interactions between hematopoietic components and the vascular matrix components. These proteins have been shown to cleave matrix proteins, and even signaling molecules: ADAM-17 converts tumor necrosis factor–α, and ADAM-10 has been implicated in the Notch signaling pathway (*135*). We have identified 19 members of the matrix metalloprotease family, and a total of 51 members of the ADAM and ADAM-TS families.

Apoptosis. Evolutionary conservation of some of the apoptotic pathway components across eukarya is consistent with its central role in developmental regulation and as a response to pathogens and stress signals. The signal transduction pathways involved in programmed cell death, or apoptosis, are mediated by interactions between well-characterized domains that include extracellular domains, adaptor (protein-protein interaction) domains, and those found in effector and regulatory enzymes (*137*). We enumerated the protein counts of central adaptor and effector enzyme domains that are found only in the apoptotic pathways to provide an estimate of divergence across eukarya and relative expansion in the human genome when compared with the fly and worm (Table 18). Adaptor domains found in proteins restricted only to apoptotic regulation such as the DED domains are vertebrate-specific, whereas others like BIR, CARD, and Bcl2 are represented in the fly and worm (although the number of Bcl2 family members in humans is significantly expanded). Although plants and yeast lack the caspases, caspase-like molecules, namely the para- and meta-caspases, have been reported in these organisms (*138*). Compared with other animal genomes, the human genome shows an expansion in the adaptor and effector domain–containing proteins involved in apoptosis, as well as in the proteases involved in the cascade such as the caspase and calpain families.

Expansions of other protein families. *Metabolic enzymes.* There are fewer cytochrome P450 genes in humans than in either the fly or worm. Lipoxygenases (six in humans), on the other hand, appear to be specific to the vertebrates and plants, whereas the lipoxygenase-activating proteins (four in human

in diverse human pathology ranging from allergic responses to cancers. One of the most surprising human expansions, however, is in the number of glyceraldehyde-3-phosphate dehydrogenase (GAPDH

is, however, evidence for many retrotransposed GAPDH pseudogenes (*139*), which may account for this apparent expansion. However, it is interesting that GAPDH, long known as a conserved enzyme involved in

bacteria to humans, has recently been shown to have other functions. It has a second cat-

Table 19. Number of proteins assigned to selected Panther families or subfamilies in *H. sapiens* (H), *D. melanogaster* (F), *C. elegans* (W), *S. cerevisiae* (Y), and *A. thaliana* (A).

Panther family/subfamily*	H	F	W	Y	A
Neural structure, function, development					
Ependymin	1	0	0	0	0
Ion channels					
Acetylcholine receptor	17	12	56	0	0
Amiloride-sensitive/degenerin	11	24	27	0	0
CNG/EAG	22	9	9	0	30
IRK	16	3	3	0	0
ITP/ryanodine	10	2	4	0	0
Neurotransmitter-gated	61	51	59	0	19
P2X purinoceptor	10	0	0	0	0
TASK	12	12	48	1	5
Transient receptor	15	3	3	1	0
Voltage-gated Ca^{2+} alpha	22	4	8	2	2
Voltage-gated Ca^{2+} alpha-2	10	3	2	0	0
Voltage-gated Ca^{2+} beta	5	2	2	0	0
Voltage-gated Ca^{2+} gamma	1	0	0	0	0
Voltage-gated K^+ alpha	33	5	11	0	0
Voltage-gated KQT	6	2	3	0	0
Voltage-gated Na^+	11	4	4	9	1
Myelin basic protein	1	0	0	0	0
Myelin PO	5	0	0	0	0
Myelin proteolipid	3	1	0	0	0
Myelin-oligodendrocyte glycoprotein	1	0	0	0	0
Neuropilin	2	0	0	0	0
Plexin	9	2	0	0	0
Semaphorin	22	6	2	0	0
Synaptotagmin	10	3	3	0	0
Immune response					
Defensin	3	0	0	0	0
Cytokine†	86	14	1	0	0
GCSF	1	0	0	0	0
GMCSF	1	0	0	0	0
Intercrine alpha	15	0	0	0	0
Intercrine beta	5	0	0	0	0
Inteferon	8	0	0	0	0
Interleukin	26	1	1	0	0
Leukemia inhibitory factor	1	0	0	0	0
MCSF	1	0	0	0	0
Peptidoglycan recognition protein	2	13	0	0	0
Pre-B cell enhancing factor	1	0	0	0	0
Small inducible cytokine A	14	0	0	0	0
SI cytokine	2	0	0	0	0
TNF	9	0	0	0	0
Cytokine receptor†	62	1	0	0	0
Bradykinin/C-C chemokine receptor	7	0	0	0	0
FI cytokine receptor	2	0	0	0	0
Interferon receptor	3	0	0	0	0
Interleukin receptor	32	0	0	0	0
Leukocyte tyrosine kinase receptor	3	0	0	0	0
MCSF receptor	1	0	0	0	0
TNF receptor	3	0	0	0	0
Immunoglobulin receptor†	59	0	0	0	0
T-cell receptor alpha chain	16	0	0	0	0
T-cell receptor beta chain	15	0	0	0	0
T-cell receptor gamma chain	1	0	0	0	0
T cell receptor delta chain					

alytic activity, as a uracil DNA glycosylase (*140*) and functions as a cell cycle regulator [illegible] ptosis (*142*).

Translation. Another striking set of human expansions has occurred in certain families involved in the translational machinery. We identified 28 different ribosomal subunits that each have at least 10 copies in the genome; on average, for all ribosomal proteins there is about an 8- to 10-fold expansion in the number of genes relative to either the worm or fly. Retrotransposed pseudogenes may account for many of these expansions [see the discussion above and (*143*)]. Recent [illegible] suggests that a number of ribosomal proteins have secondary functions independent of their involvement in protein biosynthesis; for example, L13a and the related L7 subunits (36 copies in humans) have been shown to induce apoptosis (*144*).

There is also a four- to fivefold expansion in the elongation factor 1-alpha family (eEF1A; 56 human genes). Many of these expansions likely represent intronless paralogs that have presumably arisen from retrotransposition, and again there is evidence tha[illegible] However, a second form (eEF1A2) of this factor has been identied with tissue-specific expression in skeletal muscle and a complementary expression pattern to the ubiquitously expressed eEF1A (*146*).

Ribonucleoproteins. Alternative splicing results in multiple transcripts from a single gene, and can therefore generate additional diversity in an organism's protein complement. We have identified 269 genes for ribonucleoproteins. This represents over 2.5 times the number of ribonucleoprotein genes in the worm, two times that of the fly, and about the same as the 265 identified in the *Arabidopsis* genome. Whether the diversity of ribonucleoprotein genes in humans contributes to gene regulation at either the splicing or translational level is unknown.

Posttranslational modifications. In this set of processes, the most prominent expansion is the transglutaminases, calcium-dependent enzymes that catalyze the cross-linking of proteins in cellular processes such as hemostasis and apoptosis (*147*). The vitamin K–dependent gamma carboxylase gene product acts on the GLA domain (missing in the fly and worm) found in coagulation factors, osteocalcin, and matrix GLA protein (*148*). Tyrosylprotein sulfotransferases participate in the posttranslational modification of proteins involved in inflammation and hemostasis, including coagulation factors and chemokine receptors (*149*). Although there is no significant numerical increase in the counts for domains involved in nuclear protein modification, there are a number of domain arrangements in the predicted human proteins that are not found in the other currently sequenced genomes. These include the tandem association of two histone deacetylase domains in HD6 with a ubiquitin finger domain, a feature lacking in the fly genome. An additional example is the co-occurrence of important nuclear regulatory enzyme PARP (poly-ADP ribosyl transferase) domain fused to protein-interaction domains—BRCT and VWA in humans.

Concluding remarks. There are several possible explanations for the differences in phenotypic complexity observed in humans when compared to the fly and worm. Some of these relate to the prominent differences in the immune system, hemostasis, neuronal, vascular, and cytoskeletal complexity. The finding that the human genome contains fewer genes than previously predicted might be [illegible] translational modification of proteins, or posttranscriptional regulation. Extensive domain shuffling to increase or alter combinatorial diversity can provide an exponential

Table 19 (*Continued*)

Panther family/subfamily*	H	F	W	Y	A
MHC class I	22	0	0	0	0
MHC class II	20	0	0	0	0
Other immunoglobulin†	114	0	0	0	0
Toll receptor–related	10	6	0	0	0
Developmental and homeostatic regulators					
Signaling molecules†					
Calcitonin	3	0	0	0	0
Ephrin	8	2	4	0	0
FGF	24	1	1	0	0
Glucagon	4	0	0	0	0
Glycoprotein hormone beta chain	2	0	0	0	0
Insulin	1	0	0	0	0
Insulin-like hormone	3	0	0	0	0
Nerve growth factor	3	0	0	0	0
Neuregulin/heregulin	6	0	0	0	0
neuropeptide Y	4	0	0	0	0
PDGF	1	1	0	0	0
Relaxin	3	0	0	0	0
Stannocalcin	2	0	0	0	0
Thymopoeitin	2	0	1	0	0
Thyomosin beta	4	2	0	0	0
TGF-β	29	6	4	0	0
VEGF	4	0	0	0	0
Wnt	18	6	5	0	0
Receptors†					
Ephrin receptor	12	2	1	0	0
FGF receptor	4	4	0	0	0
Frizzled receptor	12	6	5	0	0
Parathyroid hormone receptor	2	0	0	0	0
VEGF receptor	5	0	0	0	0
BDNF/NT-3 nerve growth factor receptor	4	0	0	0	0
Kinases and phosphatases					
Dual-specificity protein phosphatase	29	8	10	4	11
S/T and dual-specificity protein kinase†	395	198	315	114	1102
S/T protein phosphatase	15	19	51	13	29
Y protein kinase†	106	47	100	5	16
Y protein phosphatase	56	22	95	5	6
Signal transduction					
ARF family	55	29	27	12	45
Cyclic nucleotide phosphodiesterase	25	8	6	1	0
G protein-coupled receptors†‡	616	146	284	0	1
G-protein alpha	27	10	22	2	5
G-protein beta	5	3	2	1	1
G-protein gamma	13	2	2	0	0
[illegible] superfamily					
[illegible]					
[illegible]					
[illegible]as GTPase-activating					
Tuberin	7	3	2	0	0
Vav proto-oncogene family	35	15	13	3	0

increase in the ability to mediate protein-protein interactions without dramatically increasing the absolute size of the protein complement (*150*). Evolution of apparently new (from the perspective of sequence analysis) protein domains and increased complexity by domain accretion both quantitatively and qualitatively (recruitment of novel domains with preexisting ones) are two features that we observe in humans. Perhaps the best illustration of this trend is the C2H2 zinc finger–containing transcription factors, where we see expansion in the number of domains per protein, together with vertebrate-specific domains such as KRAB and SCAN. Recent reports on the prominent use of internal ribosomal entry sites in the human genome to regulate translation of specific classes of proteins suggests that this is an area that needs further research to identify the full extent of this process in the human genome (*151*). At the posttranslational level, although we provide examples of expansions of some protein families involved in these modifications, further experimental evidence is required to evaluate whether this is correlated with increased complexity in protein processing. Posttranscriptional processing and the extent of isoform generation in the human remain to be cataloged in their entirety. Given the conserved nature of the spliceosomal machinery, further analysis will be required to dissect regulation at this level.

8 Conclusions

8.1 The whole-genome sequencing approach versus BAC by BAC

Experience in applying the whole-genome shotgun sequencing approach to a diverse group of organisms with a wide range of genome sizes and repeat content allows us to assess its strengths and weaknesses. With the success of the method for a large number of microbial genomes, *Drosophila*, and now the human, there can be no doubt concerning the utility of this method. The large number of microbial genomes that have been sequenced by this method (*15*, *80*, *152*) demonstrate that megabase-sized genomes can be sequenced efficiently without any input other that the de novo mate-paired sequences. With more complex genomes like those of *Drosophila* or human, map information, in the form of well-ordered markers, has been critical for long-range ordering of scaffolds. For joining scaffolds into chromosomes, the quality of the map (in terms of the order of the markers) is more important than the number of markers per se. Although this mapping could have been performed concurrently with sequencing, the prior existence of mapping data was

Table 19 (*Continued*)

Panther family/subfamily*	H	F	W	Y	A
Transcription factors/chromatin organization					
COE	[illegible]	232	79	28	8
CREB	7	1	1	0	0
ETS-related	7	1	2	0	0
Forkhead-related	25	8	10	0	0
FOS	34	19	15	4	0
Groucho	8	2	1	0	0
Histone H1	13	2	1	0	0
Histone H2A	5	0	1	0	0
Histone H2B	24	1	17	3	13
Histone H3	21	1	17	2	12
Histone H4	28	2	24	2	16
Homeotic†	9	1	16	1	8
ABD-B	168	104	74	4	78
Bithoraxoid	5	0	0	0	0
Iroquois class	1	8	1	0	0
Distal-less	7	3	1	0	0
Engrailed	5	2	1	0	0
LIM-containing	2	2	1	0	0
MEIS/KNOX class	17	8	3	0	0
NK-3/NK-2 class	9	4	4	2	26
Paired box	9	4	5	0	0
Six	38	28	23	0	2
Leucine zipper	5	3	4	0	0
Nuclear hormone receptor†	6	0	0	0	0
Pou-related	59	25	183	1	4
Runt-related	15	5	4	1	0
	3	4	2	0	0
ECM adhesion					
Cadherin	113	17	16	0	0
Claudin	20	0	0	0	0
Complement receptor-related	22	8	6	0	0
Connexin	14	0	0	0	0
Galectin	12	5	22	0	0
Glypican	13	2	1	0	0
ICAM	6	0	0	0	0
Integrin alpha	24	7	4	0	1
Integrin beta	9	2	2	0	0
LDL receptor family	26	19	20	0	2
Proteoglycans	22	9	7	0	5
Apoptosis					
Bcl-2	12	1	0	0	0
Calpain	22	4	11	1	3
Calpain inhibitor	4	0	0	0	1
Caspase	13	7	3	0	0
Hemostasis					
ADAM/ADAMTS	51	9	12	0	0
Fibronectin	3	0	0	0	0
Globin	10	2	3	0	3
Matrix metalloprotease	19	2	7	0	3
Serum amyloid A	4	0	0	0	0
Serum amyloid P (subfamily of Pentaxin)	2	0	0	0	0
Serum paraoxonase/arylesterase	4	0	3	0	0
Serum albumin	4	0	0	0	0
Transglutaminase	10	1	0	0	0
Other enzymes					
Cytochrome p450	60	89	83	3	256
GAPDH	46	3	4	3	8
Heparan sulfotransferase	11	4	2	0	0
Splicing and translation					
EF-1alpha	56	13	10	6	13
Ribonucleoproteins†	269	135	104	60	265
Ribosomal proteins†	812	111	80	[illegible]	[illegible]

[illegible] metabotropic glutamate class GPCR

[illegible] rhodopsin-class, secret

quence well into centromeric regions and allowed high-quality resolution of complex repeat regions. Likewise, in *Drosophila*, the BAC physical map was most useful in regions near the highly repetitive centromeres and telomeres. WGA has been found to deliver excellent-quality reconstructions of the unique regions of the genome. As the genome size, and more importantly the repetitive content, increases, the WGA approach delivers less of the repetitive sequence.

The cost and overall efficiency of clone-by-clone approaches makes them difficult to justify as a stand-alone strategy for future large-scale genome-sequencing projects. Specific applications of BAC-based or other clone mapping and sequencing strategies to resolve ambiguities in sequence assembly that cannot be efficiently resolved with computational approaches alone are clearly worth exploring. Hybrid approaches to whole-genome sequencing will only work if there is sufficient coverage in both the whole-genome shotgun phase and the BAC clone sequencing phase. Our experience with human genome assembly suggests that this will require at least 3× coverage of both whole-genome and BAC shotgun sequence data.

8.2 The low gene number in humans

We have sequenced and assembled ~95% of the euchromatic sequence of *H. sapiens* and used a new automated gene prediction method to produce a preliminary catalog of the human genes. This has provided a major surprise: We have found far fewer genes (26,000 to 38,000) than the earlier molecular predictions (50,000 to over 140,000). Whatever the reasons for this current disparity, only detailed annotation, comparative genomics (particularly using the *Mus musculus* genome), and careful molecular dissection of complex phenotypes will clarify this critical issue of the basic "parts list" of our genome. Certainly, the analysis is still incomplete and considerable refinement will occur in the years to come as the precise structure of each transcription unit is evaluated. A good place to start is to determine why the gene estimates derived from EST data are so discordant with our predictions. It is likely that the following contribute to an inflated gene number derived from ESTs: the variable lengths of 3′- and 5′-untranslated leaders and trailers; the little-understood vagaries of RNA processing that often leave intronic regions in an unspliced condition; the finding that nearly 40% of human genes are alternatively spliced (*153*); and finally, the unsolved technical problems in EST [illegible]

predicting genes should limit this number. As was true at the beginning of [illegible]ing, ultimately it will be necessary to measure mRNA in specific cell types to demonstrate the presence of a gene.

J. B. S. Haldane speculated in 1937 that a population of organisms might have to pay a price for the number of genes it can possibly carry. He theorized that when the number of genes becomes too large, each zygote carries so many new deleterious mutations that the population simply cannot maintain itself. On the basis of this premise, and on the basis of available mutation rates and x-ray–induced mutations at specific loci, Muller, in 1967 (*154*), calculated that the mammalian genome would contain a maximum of not much more than 30,000 genes (*155*). An estimate of 30,000 gene loci for humans was also arrived at by Crow and Kimura (*156*). Muller's estimate for *D. melanogaster* was 10,000 genes, compared to 13,000 derived by annotation of the fly genome (*26*, *27*). These arguments for the theoretical maximum gene number were based on simplified ideas of genetic load—that all genes have a certain low rate of mutation to a deleterious state. However, it is clear that many mouse, fly, worm, and yeast knockout mutations lead to almost no discernible phenotypic perturbations.

The modest number of human genes means that we must look elsewhere for the mechanisms that generate the complexities inherent in human development and the sophisticated signaling systems that maintain homeostasis. There are a large number of ways in which the functions of individual genes and gene products are regulated. The degree of "openness" of chromatin structure and hence transcriptional activity is regulated by protein complexes that involve histone and DNA enzymatic modifications. We enumerate many of the proteins that are likely involved in nuclear regulation in Table 19. The location, timing, and quantity of transcription are intimately linked to nuclear signal transduction events as well as by the tissue-specific expression of many of these proteins. Equally important are regulatory DNA elements that include insulators, repeats, and endogenous viruses (*157*); methylation of CpG islands in imprinting (*158*); and promoter-enhancer and intronic regions that modulate transcription. The spliceosomal machinery consists of multisubunit proteins (Table 19) as well as structural and catalytic RNA elements (*159*) that regulate transcript structure through alternative start and termi-

of RNA editing in which coding changes

clinical and biological relevance (*161*). Finally, examples of translational control include internal ribosomal entry sites that are found in proteins involved in cell cycle regulation and apoptosis (*162*). At the protein level, minor alterations in the nature of protein-protein interactions, protein modifications, and localization can have dramatic effects on cellular physiology (*163*). This dynamic system therefore has many ways to modulate activity, which suggests that definition of complex systems by analysis of single genes is unlikely to be entirely successful.

In situ studies have shown that the human genome is asymmetrically populated with G+C content, CpG islands, and genes (*68*). However, the genes are not distributed quite as unequally as had been predicted (Table 9) (*69*). The most G+C-rich fraction of the genome, H3 isochores, constitute more of the genome than previously thought (about 9%), and are the most gene-dense fraction, but contain only 25% of the genes, rather than the predicted ~40%. The low G+C L isochores make up 65% of the genome, and 48% of the genes. This inhomogeneity, the net result of millions of years of mammalian gene duplication, has been described as the "desertification" of the vertebrate genome (*71*). Why are there clustered regions of high and low gene density, and are these accidents of history or driven by selection and evolution? If these deserts are dispensable, it ought to be possible to find mammalian genomes that are far smaller in size than the human genome. Indeed, many species of bats have genome sizes that are much smaller than that of humans; for example, *Miniopterus*, a species of Italian bat, has a genome size that is only 50% that of humans (*164*). Similarly, *Muntiacus*, a species of Asian barking deer, has a genome size that is ~70% that of humans.

8.3 Human DNA sequence variation and its distribution across the genome

This is the first eukaryotic genome in which a nearly uniform ascertainment of polymorphism has been completed. Although we have identified and mapped more than 3 million SNPs, this by no means implies that the task of finding and cataloging SNPs is complete. These represent only a fraction of the SNPs present in the human population as a whole. Nevertheless, this first glimpse at genome-wide variation has revealed strong inhomogeneities in the distribution of SNPs across the genome. Polymorphism

course, it is possible that there are genes that remain unpredicted owing to the absence of EST or protein data to support them, although our use of mouse genome data for

antisense riboregulator RNA, RNA involved in X-dosage compensation, and other structural RNAs to appreciate their precise role in regulating gene expression. The phenomenon

[illegible] The availability of a dense array of SNPs will allow questions related to each of these factors to be addressed on a genome-wide basis. SNP studies can establish the range of haplo-

types present in subjects of different ethnogeographic origins, providing insights into population history and migration patterns. Although such studies have suggested that modern human lineages derive from Africa, many important [illegible] answered, and more analyses using detailed SNP maps will be needed to settle these controversies. In addition to providing evidence for population expansions, migration, and admixture, SNPs can serve as markers for the extent of evolutionary constraint acting on particular genes. The correlation between patterns of intraspecies and interspecies genetic variation may prove to be especially informative to identify sites of reduced genetic diversity that may mark loci where sequence variations are not tolerated.

The remarkable heterogeneity in SNP density implies that there are a variety of forces acting on polymorphism—sparse regions may have lower SNP density because the mutation rate is lower, because most of those regions have a lower fraction of mutations that are tolerated, or because recent strong selection in favor of a newly arisen allele "swept" the linked variation out of the population (*165*). The effect of random genetic drift also varies widely across the genome. The nonrecombining portion of the Y chromosome faces the strongest pressure from random drift because there are roughly one-quarter as many Y chromosomes in the population as there are autosomal chromosomes, and the level of polymorphism on the Y is correspondingly less. Similarly, the X chromosome has a smaller effective population size than the autosomes, and its nucleotide diversity is also reduced. But even across a single autosome, the effective population size can vary because the density of deleterious mutations may vary. Regions of high density of deleterious mutations will see a greater rate of elimination by selection, and the effective population size will be smaller (*166*). As a result, the density of even completely neutral SNPs will be lower in such regions. There is a large literature on the association between SNP density and local recombination rates in *Drosophila*, and it remains an important task to assess the strength of this association in the human genome, because of its impact on the design of local SNP densities for disease-association studies. It also remains an important task to validate SNPs on a genomic scale in order to assess the degree of heterogeneity among geographic and ethnic populations.

8.4 Genome complexity

We will soon be in a position [illegible]

[illegible]

[illegible] complete sequence of the human g[illegible]

then docks on this, and then the complex moves there. . . ." (*167*) to the exciting area of network perturbations, nonlinear responses and thresholds, and their pivotal role in human diseases.

The enumeration of other "parts lists" reveals that in organisms with complex nervous systems, neither gene number, neuron number, nor number of cell types correlates in any meaningful manner with even simplistic measures of structural or behavioral complexity. Nor would they be expected to; this is the realm of nonlinearities and epigenesis (*168*). The 520 million neurons of the common octopus exceed the neuronal number in the brain of a mouse by an order of magnitude. It is apparent from a comparison of genomic data on the mouse and human, and from comparative mammalian neuroanatomy (*169*), that the morphological and behavioral diversity found in mammals is underpinned by a similar gene repertoire and similar neuroanatomies. For example, when one compares a pygmy marmoset (which is only 4 inches tall and weighs about 6 ounces) to a chimpanzee, the brain volume of this minute primate is found to be only about 1.5 cm^3, two orders of magnitude less than that of a chimp and three orders less than that of humans. Yet the neuroanatomies of all three brains are strikingly similar, and the behavioral characteristics of the pygmy marmoset are little different from those of chimpanzees. Between humans and chimpanzees, the gene number, gene structures and functions, chromosomal and genomic organizations, and cell types and neuroanatomies are almost indistinguishable, yet the developmental modifications that predisposed human lineages to cortical expansion and development of the larynx, giving rise to language, culminated in a massive singularity that by even the simplest of criteria made humans more complex in a behavioral sense.

Simple examination of the number of neurons, cell types, or genes or of the genome size does not alone account for the differences in complexity that we observe. Rather, it is the interactions within and among these sets that result in such great variation. In addition, it is possible that there are "special cases" of regulatory gene networks that have a disproportionate effect on the overall system. We have presented several examples of "regulatory genes" that are significantly increased in the human genome compared with the fly and worm. These include extracellular ligands and their cognate receptors (e.g., wnt, frizzled, TGF-β, ephrins, and connexins), as well as nuclear regulators (e.g., the KRAB and homeodomain transcription factor families), where a few proteins control broad developmental processes. The answers to these

8.5 Beyond single components

While few would disagree with the intuitive conclusion that Einstein's brain was more complex than that of *Drosophila*, closer com[illegible]

human proteins is more complex than the protein set of *Drosophila*, and if so, to what degree, are not straightforward, since protein, protein domain, or protein-protein interaction measures do not capture context-dependent interactions that underpin the dynamics underlying phenotype.

Currently, there are more than 30 different mathematical descriptions of complexity (*170*). However, we have yet to understand the mathematical dependency relating the number of genes with organism complexity. One pragmatic approach to the analysis of biological systems, which are composed of nonidentical elements (proteins, protein complexes, interacting cell types, and interacting neuronal populations), is through graph theory (*171*). The elements of the system can be represented by the vertices of complex topographies, with the edges representing the interactions between them. Examination of large networks reveals that they can self-organize, but more important, they can be particularly robust. This robustness is not due to redundancy, but is a property of inhomogeneously wired networks. The error tolerance of such networks comes with a price; they are vulnerable to the selection or removal of a few nodes that contribute disproportionately to network stability. Gene knockouts provide an illustration. Some knockouts may have minor effects, whereas others have catastrophic effects on the system. In the case of vimentin, a supposedly critical component of the cytoplasmic intermediate filament network of mammals, the knockout of the gene in mice reveals them to be reproductively normal, with no obvious phenotypic effects (*172*), and yet the usually conspicuous vimentin network is completely absent. On the other hand, ~30% of knockouts in *Drosophila* and mice correspond to critical nodes whose reduction in gene product, or total elimination, causes the network to crash most of the time, although even in some of these cases, phenotypic normalcy ensues, given the appropriate genetic background. Thus, there are no "good" genes or "bad" genes, but only networks that exist at various levels and at different connectivities, and at different states of sensitivity to perturbation. Sophisticated mathematical analysis needs to be constantly evaluated against hard biological data sets that specifically address network dynamics. Nowhere is this more critical than in attempts to come to grips with "complexity," particularly because deconvoluting and correcting complex networks that have undergone perturbation, and

nome would open up new strategies for human biological research, and would have a major impact on medicine, and through medicine and public health, on society. Effects on biomedical research are already being felt. This assembly of the human genome sequence is but a first, hesitant step on a long and exciting journey toward understanding the role of the genome in human biology. It has been possible only because of innovations in instrumentation and software that have allowed automation of almost every step of the process from DNA preparation to annotation. The next steps are clear: We must define the complexity that ensues when this relatively modest set of about 30,000 genes is expressed. The sequence provides the framework upon which all the genetics, biochemistry, physiology, and ultimately phenotype depend. It provides the boundaries for scientific inquiry. The sequence is only the first level of understanding of the genome. All genes and their control elements must be identified; their functions, in concert as well as in isolation, defined; their sequence variation worldwide described; and the relation between genome variation and specific phenotypic characteristics determined. Now we know what we have to explain.

Another paramount challenge awaits: public discussion of this information and its potential for improvement of personal health. Many diverse sources of data have shown that any two individuals are more than 99.9% identical in sequence, which means that all the glorious differences among individuals in our species that can be attributed to genes falls in a mere 0.1% of the sequence. There are two fallacies to be avoided: determinism, the idea that all characteristics of the person are "hard-wired" by the genome; and reductionism, the view that with complete knowledge of the human genome sequence, it is only a matter of time before our understanding of gene functions and interactions will provide a complete causal description of human variability. The real challenge of human biology, beyond the task of finding out how genes orchestrate the construction and maintenance of the miraculous mechanism of our bodies, will lie ahead as we seek to explain how our minds have come to organize thoughts sufficiently well to investigate our own existence.

References and Notes

1. R. L. Sinsheimer, *Genomics* **5**, 954 (1989); U.S. Department of Energy, Office of Health and Environmental Research, Publication [illegible]
2. [illegible] Weigall, *The Gene Wars: Science, Politics and the Human Genome* (Norton, New York, 1999).
3. F. Sanger *et al.*, *Nature* **265**, 687 (1977).
4. P. H. Seeburg *et al.*, *Trans. Assoc. Am. Physicians* **90**, 109 (1977).
5. E. C. Strauss, J. A. Kobori, G. Siu, L. E. Hood, *Anal. Biochem.* **154**, 353 (1986).
6. [illegible] *Proc. Natl. Acad. Sci. U.S.A.* **84**, 8296 (1987).
7. A. Martin-Gallardo *et al.*, *DNA Sequence* **3**, 237 (1992); W. R. McCombie *et al.*, *Nature Genet.* **1**, 348 (1992); M. A. Jensen *et al.*, *DNA Sequence* **1**, 233 (1991).
8. M. D. Adams *et al.*, *Science* **252**, 1651 (1991).
9. M. D. Adams *et al.*, *Nature* **355**, 632 (1992); M. D. Adams, A. R. Kerlavage, C. Fields, J. C. Venter, *Nature Genet.* **4**, 256 (1993); M. D. Adams, M. B. Soares, A. R. Kerlavage, C. Fields, J. C. Venter, *Nature Genet.* **4**, 373 (1993); M. H. Polymeropoulos *et al.*, *Nature Genet.* **4**, 381 (1993), M. Marra *et al.*, *Nature Genet.* **21**, 191 (1999).
10. M. D. Adams *et al.*, *Nature* **377**, 3 (1995); O. White *et al.*, *Nucleic Acids Res.* **21**, 3829 (1993).
11. F. Sanger, A. R. Coulson, G. F. Hong, D. F. Hill, G. B. Petersen, *J. Mol. Biol* **162**, 729 (1982).
12. B. W. J. Mahy, J. J. Esposito, J. C. Venter, *Am. Soc. Microbiol. News* **57**, 577 (1991).
13. R. D. Fleischmann *et al.*, *Science* **269**, 496 (1995).
14. C. M. Fraser *et al.*, *Science* **270**, 397 (1995).
15. C. J. Bult *et al.*, *Science* **273**, 1058 (1996); J. F. Tomb *et al.*, *Nature* **388**, 539 (1997); H. P. Klenk *et al.*, *Nature* **390**, 364 (1997).
16. J. C. Venter, H. O. Smith, L. Hood, *Nature* **381**, 364 (1996).
17. H. Schmitt *et al.*, *Genomics* **33**, 9 (1996).
18. S. Zhao *et al.*, *Genomics* **63**, 321 (2000).
19. X. Lin *et al.*, *Nature* **402**, 761 (1999).
20. J. L. Weber, E. W. Myers, *Genome Res.* **7**, 401 (1997).
21. P. Green, *Genome Res.* **7**, 410 (1997).
22. E. Pennisi, *Science* **280**, 1185 (1998).
23. J. C. Venter *et al.*, *Science* **280**, 1540 (1998).
24. M. D. Adams *et al.*, *Nature* **368**, 474 (1994).
25. E. Marshall, E. Pennisi, *Science* **280**, 994 (1998).
26. M. D. Adams *et al.*, *Science* **287**, 2185 (2000).
27. G. M. Rubin *et al.*, *Science* **287**, 2204 (2000).
28. E. W. Myers *et al.*, *Science* **287**, 2196 (2000).
29. F. S. Collins *et al.*, *Science* **282**, 682 (1998).
30. International Human Genome Sequencing Consortium (2001), *Nature* **409**, 860 (2001).
31. Institutional review board: P. Calabresi (chairman), H. P. Freeman, C. McCarthy, A. L. Caplan, G. D. Rogell, J. Karp, M. K. Evans, B. Margus, C. L. Carter, R. A. Millman, S. Broder.
32. Eligibility criteria for participation in the study were as follows: prospective donors had to be 21 years of age or older, not pregnant, and capable of giving an informed consent. Donors were asked to self-define their ethnic backgrounds. Standard blood bank screens (screening for HIV, hepatitis viruses, and so forth) were performed on all samples at the clinical laboratory prior to DNA extraction in the Celera laboratory. All samples that tested positive for transmissible viruses were ineligible and were discarded. Karyotype analysis was performed on peripheral blood lymphocytes from all samples selected for sequencing; all were normal. A two-staged consent process for prospective donors was employed. The first stage of the consent process provided information about the genome project, procedures, and risks and benefits of participating. The second stage of the consent process involved answering follow-up questions and signing consent forms, and was conducted about 48 hours after the first.
33. DNA was isolated from blood (*173*) or sperm. For sperm, a washed pellet (100 μl) was lysed in a suspension (1 ml) containing 0.1 M NaCl, 10 mM tris-Cl–20 mM EDTA (pH 8), 1% SDS, 1 mg proteinase K, and 10 mM dithiothreitol for 1 hour at 37°C. The lysate was extracted with aqueous phenol and with phenol/chloroform. The DNA was ethanol pre[illegible] sheet with [illegible] and size-selected by electrophoresis on 1% low melting point agarose. After ligation to Bst XI adapters (Invitrogen, catalog no. N408-18), DNA was purified by three rounds of gel electrophoresis to remove excess adapters, and the fragments, now with 3′-CACA overhangs, were inserted into Bst XI–linearized plasmid vector with [illegible] average sizes of inserts were constructed: 2, 10, and 50 kbp. The 2-kbp fragments were cloned in a high-copy pUC18 derivative. The 10- and 50-kbp fragments were cloned in a medium-copy pBR322 derivative. The 2- and 10-kbp libraries yielded uniform-sized large colonies on plating. However, the 50-kbp libraries produced many small colonies and inserts were unstable. To remedy this, the 50-kbp libraries were digested with Bgl II, which does not cleave the vector, but generally cleaved several times within the 50-kbp insert. A 1264-bp Bam HI kanamycin resistance cassette (purified from pUCK4; Amersham Pharmacia, catalog no. 27-4958-01) was added and ligation was carried out at 37°C in the continual presence of Bgl II. As Bgl II–Bgl II ligations occurred, they were continually cleaved, whereas Bam HI–Bgl II ligations were not cleaved. A high yield of internally deleted circular library molecules was obtained in which the residual insert ends were separated by the kanamycin cassette DNA. The internally deleted libraries, when plated on agar containing ampicillin (50 μg/ml), carbenicillin (50 μg/ml), and kanamycin (15 μg/ml), produced relatively uniform large colonies. The resulting clones could be prepared for sequencing using the same procedures as clones from the 10-kbp libraries.
34. Transformed cells were plated on agar diffusion plates prepared with a fresh top layer containing no antibiotic poured on top of a previously set bottom layer containing excess antibiotic, to achieve the correct final concentration. This method of plating permitted the cells to develop antibiotic resistance before being exposed to antibiotic without the potential clone bias that can be introduced through liquid outgrowth protocols. After colonies had grown, QBot (Genetix, UK) automated colony-picking robots were used to pick colonies meeting stringent size and shape criteria and to inoculate 384-well microtiter plates containing liquid growth medium. Liquid cultures were incubated overnight, with shaking, and were scored for growth before passing to template preparation. Template DNA was extracted from liquid bacterial culture using a procedure based upon the alkaline lysis miniprep method (*173*) adapted for high throughput processing in 384-well microtiter plates. Bacterial cells were lysed; cell debris was removed by centrifugation; and plasmid DNA was recovered by isopropanol precipitation and resuspended in 10 mM tris-HCl buffer. Reagent dispensing operations were accomplished using Titertek MAP 8 liquid dispensing systems. Plate-to-plate liquid transfers were performed using Tomtec Quadra 384 Model 320 pipetting robots. All plates were tracked throughout processing by unique plate barcodes. Mated sequencing reads from opposite ends of each clone insert were obtained by preparing two 384-well cycle sequencing reaction plates from each plate of plasmid template DNA using ABI-PRISM BigDye Terminator chemistry (Applied Biosystems) and standard M13 forward and reverse primers. Sequencing reactions were prepared using the Tomtec Quadra 384-320 pipetting robot. Parent-child plate relationships and, by extension, forward-reverse sequence mate pairs were established by automated plate barcode reading by the onboard barcode reader and were recorded by direct LIMS communication. Sequencing reaction products were purified by alcohol precipitation and were dried, sealed, and stored at 4°C in the dark until needed for sequencing, at which time the reaction products were resuspended in deionized formamide and sealed immediately to prevent deg[illegible] [illegible] sample sheet was created at [illegible] code scanning of the sequencing plate barcode. retrieves sample information from the central LIMS, and reserves unique trace identifiers. The application permitted a single sample sheet file in the linking directory and deleted previously created sample sheet files immediately upon scanning of a

sample plate barcode, thus enhancing sample-to-plate associations.
35. F. Sanger, S. Nicklen, A. R. Coulson, *Proc. Natl. Acad. Sci. U.S.A.* **74**, 5463 (1977); J. M. Prober *et al.*, *Science* **238**, 336 (1987).
36. Celera's computing environment is based on Compaq Computer Corporation's Alpha system technol-

Celera uses these Alphas as Data Servers and as nodes in a Virtual Compute Farm, all of which are connected to a fully switched network operating at Fast Ethernet speed (for the VCF) and gigabit Ethernet speed (for data servers). Load balancing and scheduling software manages the submission and execution of jobs, based on central processing unit (CPU) speed, memory requirements, and priority. The Virtual Compute Farm is composed of 440 Alpha CPUs, which includes model EV6 running at a clock speed of 400 MHz and EV67 running at 667 MHz. Available memory on these systems ranges from 2 GB to 8 GB. The VCF is used to manage trace file processing, and annotation. Genome assembly was performed on a GS 160 running 16 EV67s (667 MHz) and 64 GB of memory, and 10 ES40s running 4 EV6s (500 MHz) and 32 GB of memory. A total of 100 terabytes of physical disk storage was included in a Storage Area Network that was available to systems across the environment. To ensure high availability, file and database servers were configured as 4-node Alpha TruClusters, so that services would fail over in the event of hardware or software failure. Data availability was further enhanced by using hardware- and software-based disk mirroring (RAID-0), disk striping (RAID-1), and disk striping with parity (RAID-5).
37. Trace processing generates quality values for base calls by means of Paracel's TraceTuner, trims sequence reads according to quality values, trims vector and adapter sequence from high-quality reads, and screens sequences for contaminants. Similar in design and algorithm to the phred program (*174*), TraceTuner reports quality values that reflect the log-odds score of each base being correct. Read quality was evaluated in 50-bp windows, each read being trimmed to include only those consecutive 50-bp segments with a minimum mean accuracy of 97%. End windows (both ends of the trace) of 1, 5, 10, 25, and 50 bases were trimmed to a minimum mean accuracy of 98%. Every read was further checked for vector and contaminant matches of 50 bp or more, and if found, the read was removed from consideration. Finally, any match to the 5′ vector splice junction in the initial part of a read was removed.
38. National Center for Biotechnology Information (NCBI); available at www.ncbi.nlm.nih.gov/.
39. NCBI; available at www.ncbi.nlm.nih.gov/HTGS/.
40. All bactigs over 3 kbp were examined for coverage by Celera mate pairs. An interval of a bactig was deemed an assembly error where there were no mate pairs spanning the interval and at least two reads that should have their mate on the other side of the interval but did not. In other words, there was no mate pair evidence supporting a join in the breakpoint interval and at least two mate pairs contradicting the join. By this criterion, we detected and broke apart bactigs at 13,037 locations, or equivalently, we found 2.13% of the bactigs to be misassembled.
41. We considered a BAC entry to be chimeric if, by the Lander-Waterman statistic (*175*), the odds were 0.99 or more that the assembly we produced was inconsistent with the sequence coming from a single source. By this criterion, 714 or 2.2% of BAC entries were deemed chimeric.
42. G. Myers, S. Selznick, Z. Zhang, W. Miller, *J. Comput. Biol.* **3**, 563 (1996).
43. E. W. Myers, J. L. Weber, in *Computational Methods in Genome Research*, S. Suhai, Ed. (Plenum, New York, 1996), pp. 73–89.
44. P. Deloukas *et al.*, *Science* **282**, 744 (1998).
45. M. A. Marra *et al.*, *Genome Res.* **9**, 1043 (1999).

fragments on the scaffolds was analyzed. If the spread of these fragments was greater than four times the reported BAC length, the BAC was considered to be chimeric. In addition, if >20% of bactigs of a given BAC were found on a different scaffolds that were not adjacent in map position, then the BAC was also considered chimeric. The number of BACs used for CSA gave the minimal estimate of chimerism rate.
48. M. Hattori *et al.*, *Nature* **405**, 311 (2000).
49. I. Dunham *et al.*, *Nature* **402**, 489 (1999).
50. A. B. Carvalho, B. P. Lazzaro, A. G. Clark, *Proc. Natl. Acad. Sci. U.S.A.* **97**, 13239 (2000).
51. The International RH Mapping Consortium, available at www.ncbi.nlm.nih.gov/genemap99/.
52. See http://ftp.genome.washington.edu/RM/RepeatMasker.html.
53. G. D. Schuler, *Trends Biotechnol.* **16**, 456 (1998).
54. S. F. Altschul, W. Gish, W. Miller, E. W. Myers, D. J. Lipman, *J. Mol. Biol.* **215**, 403 (1990).
55a. M. Olivier *et al.*, *Science* **291**, 1298 (2001).
55b. See http://genome.ucsc.edu/.
56. N. Chaudhari, W. E. Hahn, *Science* **220**, 924 (1983); R. J. Milner, J. G. Sutcliffe, *Nucleic Acids Res.* **11**, 5497 (1983).
57. D. Dickson, *Nature* **401**, 311 (1999).
58. B. Ewing, P. Green, *Nature Genet.* **25**, 232 (2000).
59. H. Roest Crollius *et al.*, *Nature Genet.* **25**, 235 (2000).
60. M. Yandell, in preparation.
61. K. D. Pruitt, K. S. Katz, H. Sicotte, D. R. Maglott, *Trends Genet.* **16**, 44 (2000).
62. Scaffolds containing greater than 10 kbp of sequence were analyzed for features of biological importance through a series of computational steps, and the results were stored in a relational database. For scaffolds greater than one megabase, the sequence was cut into single megabase pieces before computational analysis. All sequence was masked for complex repeats using Repeatmasker (*52*) before gene finding or homology-based analysis. The computational pipeline required ~7 hours of CPU time per megabase, including repeat masking, or a total compute time of about 20,000 CPU hours. Protein searches were performed against the nonredundant protein database available at the NCBI. Nucleotide searches were performed against human, mouse, and rat Celera Gene Indices (assemblies of cDNA and EST sequences), mouse genomic DNA reads generated at Celera (3×), the Ensembl gene database available at the European Bioinformatics Institute (EBI), human and rodent (mouse and rat) EST data sets parsed from the dbEST database (NCBI), and a curated subset of the RefSeq experimental mRNA database (NCBI). Initial searches were performed on repeat-masked sequence with BLAST 2.0 (*54*) optimized for the Compaq Alpha computeserver and an effective database size of 3×10^9 for BLASTN searches and 1×10^9 for BLASTX searches. Additional processing of each query-subject pair was performed to improve the alignments. All protein BLAST results having an expectation score of $<1 \times 10^{-4}$, human nucleotide BLAST results having an expectation score of $<1 \times 10^{-8}$ with >94% identity, and rodent nucleotide BLAST results having an expectation score of $<1 \times 10^{-8}$ with >80% identity were then examined on the basis of their high-scoring pair (HSP) coordinates on the scaffold to remove redundant hits, retaining hits that supported possible alternative splicing. For BLASTX searches, analysis was performed separately for selected model organisms (yeast, mouse, human, *C. elegans*, and *D. melanogaster*) so as not to exclude HSPs from these organisms that support the same gene structure. Sequences producing BLAST hits judged to be informative, nonredundant, and sufficiently similar to the scaffold sequence were then realigned to the genomic sequence with Sim4 for ESTs, and with Lap for proteins. Because both of these algorithms take splicing into account, the

homology-based analysis described above, three ab initio gene prediction programs were used (*63*).
63. E. C. Uberbacher, Y. Xu, R. J. Mural, *Methods Enzymol.* **266**, 259 (1996); C. Burge, S. Karlin, *J. Mol. Biol.* **268**, 78 (1997); R. J. Mural, *Methods Enzymol.* **303**, 77 (1999); A. A. Salamov, V. V. Solovyev, *Genome Res.* **8**, 967 (1998).
64. G. L. Miklos, B. John, *Am. J. Hum. Genet.* **31**, 264 (1979); U. Francke, *Cytogenet. Cell Genet.* **65**, 206 (1994).
65. P. E. Warburton, H. F. Willard, in *Human Genome Evolution*, M. S. Jackson, T. Strachan, G. Dover, Eds. (BIOS Scientific, Oxford, 1996), pp. 121–145.
66. J. E. Horvath, S. Schwartz, E. E. Eichler, *Genome Res.* **10**, 839 (2000).
67. W. A. Bickmore, A. T. Sumner, *Trends Genet.* **5**, 144 (1989).
68. G. P. Holmquist, *Am. J. Hum. Genet.* **51**, 17 (1992).
69. G. Bernardi, *Gene* **241**, 3 (2000).
70. S. Zoubak, O. Clay, G. Bernardi, *Gene* **174**, 95 (1996).
71. S. Ohno, *Trends Genet.* **1**, 160 (1985).
72. K. W. Broman, J. C. Murray, V. C. Sheffield, R. L. White, J. L. Weber, *Am. J. Hum. Genet.* **63**, 861 (1998).
73. M. J. McEachern, A. Krauskopf, E. H. Blackburn, *Annu. Rev. Genet.* **34**, 331 (2000).
74. A. Bird, *Trends Genet.* **3**, 342 (1987).
75. M. Gardiner-Garden, M. Frommer, *J. Mol. Biol.* **196**, 261 (1987).
76. F. Larsen, G. Gundersen, R. Lopez, H. Prydz, *Genomics* **13**, 1095 (1992).
77. S. H. Cross, A. Bird, *Curr. Opin. Genet. Dev.* **5**, 309 (1995).
78. J. Peters, *Genome Biol.* **1**, reviews1028.1 (2000) (http://genomebiology.com/2000/1/5/reviews/1028).
79. C. Grunau, W. Hindermann, A. Rosenthal, *Hum. Mol. Genet.* **9**, 2651 (2000).
80. F. Antequera, A. Bird, *Proc. Natl. Acad. Sci. U.S.A.* **90**, 11995 (1993).
81. S. H. Cross *et al.*, *Mamm. Genome* **11**, 373 (2000).
82. D. Slavov *et al.*, *Gene* **247**, 215 (2000).
83. A. F. Smit, A. D. Riggs, *Nucleic Acids Res.* **23**, 98 (1995).
84. D. J. Elliott *et al.*, *Hum. Mol. Genet.* **9**, 2117 (2000).
85. A. V. Makeyev, A. N. Chkheidze, S. A. Lievhaber, *J. Biol. Chem.* **274**, 24849 (1999).
86. Y. Pan, W. K. Decker, A. H. H. M. Huq, W. J. Craigen, *Genomics* **59**, 282 (1999).
87. P. Nouvel, *Genetica* **93**, 191 (1994).
88. I. Goncalves, L. Duret, D. Mouchiroud, *Genome Res.* **10**, 672 (2000).
89. Lek first compares all proteins in the proteome to one another. Next, the resulting BLAST reports are parsed, and a graph is created wherein each protein constitutes a node; any hit between two proteins with an expectation beneath a user-specified threshold constitutes an edge. Lek then uses this graph to compute a similarity between each protein pair *ij* in the context of the graph as a whole by simply dividing the number of BLAST hits shared in common between the two proteins by the total number of proteins hit by *i* and *j*. This simple metric has several interesting properties. First, because the similarity metric takes into account both the similarity and the differences between the two sequences at the level of BLAST hits, the metric respects the multidomain nature of protein space. Two multidomain proteins, for instance, each containing domains A and B, will have a greater pairwise similarity to each other than either one will have to a protein containing only A or B domains, so long as A-B–containing multidomain proteins are less frequent in the proteome than are single-domain proteins containing A or B domains. A second interesting property of this similarity metric is that it can be used to produce a similarity matrix for the proteome as a whole without having to first produce a multiple

share at least one significant BLAST hit in common. This is an especially interesting property of the metric, because it allows the rapid recovery of pro-

tiple alignment is possible, thus providing a computational basis for the extension of protein homology searches beyond those of current HMM- and profile-based search methods. Once the whole-proteome similarity matrix has been calculated, Lek first partitions the proteome into single-linkage clusters (*27*) on the basis of one or more shared BLAST hits between two sequences. Next, these single-linkage clusters are further partitioned into subclusters, each member of which shares a user-specified pairwise similarity with the other members of the cluster, as described above. For the purposes of this publication, we have focused on the analysis of single-linkage clusters and what we have termed "complete clusters," e.g., those subclusters for which every member has a similarity metric of 1 to every other member of the subcluster. We believe that the single-linkage and complete clusters are of special interest, in part, because they allow us to estimate and to compare sizes of core protein sets in a rigorous manner. The rationale for this is as follows: if one imagines for a moment a perfect clustering algorithm capable of perfectly partitioning one or more perfectly annotated protein sets into protein families, it is reasonable to assume that the number of clusters will always be greater than, or equal to, the number of single-linkage clusters, because single-linkage clustering is a maximally agglomerative clustering method. Thus, if there exists a single protein in the predicted protein set containing domains A and B, then it will be clustered by single linkage together with all single-domain proteins containing domains A or B. Likewise, for a predicted protein set containing a single multidomain protein, the number of real clusters must always be less than or equal to the number of complete clusters, because it is impossible to place a unique multidomain protein into a complete cluster. Thus, the single-linkage and complete clusters plus singletons should comprise a lower and upper bound of sizes of core protein sets, respectively, allowing us to compare the relative size and complexity of different organisms' predicted protein set.

90. T. F. Smith, M. S. Waterman, *J. Mol. Biol.* **147**, 195 (1981).
91. A. L. Delcher *et al.*, *Nucleic Acids Res.* **27**, 2369 (1999).
92. *Arabidopsis* Genome Initiative, *Nature* **408**, 796 (2000).

93. The probability that a contiguous set of proteins is the result of a segmental duplication can be estimated approximately as follows. Given that protein A and B occur on one chromosome, and that A′ and B′ (paralogs of A and B) also exist in the genome, the probability that B′ occurs immediately after A′ is $1/N$, where N is the number of proteins in the set (for this analysis, N = 26,588). Allowing for B′ to occur as any of the next J-1 proteins [leaving a gap between A′ and B′ increases the probability to $(J - 1)/N$; allowing B′A′ or A′B′ gives a probability of $2(J - 1)/N$]. Considering three genes ABC, the probability of observing A′B′C′ elsewhere in the genome, given that the paralogs exist, is $1/N^2$. Three proteins can occur across a spread of five positions in six ways; more generally, we compute the number of ways that K proteins can be spread across J positions by counting all possible arrangements of $K - 2$ proteins in the $J - 2$ positions between the first and last protein. Allowing for a spread to vary from K positions (no gaps) to J gives

$$L = \sum_{K=2}^{J-2} \binom{X}{K-2}$$

[illegible] duplicated segments might be rearranged by the operations of reversal or translocation, allowing for M such rearrangements gives us a probability $P = L^2M/N^{K-1}$. For example, the probability of observing a duplicated set of three genes in two different locations, where the three genes occur across a spread of five positions in both matched sets in the predicted protein set is approximately $(N)36/N^2 = 36/N$, a value $\ll 1$. Therefore, any such duplications of three genes are unlikely to result from random rearrangements of the genome. If any of the genes occur in more than two copies, the probability that the apparent duplication has occurred by chance increases. The algorithm for selecting candidate duplications only generates matched protein sets with $P \ll 1$.

94. B. J. Trask *et al.*, *Hum. Mol. Genet.* **7**, 13 (1998); D. Sharon *et al.*, *Genomics* **61**, 24 (1999).
95. W. B. Barbazuk *et al.*, *Genome Res.* **10**, 1351 (2000); A. McLysaght, A. J. Enright, L. Skrabanek, K. H. Wolfe, *Yeast* **17**, 22 (2000); D. W. Burt *et al.*, *Nature* **402**, 411 (1999).
96. Reviewed in L. Skrabanek, K. H. Wolfe, *Curr. Opin. Genet. Dev.* **8**, 694 (1998).
97. P. Taillon-Miller, Z. Gu, Q. Li, L. Hillier, P. Y. Kwok, *Genome Res.* **8**, 748 (1998); P. Taillon-Miller, E. E. Piernot, P. Y. Kwok, *Genome Res.* **9**, 499 (1999).
98. D. Altshuler *et al.*, *Nature* **407**, 513 (2000).
99. G. T. Marth *et al.*, *Nature Genet.* **23**, 452 (1999).
100. W.-H. Li, *Molecular Evolution* (Sinauer, Sunderland, MA, 1997).
101. M. Cargill *et al.*, *Nature Genet.* **22**, 231 (1999).
102. M. K. Halushka *et al.*, *Nature Genet.* **22**, 239 (1999).
103. J. Zhang, T. L. Madden, *Genome Res.* **7**, 649 (1997).
104. M. Nei, *Molecular Evolutionary Genetics* (Columbia Univ. Press, New York, 1987).

105. From the observed coverage of the sequences at each site for each individual, we calculated the probability that a SNP would be detected at the site if it were present. For each level of coverage, there is a binomial sampling of the two homologs for each individual, and a heterozygous site could only be ascertained if both homologs are present, or if two alleles from different individuals are present. With coverage x from a given individual, both homologs are present in the assembly with probability $1 - (1/2)x^{-1}$. Even if both homologs are present, the probability that a SNP is detected is <1 because a fraction of sites failed the quality criteria. Integrating over coverage levels, the binomial sampling, and the quality distribution, we derived an expected number of sites in the genome that were ascertained for polymorphism for each individual. The nucleotide diversity was then the observed number of variable sites divided by the expected number of sites ascertained.

106. M. W. Nachman, V. L. Bauer, S. L. Crowell, C. F. Aquadro, *Genetics* **150**, 1133 (1998).
107. D. A. Nickerson *et al.*, *Nature Genet.* **19**, 233 (1998); D. A. Nickerson *et al.*, *Genomic Res.* **10**, 1532 (2000); L. Jorde *et al.*, *Am. J. Hum. Genet.* **66**, 979 (2000); D. G. Wang *et al.*, *Science* **280**, 1077 (1998).
108. M. Przeworski, R. R. Hudson, A. Di Rienzo, *Trends Genet.* **16**, 296 (2000).
109. S. Tavare, *Theor. Popul. Biol.* **26**, 119 (1984).
110. R. R. Hudson, in *Oxford Surveys in Evolutionary Biology*, D. J. Futuyma, J. D. Antonovics, Eds. (Oxford Univ. Press, Oxford, 1990), vol. 7, pp. 1–44.
111. A. G. Clark *et al.*, *Am. J. Hum. Genet.* **63**, 595 (1998).
112. M. Kimura, *The Neutral Theory of Molecular Evolution* (Cambridge Univ. Press, Cambridge, 1983).
113. H. Kaessmann, F. Heissig, A. von Haeseler, S. Paabo, *Nature Genet.* **22**, 78 (1999).
114. E. L. Sonnhammer, S. R. Eddy, R. Durbin, *Proteins* **28**, 405 (1997).
115. A. Bateman *et al.*, *Nucleic Acids Res.* **28**, 263 (2000).

116. Brief description of the methods used to build the Panther classification. First, the June 2000 release of the GenBank NR protein database (excluding se-

[illegible] seed to statistical significance (E-value [illegible] "globally" alignable (the length of the match region must be >70% and <130% of the length of the seed). If the cluster had more than five members, and at least one from a multicellular eukaryote, the cluster was extended. For the extension step, a hidden Markov Model (HMM) was trained for [illegible] NR (excluding mutants but including fragments for this step), and all sequences scoring better than a specific (NLL-NULL) score were added to the cluster. The HMM was then retrained (with fixed model length) and all sequences in the cluster were aligned to the HMM to produce a multiple sequence alignment. This alignment was assessed by a number of quality measures. If the alignment failed the quality check, the initial cluster was rebuilt around the seed using a more restrictive E-value, followed by extension, alignment, and reassessment. This process was repeated until the alignment quality was good. The multiple alignment and "general" (i.e., describing the entire cluster, or "family") HMM (*176*) were then used as input into the BETE program (*177*). BETE calculates a phylogenetic tree for the sequences in the alignment. Functional information about the sequences in each cluster were parsed from SwissProt (*178*) and GenBank records. "Tree-attribute viewer" software was used by biologist curators to correlate the phylogenetic tree with protein function. Subfamilies were manually defined on the basis of shared function across subtrees, and were named accordingly. HMMs were then built for each subfamily, using information from both the subfamily and family (K. Sjölander, In preparation). Families were also manually named according to the functions contained within them. Finally, all of the families and subfamilies were classified into categories and subcategories based on their molecular functions. The categorization was done by manual review of the family and subfamily names, by examining SwissProt and GenBank records, and by review of the literature as well as resources on the World Wide Web. The current version (2.0) of the Panther molecular function schema has four levels: category, subcategory, family, and subfamily. Protein sequences for whole eukaryotic genomes (for the predicted human proteins and annotated proteins for fly, worm, yeast, and *Arabidopsis*) were scored against the Panther library of family and subfamily HMMs. If the score was significant (the NLL-NULL score cutoff depends on the protein family), the protein was assigned to the family or subfamily function with the most significant score.

117. C. P. Ponting, J. Schultz, F. Milpetz, P. Bork, *Nucleic Acids Res.* **27**, 229 (1999).
118. A. Goffeau *et al.*, *Science* **274**, 546, 563 (1996).
119. *C. elegans* Sequencing Consortium, *Science* **282**, 2012 (1998).
120. S. A. Chervitz *et al.*, *Science* **282**, 2022 (1998).
121. E. R. Kandel, J. H. Schwartz, T. Jessell, *Principles of Neural Science* (McGraw-Hill, New York, ed. 4, 2000)
122. D. A. Goodenough, J. A. Goliger, D. L. Paul, *Annu. Rev. Biochem.* **65**, 475 (1996).
123. D. G. Wilkinson, *Int. Rev. Cytol.* **196**, 177 (2000).
124. F. Nakamura, R. G. Kalb, S. M. Strittmatter, *J. Neurobiol.* **44**, 219 (2000).
125. P. J. Horner, F. H. Gage, *Nature* **407**, 963 (2000); P. Casaccia-Bonnefil, C. Gu, M. V. Chao, *Adv. Exp. Med. Biol.* **468**, 275 (1999).
126. S. Wang, B. A. Barres, *Neuron* **27**, 197 (2000).
127. M. Geppert, T. C. Sudhof, *Annu. Rev. Neurosci.* **21**, 75 (1998); J. T. Littleton, H. J. Bellen, *Trends Neurosci.* **18**, 177 (1995).
128. A. Maximov, T. C. Sudhof, I. Bezprozvanny, *J. Biol. Chem.* **274**, 24453 (1999).
129. B. Sampo *et al.*, *Proc. Natl. Acad. Sci. U.S.A.* **97**, 3666 (2000).
130. G. Lemke, *Glia* **7**, 263 (1993).
131. M. Bernfield *et al.*, *Annu. Rev. Biochem.* **68**, 729 [illegible]
[illegible] Freedman *et al.*, *Science* **290**, [illegible] (2000).
135. T. L. Hurskainen, S. Hirohata, M. F. Seldin, S. S. Apte, *J. Biol. Chem* **274**, 25555 (1999).

136. R. A. Black, J. M. White, *Curr. Opin. Cell Biol.* **10**, 654 (1998).
137. L. Aravind, V. M. Dixit, E. V. Koonin, *Trends Biochem. Sci.* **24**, 47 (1999).
138. A. G. Uren *et al.*, *Mol. Cell* **6**, 961 (2000).
139. P. Garcia-Meunier, M. Etienne-Julan, P. Fort, M. Piec- (1993).
140. K. Meyer-Siegler *et al.*, *Proc. Natl. Acad. Sci. U.S.A.* **88**, 8460 (1991).
141. N. R. Mansur, K. Meyer-Siegler, J. C. Wurzer, M. A. Sirover, *Nucleic Acids Res.* **21**, 993 (1993).
142. N. A. Tatton, *Exp. Neurol.* **166**, 29 (2000).
143. N. Kenmochi *et al.*, *Genome Res.* **8**, 509 (1998).
144. F. W. Chen, Y. A. Ioannou, *Int. Rev. Immunol.* **18**, 429 (1999).
145. H. O. Madsen, K. Poulsen, O. Dahl, B. F. Clark, J. P. Hjorth, *Nucleic Acids Res.* **18**, 1513 (1990).
146. D. M. Chambers, J. Peters, C. M. Abbott, *Proc. Natl. Acad. Sci. U.S.A.* **95**, 4463 (1998); A. Khalyfa, B. M. Carlson, J. A. Carlson, E. Wang, *Dev. Dyn.* **216**, 267 (1999).
147. D. Aeschlimann, V. Thomazy, *Connect. Tissue Res.* **41**, 1 (2000).
148. P. Munroe *et al.*, *Nature Genet.* **21**, 142 (1999); S. M. Wu, W. F. Cheung, D. Frazier, D. W. Stafford, *Science* **254**, 1634 (1991); B. Furie *et al.*, *Blood* **93**, 1798 (1999).
149. J. W. Kehoe, C. R. Bertozzi, *Chem. Biol.* **7**, R57 (2000).
150. T. Pawson, P. Nash, *Genes Dev.* **14**, 1027 (2000).
151. A. W. van der Velden, A. A. Thomas, *Int. J. Biochem. Cell Biol.* **31**, 87 (1999).
152. C. M. Fraser *et al.*, *Science* **281**, 375 (1998); H. Tettelin *et al.*, *Science* **287**, 1809 (2000).
153. D. Brett *et al.*, *FEBS Lett.* **474**, 83 (2000).
154. H. J. Muller, H. Kern, *Z. Naturforsch. B* **22**, 1330 (1967).
155. H. J. Muller, in *Heritage from Mendel*, R. A. Brink, Ed. (Univ. of Wisconsin Press, Madison, WI, 1967), p. 419.
156. J. F. Crow, M. Kimura, *Introduction to Population Genetics Theory* (Harper & Row, New York, 1970).
157. K. Kobayashi *et al.*, *Nature* **394**, 203 (1998).
158. [illegible] 87 (2000).
159. C. A. Collins, C. Guthrie, *Nature Struct. Biol.* **7**, 850 (2000).
160. S. R. Eddy, *Curr. Opin. Genet. Dev.* **9**, 695 (1999).
161. Q. Wang, J. Khillan, P. Gadue, K. Nishikura, *Science* **290**, 1765 (2000).
162. M. Holcik, N. Sonenberg, R. G. Korneluk, *Trends Genet.* **16**, 469 (2000).
163. T. A. McKinsey, C. L. Zhang, J. Lu, E. N. Olson, *Nature* **408**, 106 (2000).
164. E. Capanna, M. G. M. Romanini, *Caryologia* **24**, 471 (1971).
165. J. Maynard Smith, *J. Theor. Biol.* **128**, 247 (1987).
166. D. Charlesworth, B. Charlesworth, M. T. Morgan, *Genetics* **141**, 1619 (1995).
167. J. E. Bailey, *Nature Biotechnol.* **17**, 616 (1999).
168. R. Maleszka, H. G. de Couet, G. L. Miklos, *Proc. Natl. Acad. Sci. U.S.A.* **95**, 3731 (1998).
169. G. L. Miklos, *J. Neurobiol.* **24**, 842 (1993).
170. J. P. Crutchfield, K. Young, *Phys. Rev. Lett.* **63**, 105 (1989); M. Gell-Mann, S. Lloyd, *Complexity* **2**, 44 (1996).
171. A. L. Barabasi, R. Albert, *Science* **286**, 509 (1999).
172. E. Colucci-Guyon *et al.*, *Cell* **79**, 679 (1994).
173. J. Sambrook, E. F. Fritch, T. Maniatis, *Molecular Cloning: A Laboratory Manual* (Cold Spring Harbor Laboratory Press, Cold Spring Harbor, NY, ed. 2, 1989).
174. B. Ewing, P. Green, *Genome Res.* **8**, 186 (1998); B. Ewing, L. Hillier, M. C. Wendl, P. Green, *Genome Res.* **8**, 175 (1998).
175. E. S. Lander, M. S. Waterman, *Genomics* **2**, 231 (1988).
176. A. Krogh, K. Sjölander, *J. Mol. Biol.* **235**, 1501 [illegible]
177. K. Sjölander, *Proc. Int. Soc. Mol. Biol.* **6**, 165 (1998).
178. A. Bairoch, R. Apweiler, *Nucleic Acids Res.* **28**, 45 (2000).
179. GO, available at www.geneontology.org/.
180. R. L. Tatusov, M. Y. Galperin, D. A. Natale, E. V. Koonin, *Nucleic Acids Res.* **28**, 33 (2000).

181. We thank E. Eichler and J. L. Goldstein for many helpful discussions and critical reading of the manuscript, and A. Caplan for advice and encouragement. We also thank T. Hein, D. Lucas, G. Edwards, and the Celera IT staff for outstanding computational support. The cost of this project was underwritten by the Celera Genomics Group of the Applera Corporation. We thank the Board of Directors of Applera Corporation: J. F. Abely Jr. (retired), R. H. Ayers, J.-L. Bélingard, R. H. Hayes, A. J. Levine, T. E. Martin, C. W. Slayman, O. R. Smith, G. C. St. Laurent Jr., and J. R. Tobin for their vision, enthusiasm, and unwavering support and T. L. White for leadership and advice. Data availability: The genome sequence and additional supporting information are available to academic scientists at the Web site (www.celera.com). Instructions for obtaining a DVD of the genome sequence can be obtained through the Web site. For commercial scientists wishing to verify the results presented here, the genome data are available upon signing a Material Transfer Agreement, which can also be found on the Web site.

5 December 2000; accepted 19 January 2001

>XM_208689 ACCESSION:XM_208689 NID: gi 30157117 ref XM_208689.3

protease precursor (LOC283471), mRNA
Length = 1457

Score = 712 bits (1819), Expect = 0.0
Identities = 344/348 (98%), Positives = 345/348 (98%), Gaps = 3/348 (0%)
Frame = +1

```
Query: 1   MRLGLLSVAL-FVGSSHL-SDHYSPSGRHRLGPSPEPAASSQQAEAVRKRLRRRREGGAH 58
           MRLGLLSVAL FVGSSHL SDHYSPSGRHRLGPSPEPAASSQQAEAVRKRLRRRREGGAH
Sbjct: 40  MRLGLLSVALLFVGSSHLYSDHYSPSGRHRLGPSPEPAASSQQAEAVRKRLRRRREGGAH 219

Query: 59  AKDCGTAPLKDVLQGSRIIGGTEAQAGAWPWVVSLQIKYGRVLVHVCGGTLVRERWVLTA 118
           A+DCGTAPLKDVLQGSRIIGGTEAQAGAWPWVVSLQIKYGRVLVHVCGGTLVRERWVLTA
Sbjct: 220 AEDCGTAPLKDVLQGSRIIGGTEAQAGAWPWVVSLQIKYGRVLVHVCGGTLVRERWVLTA 399

Query: 119 AHCTKD-SDPLMWTAVIGTNNIHGRYPHTKKIKIKAIIIHPNFILESYVNDIALFHLKKA 177
           AHCTKD SDPLMWTAVIGTNNIHGRYPHTKKIKIKAIIIHPNFILESYVNDIALFHLKKA
Sbjct: 400 AHCTKDASDPLMWTAVIGTNNIHGRYPHTKKIKIKAIIIHPNFILESYVNDIALFHLKKA 579

Query: 178 VRYNDYIQPICLPFDVFQILDGNTKCFISGWGRTKEEGNATNILQDAEVHYISREMCNSE 237
           VRYNDYIQPICLPFDVFQILDGNTKCFISGWGRTKEEGNATNILQDAEVHYISREMCNSE
Sbjct: 580 VRYNDYIQPICLPFDVFQILDGNTKCFISGWGRTKEEGNATNILQDAEVHYISREMCNSE 759

Query: 238 RSYGGIIPNTSFCAGDEDGAFDTCRGDSGGPLMCYLPEYKRFFVMGITSYGHGCGRRGFP 297
           RSYGGIIPNTSFCAGDEDGAFDTCRGDSGGPLMCYLPEYKRFFVMGITSYGHGCGRRGFP
Sbjct: 760 RSYGGIIPNTSFCAGDEDGAFDTCRGDSGGPLMCYLPEYKRFFVMGITSYGHGCGRRGFP 939

Query: 298 GVYIGPSFYQKWLTEHFFHASTQGILTINILRGQILIALCFVILLATT 345
           GVYIGPSFYQKWLTEHFFHASTQGILTINILRGQILIALCFVILLATT
Sbjct: 940 GVYIGPSFYQKWLTEHFFHASTQGILTINILRGQILIALCFVILLATT 1083
```

NCBI Nucleotide

PubMed Nucleotide Protein Genome Structure

Search Nucleotide for Go Clear

Limits Preview/Index History Clipboard Details

Display default Show: 20 Send to File Get Subsequence

1: XM_208689. Homo sapiens simi...[gi:30157117]

Links

```
LOCUS       LOC283471               1457 bp    mRNA    linear   PRI 28-APR-2003
DEFINITION  Homo sapiens similar to adrenal secretory serine protease precursor
            (LOC283471), mRNA.
ACCESSION   XM_208689
VERSION     XM_208689.3  GI:30157117
KEYWORDS    .
SOURCE      Homo sapiens (human)
  ORGANISM  Homo sapiens
            Eukaryota; Metazoa; Chordata; Craniata; Vertebrata; Euteleostomi;
            Mammalia; Eutheria; Primates; Catarrhini; Hominidae; Homo.
REFERENCE   1  (bases 1 to 1457)
  AUTHORS   International Human Genome Sequencing Consortium.
  TITLE     The DNA sequence of Homo sapiens
  JOURNAL   Unpublished (2003)
COMMENT     GENOME ANNOTATION REFSEQ:  This model reference sequence was
            predicted from NCBI contig NT_029419 by automated computational
            analysis using gene prediction method: BLAST, supported by mRNA and
            EST evidence.
            Also see:
                Documentation of NCBI's Annotation Process

            On Apr 28, 2003 this sequence version replaced gi:29743195.
FEATURES             Location/Qualifiers
     source          1..1457
                     /organism="Homo sapiens"
                     /mol_type="mRNA"
                     /db_xref="taxon:9606"
                     /chromosome="12"
     gene            1..1457
                     /gene="LOC283471"
                     /db_xref="InterimID:283471"
     CDS             40..1086
                     /gene="LOC283471"
                     /codon_start=1
                     /product="similar to adrenal secretory serine protease
                     precursor"
                     /protein_id="XP_208689.3"
                     /db_xref="GI:30157118"
                     /db_xref="InterimID:283471"
                     /translation="MRLGLLSVALLFVGSSHLYSDHYSPSGRHRLGPSPEPAASSQQA
                     EAVRKRLRRRREGGAHAEDCGTAPLKDVLQGSRIIGGTEAQAGAWPWVVSLQIKYGRV
                     LVHVCGGTLVRERWVLTAAHCTKDASDPLMWTAVIGTNNIHGRYPHTKKIKIKAIIIH
```

```
                     /gene="LOC283471"
                     /note="COG5640; Region: Secreted trypsin-like serine
                     protease [Posttranslational modification, protein
                     turnover, chaperones]"
                     /db_xref="CDD:COG5640"
     misc_feature    268..978
                     /gene="LOC283471"
                     /note="Tryp_SPc; Region: Trypsin-like serine protease"
                     /db_xref="CDD:smart00020"
     misc_feature    271..978
                     /gene="LOC283471"
                     /note="trypsin; Region: Trypsin"
                     /db_xref="CDD:pfam00089"
BASE COUNT      419 a    269 c    327 g    442 t
ORIGIN
        1 gggaagtacc tgccgccatc ttgctcacca gcctccaaaa tgcggctggg gctcctgagc
       61 gtggcgctgt tgtttgtggg gagctctcac ttatactcag accactactc gccctctgga
      121 aggcacaggc tcggcccctc gccggaaccg gcggctagtt cccagcaggc tgaggccgtc
      181 cgcaagaggc tccggcggcg gagggaggga ggggcgcatg cagaggattg tggaacagca
      241 ccgcttaagg atgtgttgca agggtctcgg attatagggg gcaccgaagc acaagctggc
      301 gcatggccgt gggtggtgag cctgcagatt aaatatggcc gtgttcttgt tcatgtatgt
      361 gggggaaccc tagtgagaga gaggtgggtc ctcacagctg cccactgcac taaagacgct
      421 agcgatcctt taatgtggac agctgtgatt ggaactaata atatacatgg acgctatcct
      481 cataccaaga agataaaaat taaagcaatc attattcatc caaacttcat tttggaatct
      541 tatgtaaatg atattgcact ttttcactta aaaaaagcag tgaggtataa tgactatatt
      601 cagcctattt gcctaccttt tgatgttttc caaatcctgg acggaaacac aaagtgtttt
      661 ataagtggct ggggaagaac aaaagaagaa ggtaacgcta caaatatttt acaagatgca
      721 gaagtgcatt atatttctcg agagatgtgt aattctgaga ggagttatgg gggaataatt
      781 cctaacactt cattttgtgc aggtgatgaa gatggagctt ttgatacttg caggggtgac
      841 agtgggggac cattaatgtg ctacttacca gaatataaaa gatttttgt aatgggaatt
      901 accagttacg gacatggctg tggtcgaaga ggttttcctg gtgtctatat tgggccatcc
      961 ttctaccaaa agtggctgac agagcatttc ttccatgcaa gcactcaagg catacttact
     1021 ataaatattt tacgtggcca gatcctcata gctttatgtt ttgtcatctt actagcaaca
     1081 acataaagaa attctgaagg ctttcatatc tttatttgc attgtgtccc tttctatgtt
     1141 ctatataatg aacatcattt attcttctag caattaattg cctacattag agatttcatg
     1201 tgaacatttt atgggctata agtattgtga cagatataca attgtaattt tggcactgaa
     1261 tcacatgtct ccttgaaata tcttgattat tttataatca taattctgta tctggaatac
     1321 tcatagagtt tgtacaaaat attcagttaa acatatattt tatgtgtata aatgccaaat
     1381 aatagtttat aattaaaatg aaagctgtca tttggttaaa ttaataaaaa ttctttctta
     1441 gattttattc taaaaaa
//
```

>XM_171629 ACCESSION:XM_171629 NID: gi 22062231 ref XM_171629.1 Homo sapiens similar to cortical granule serine protease 1 precursor (LOC257236), mRNA

Length = 1295

Identities = 141/153 (92%), Positives = 141/153 (92%)
Frame = +3

```
Query: 62   CGTAPLKDVLQGSRIIGGTEAQAGAWPWVVSLQIKYGRVLVHVCGGTLVRERWVLTAAHC 121
            CGTAPLKDVLQGSRIIGGTEAQAGAWPWVVSLQIKYGRVLVHVCGGTLVRE
Sbjct: 3    CGTAPLKDVLQGSRIIGGTEAQAGAWPWVVSLQIKYGRVLVHVCGGTLVRE--------- 155

Query: 122  TKDSDPLMWTAVIGTNNIHGRYPHTKKIKIKAIIIHPNFILESYVNDIALFHLKKAVRYN 181
                SDPLMWTAVIGTNNIHGRYPHTKKIKIKAIIIHPNFILESYVNDIALFHLKKAVRYN
Sbjct: 156  ---SDPLMWTAVIGTNNIHGRYPHTKKIKIKAIIIHPNFILESYVNDIALFHLKKAVRYN 326

Query: 182  DYIQPICLPFDVFQILDGNTKCFISGWGRTKEE 214
            DYIQPICLPFDVFQILDGNTKCFISGWGRTKEE
Sbjct: 327  DYIQPICLPFDVFQILDGNTKCFISGWGRTKEE 427
```

Identities = 131/131 (100%), Positives = 131/131 (100%)
Frame = +3

```
Query: 215  GNATNILQDAEVHYISREMCNSERSYGGIIPNTSFCAGDEDGAFDTCRGDSGGPLMCYLP 274
            GNATNILQDAEVHYISREMCNSERSYGGIIPNTSFCAGDEDGAFDTCRGDSGGPLMCYLP
Sbjct: 900  GNATNILQDAEVHYISREMCNSERSYGGIIPNTSFCAGDEDGAFDTCRGDSGGPLMCYLP 1079

Query: 275  EYKRFFVMGITSYGHGCGRRGFPGVYIGPSFYQKWLTEHFFHASTQGILTINILRGQILI 334
            EYKRFFVMGITSYGHGCGRRGFPGVYIGPSFYQKWLTEHFFHASTQGILTINILRGQILI
Sbjct: 1080 EYKRFFVMGITSYGHGCGRRGFPGVYIGPSFYQKWLTEHFFHASTQGILTINILRGQILI 1259

Query: 335  ALCFVILLATT 345
            ALCFVILLATT
Sbjct: 1260 ALCFVILLATT 1292
```

NCBI Entrez Nucleotide

Search Nucleotide for [ ] Go Clear

Limits Preview/Index History Clipboard Details

Display default Save Text Add to Clipboard Get Subsequence

Links

1: XM_171629. Homo sapiens simi...[gi:22062231]

```
LOCUS       LOC257238               1295 bp    mRNA    linear   PRI 01-AUG-2002
DEFINITION  Homo sapiens similar to cortical granule serine protease 1
            precursor (LOC257238), mRNA.
ACCESSION   XM_171629
VERSION     XM_171629.1  GI:22062231
KEYWORDS    .
SOURCE      Homo sapiens (human)
  ORGANISM  Homo sapiens
            Eukaryota; Metazoa; Chordata; Craniata; Vertebrata; Euteleostomi;
            Mammalia; Eutheria; Primates; Catarrhini; Hominidae; Homo.
REFERENCE   1  (bases 1 to 1295)
  AUTHORS   NCBI Annotation Project.
  TITLE     Direct Submission
  JOURNAL   Submitted (31-JUL-2002) National Center for Biotechnology
            Information, NIH, Bethesda, MD 20894, USA
COMMENT     GENOME ANNOTATION REFSEQ:  This model reference sequence was
            predicted from NCBI contig NT_009782 by automated computational
            analysis using gene prediction method: GenomeScan, supported by EST
            evidence.
            Also see:
                Documentation of NCBI's Annotation Process

FEATURES             Location/Qualifiers
     source          1..1295
                     /organism="Homo sapiens"
                     /db_xref="taxon:9606"
                     /chromosome="12"
     gene            1..1295
                     /gene="LOC257238"
                     /db_xref="InterimID:257238"
     CDS             168..1295
                     /gene="LOC257238"
                     /codon_start=1
                     /product="similar to cortical granule serine protease 1
                     precursor"
                     /protein_id="XP_171629.1"
                     /db_xref="GI:22062232"
                     /db_xref="InterimID:257238"
                     /translation="MWTAVIGTNNIHGRYPHTKKIKIKAIIIHPNFILESYVNDIALF
                     HLKKAVRYNDYIQPICLPFDVFQILDGNTKCFISGWGRTKEEGIAGFVTVVSCGLYKL
                     KYRRDQKMSIHLIHMRVAAQGFVVGAVTLARGFAGGAPAMALPPGEPGGLSSPQPEIP
                     TAGSAPPLARACFRRMARILASDGYLLPFPSKPSVVTLCPLSPQFWAQESEKKMSSDN

                     /gene="LOC257238"
```

/note="Region: smart00020, Tryp_SPc, Trypsin-like serine protease; Many of these are synthesised as inactive precursor zymogens that are cleaved during limited proteolysis to generate their active forms. A few, however, are active as single chain molecules, and others are inactive due to substitutions of the catalytic triad residues"

misc_feature 171..434
/gene="LOC257238"
/note="Region: pfam00089, trypsin, Trypsin"

misc_feature 819..1199
/gene="LOC257238"
/note="Region: pfam02395, IGA1, Immunoglobulin A1 protease. This family consists of immunoglobulin A1 protease proteins. The immunoglobulin A1 protease cleaves immunoglobulin IgA and is found in pathogenic bacteria such as Neisseria gonorrhoeae. Not all of the members of this family are IgA proteases (one member from E. coli cleaves human coagulation factor V, another one is a hemoglobin protease)"

misc_feature 900..1187
/gene="LOC257238"
/note="Region: smart00020, Tryp_SPc, Trypsin-like serine protease; Many of these are synthesised as inactive precursor zymogens that are cleaved during limited proteolysis to generate their active forms. A few, however, are active as single chain molecules, and others are inactive due to substitutions of the catalytic triad residues"

misc_feature 903..1187
/gene="LOC257238"
/note="Region: pfam00089, trypsin, Trypsin"

variation 681
/gene="LOC257238"
/allele="C"
/allele="T"
/db_xref="dbSNP:3742071"

BASE COUNT 352 a 265 c 314 g 364 t
ORIGIN

```
      1 attgtggaac agcaccgctt aaggatgtgt tgcaagggtc tcggattata gggggcaccg
     61 aagcacaagc tggcgcatgg ccgtgggtgg tgagcctgca gattaaatat ggccgtgttc
    121 ttgttcatgt atgtggggga accctagtga gagagagcga tcctttaatg tggacagctg
    181 tgattggaac taataatata catggacgct atcctcatac caagaagata aaaattaaag
    241 caatcattat tcatccaaac ttcattttgg aatcttatgt aaatgatatt gcacttttc
    301 acttaaaaaa agcagtgagg tataatgact atattcagcc tatttgccta ccttttgatg
    361 ttttccaaat cctggacgga aacacaaagt gttttataag tggctgggga agaacaaaag
    421 aagaaggtat agcaggcttt gtgactgtgg tgtcctgtgg tctttacaag ctaaagtaca
    481 gaagagatca gaaaatgtca attcatctta ttcacatgag agttgctgcc caaggatttg
    541 ttgttggagc tgtgactcta gctcgaggct ttgcaggagg cgcacctgcg atggccttac
    601 cgccaggtga gcccggcggg ctctcatcgc ctcagccgga gattccaact gcagggagcg
    661 cacctcctct ggctagggcg tgtttccgaa ggatggcaag aatcctggcc tctgatggct
    721 atcttctccc cttcccctcc aagcccagtg ttgtgaccct gtgccctctt tcccctcaat
    781 tttgggccca ggagtcagag aaaaaaatgt cttcagataa ccagtggtca gcagatgagg
    841 atgaaggcca attatcccga ctaatcagga aatctagaga ctccccctt gtccctatag
    901 gtaacgctac aaatatttta caagatgcag aagtgcatta tatttctcga gagatgtgta
    961 attctgagag gagttatggg ggaataattc ctaacacttc attttgtgca ggtgatgaag
```

```
     1261 ctttatgttt tgtcatctta ctagcaacaa cataa
//
```

Revised: July 5, 2002.

Dec 2 2002 13:45:47

THE HUMAN GENOME

Humanity has been given a great gift. With the completion of the human genome sequence, we have received a powerful tool for unlocking the secrets of our genetic heritage and for finding our place among the other participants in the adventure of life.

This week's issue of *Science* contains the report of the sequencing of the human genome from a group of authors led by Craig Venter of Celera Genomics. The report of the sequencing of the human genome from the publicly funded consortium of laboratories led by Francis Collins appears in this week's *Nature*. This stunning achievement has been portrayed—often unfairly—as a competition between two ventures, one public and one private. That characterization detracts from the awesome accomplishment jointly unveiled this week. In truth, each project contributed to the other. The inspired vision that launched the publicly funded project roughly 10 years ago reflected, and now rewards, the confidence of those who believe that the pursuit of large-scale fundamental problems in the life sciences is in the national interest. The technical innovation and drive of Craig Venter and his colleagues made it possible to celebrate this accomplishment far sooner than was believed possible. Thus, we can salute what has become, in the end, not a contest but a marriage (perhaps encouraged by shotgun) between public funding and private entrepreneurship.

A historic moment for the scientific endeavor.

There are excellent scientific reasons for applauding an outcome that has given us two winners. Two sequences are better than one; the opportunity for comparison and convergence is invaluable. Indeed, a real-world proof of the importance of access to both sets of data can be found in the pages of this issue of *Science*, in the comparative analysis by Olivier *et al.* (p. 1298).

Although we have made the point before, it is worth repeating that the sequencing of the human genome represents, not an ending, but the beginning of a new approach to biology. As Galas says in his Viewpoint (p. 1257), the knowledge that all of the genetic components of any process can be identified will give extraordinary new power to scientists. Because of this breakthrough, research can evolve from analyzing the effects of individual genes to a more integrated view that examines whole ensembles of genes as they interact to form a living human being. Several articles in this issue highlight how this approach is already beginning to revolutionize the way we look at human disease.

This has been a massive project, on a scale unparalleled in the history of biology, but of course it has built on the scientific insights of centuries of investigators. By coincidence, this landmark announcement falls during the week of the anniversary of the birth of Charles Darwin. Darwin's message that the survival of a species can depend on its ability to evolve in the face of change is peculiarly pertinent to discussions that have gone on in the past year over access to the Celera data. (Full information regarding the agreements that were reached to make the data available can be found at www.sciencemag.org/feature/data/announcement/gsp.shl.) We are willing to be flexible in allowing data repositories other than the traditional GenBank, while insisting on access to all the data needed to verify conclusions. In this domain, change is everywhere: Commercial researchers are producing more and more potentially valuable sequences, yet (at least in the United States) laws governing databases provide scant protection against piracy. Had the Celera data been kept secret, it would have been a serious loss to the scientific community. We hope that our adaptability in the face of change will enable other proprietary data to be published after peer review, in a way that satisfies our continuing commitment to full access.

It should be no surprise that an achievement so stunning, and so carefully watched, has created new challenges for the scientific venture. *Science* is proud to have played a role in bringing this discovery onto the public stage. It is literally true that this is a historic moment for the scientific endeavor. The human genome has been called the Book of Life. Rather, it is a library, in which, with rules that encourage exploration and reward creativity, we can find many of the books that will

Query= SEQ ID NO:3

Sequences producing significant alignments:	Score (bits)	E Value
AC008121.33.67777.200926	546	e-153

>AC008121.33.67777.200926
Length = 133150

Score = 546 bits (275), Expect = e-153
Identities = 275/275 (100%)
Strand = Plus / Plus

```
Query: 382   agcgatcctttaatgtggacagctgtgattggaactaataatatacatggacgctatcct 441
              |||||||||||||||||||||||||||||||||||||||||||||||||||||||||||
Sbjct: 51038 agcgatcctttaatgtggacagctgtgattggaactaataatatacatggacgctatcct 51097

Query: 442   cataccaagaagataaaaattaaagcaatcattattcatccaaacttcattttggaatct 501
              |||||||||||||||||||||||||||||||||||||||||||||||||||||||||||
Sbjct: 51098 cataccaagaagataaaaattaaagcaatcattattcatccaaacttcattttggaatct 51157

Query: 502   tatgtaaatgatattgcacttttcacttaaaaaaagcagtgaggtataatgactatatt 561
              |||||||||||||||||||||||||||||||||||||||||||||||||||||||||||
Sbjct: 51158 tatgtaaatgatattgcacttttcacttaaaaaaagcagtgaggtataatgactatatt 51217

Query: 562   cagcctatttgcctacctttgatgttttccaaatcctggacggaaacacaaagtgtttt 621
              |||||||||||||||||||||||||||||||||||||||||||||||||||||||||||
Sbjct: 51218 cagcctatttgcctacctttgatgttttccaaatcctggacggaaacacaaagtgtttt 51277

Query: 622   ataagtggctggggaagaacaaaagaagaaggtaa 656
              |||||||||||||||||||||||||||||||||
Sbjct: 51278 ataagtggctggggaagaacaaaagaagaaggtaa 51312
```

Score = 502 bits (253), Expect = e-139
Identities = 253/253 (100%)
Strand = Plus / Plus

```
Query: 795   gggtgacagtgggggaccattaatgtgctacttaccagaatataaaagatttttgtaat 854
              ||||||||||||||||||||||||||||||||||||||||||||||||||||||||||||
Sbjct: 79588 gggtgacagtgggggaccattaatgtgctacttaccagaatataaaagatttttgtaat 79647

Query: 855   gggaattaccagttacggacatggctgtggtcgaagaggttttcctggtgtctatattgg 914
              ||||||||||||||||||||||||||||||||||||||||||||||||||||||||||||
```

```
Query: 915    gccatccttctaccaaaagtggctgacagagcatttcttccatgcaagcactcaaggcat 974
              ||||||||||||||||||||||||||||||||||||||||||||||||||||||||||||
Sbjct: 79708  gccatccttctaccaaaagtggctgacagagcatttcttccatgcaagcactcaaggcat 79767


Query: 975    acttactataaatattttacgtggccagatcctcatagctttatgttttgtcatcttact 1034
              ||||||||||||||||||||||||||||||||||||||||||||||||||||||||||||
Sbjct: 79768  acttactataaatattttacgtggccagatcctcatagctttatgttttgtcatcttact 79827


Query: 1035   agcaacaacataa 1047
              |||||||||||||
Sbjct: 79828  agcaacaacataa 79840
```

Score = 387 bits (195), Expect = e-105
Identities = 196/197 (99%)
Strand = Plus / Plus

```
Query: 187    gattgtggaacagcaccgcttaaggatgtgttgcaagggtctcggattatagggggcacc 246
              ||||||||||||||||||||||||||||||||||||||||||||||||||||||||||||
Sbjct: 36091  gattgtggaacagcaccgcttaaggatgtgttgcaagggtctcggattatagggggcacc 36150


Query: 247    gaagcacaagctggcgcatggccgtgggtggtgagcctgcagattaaatatggccgtgtt 306
              ||||||||||||||||||||||||||||||||||||||||||||||||||||||||||||
Sbjct: 36151  gaagcacaagctggcgcatggccgtgggtggtgagcctgcagattaaatatggccgtgtt 36210


Query: 307    cttgttcatgtatgtgggggaaccctagtgagagagaggtgggtcctcacagctgcccac 366
              ||||||||||||||||||||||||||||||||||||||||||||||||||||||||||||
Sbjct: 36211  cttgttcatgtatgtgggggaaccctagtgagagagaggtgggtcctcacagctgcccac 36270


Query: 367    tgcactaaagacrctag 383
              |||||||||||| ||||
Sbjct: 36271  tgcactaaagacactag 36287
```

Score = 363 bits (183), Expect = 9e-98
Identities = 185/187 (98%)
Strand = Plus / Plus

```
Query: 1      atgcggctggggctcctgagcgtggcgytgttgtttgtggggagctctcacttayactca 60
              |||||||||||||||||||||||| |||||||||||||||||||||||| |||||
Sbjct: 35215  atgcggctggggctcctgagcgtggcgctgttgtttgtggggagctctcacttatactca 35274


Query: 61     gaccactactcgccctctggaaggcacaggctcggcccctcgccggaaccggcggctagt 120
              ||||||||||||||||||||||||||||||||||||||||||||||||||||||||||||
```

```
Query: 121   tcccagcaggctgaggccgtccgcaagaggctccggcggcggagggagggaggggcgcat 180
              ||||||||||||||||||||||||||||||||||||||||||||||||||||||||||||
Sbjct: 35335 tcccagcaggctgaggccgtccgcaagaggctccggcggcggagggagggaggggcgcat 35394


Query: 181   gcaaagg 187
              |||||||
Sbjct: 35395 gcaaagg 35401
```

Score = 290 bits (146), Expect = 1e-75
Identities = 146/146 (100%)
Strand = Plus / Plus

```
Query: 651   aggtaacgctacaaatattttacaagatgcagaagtgcattatatttctcgagagatgtg 710
              ||||||||||||||||||||||||||||||||||||||||||||||||||||||||||||
Sbjct: 77571 aggtaacgctacaaatattttacaagatgcagaagtgcattatatttctcgagagatgtg 77630


Query: 711   taattctgagaggagttatgggggaataattcctaacacttcattttgtgcaggtgatga 770
              ||||||||||||||||||||||||||||||||||||||||||||||||||||||||||||
Sbjct: 77631 taattctgagaggagttatgggggaataattcctaacacttcattttgtgcaggtgatga 77690


Query: 771   agatggagcttttgatacttgcaggg 796
              |||||||||||||||||||||||||
Sbjct: 77691 agatggagcttttgatacttgcaggg 77716
```

NCBI Nucleotide

PubMed Nucleotide Protein Genome Structure PMC Taxonomy

Search Nucleotide for Go Clear

Limits Preview/Index History Clipboard Details

Display default Show: 20 Send to File Get Subsequence

Links

1: AC008121. Homo sapiens 12 B...[gi:28626577]

LOCUS AC008121 105989 bp DNA linear PRI 01-MAR-2003
DEFINITION Homo sapiens 12 BAC RP11-407N8 (Roswell Park Cancer Institute Human BAC Library) complete sequence.
ACCESSION AC008121
VERSION AC008121.43 GI:28626577
KEYWORDS HTG.
SOURCE Homo sapiens (human)
ORGANISM Homo sapiens
Eukaryota; Metazoa; Chordata; Craniata; Vertebrata; Euteleostomi; Mammalia; Eutheria; Primates; Catarrhini; Hominidae; Homo.
REFERENCE 1 (bases 1 to 105989)
AUTHORS Muzny,D.M., Adams,C., Adio-Oduola,B., Ali-osman,F.R., Allen,C., Alsbrooks,S.L., Amaratunge,H.C., Are,J.R., Ayele,M., Banks,T., Barbaria,J., Benton,J., Bimage,K., Blankenburg,K., Bonnin,D., Bouck,J., Bowie,S., Brieva,M., Brown,E., Brown,M., Bryant,N.P., Buhay,C., Burch,P., Burkett,C., Burrell,K.L., Byrd,N.C., Carron,T.F., Carter,M., Cavazos,S.R., Chacko,J., Chavez,D., Chen,G., Chen,R., Chen,Z., Chiu,D., Chowdhry,I., Christopoulos,C., Cleveland,C.D., Cox,C., Coyle,M.D., Dathorne,S.R., David,R., Davila,M.L., Davis,C., Davy-Carroll,L., Dederich,D.A., Delaney,K.R., Delgado,O., Denn,A.L., Ding,Y., Dinh,H.H., Douthwaite,K.J., Draper,H., Dugan-Rocha,S., Durbin,K.J., Earnhart,C., Edgar,D., Edwards,C.C., Elhaj,C., Emerling,S., Escotto,M., Falls,T., Ferraguto,D., Flagg,N., Ford,J., Foster,P., Frantz,P., Gabisi,A., Gao,J., Garcia,A., Garner,T., Garza,N., Gill,R., Gorrell,J.H., Guevara,W., Gunaratne,P., Hale,S., Hamilton,K., Han,J., Harris,C., Harris,K., Hart,M., Havlak,P., Hawes,A., Hernandez,J., Hernandez,O., Hodgson,A., Hogues,M., Holloway,C., Hollins,B., Homsi,F., Howard,S., Huber,J., Hulyk,S., Hume,J., Ioshikhes,I., Jackson,L.E., Jacobson,B., Jia,Y., Johnson,R., Jolivet,S., Joudah,S., Karlsson,E., Kelly,S., Khan,U., King,L., Korvah,J., Kovar,C., Kratovic,J., Kureshi,A., Landry,N., Leal,B., Lee,E., Lewis,L.C., Lewis,L., Li,J., Li,Z., Lichtarge,O., Lieu,C., Liu,J., Liu,W., Loulseged,H., Lozado,R.J., Lu,X., Lucier,A., Lucier,R., Luna,R., Ma,J., Maheshwari,M., Mapua,P., Marondel,I., Martin,R., Martindale,A., Martinez,E., Massey,E., Mawhiney,E., McLeod,M.P., Meador,M., Mei,G., Merscher,S., Metzker,M., Miller,A., Miner,G., Miner,Z., Mitchell,T., Mohabbat,K., Montgomery,K.T., Morgan,M., Morris,S., Moser,M., Neal,D., Nelson,D., Newtson,J., Newtson,N., Nguyen,A., Nguyen,N., Nguyen,N., Nickerson,E., Nwokenkwo,S., Oguh,M., Okwuonu,G., Oragunye,N., Oviedo,R., Pace,A., Payton,B., Peery,J., Perez,L.,

Sutton,A., Svatek,A., [illegible]